Dissertation

submitted to the
Combined Faculties for the Natural Sciences and for Mathematics
of the Ruperto-Carola University of Heidelberg, Germany
for the degree of
Doctor of Natural Sciences

presented by

Diplom-Biochemist Lars Gredsted
Born in Copenhagen, Denmark

Oral examination:

The Role of Men1 in Pituitary Gland Tumourigenesis

Referees: Priv. Doz. Jochen Wittbrodt
Prof. Dr. Günther Schütz

Acknowledgements

The work presented in this thesis would not have been possible without the help and assistance from many people both inside and outside the lab.

First of all I would like to thank Mathias Treier for his advise and support throughout my four years in his lab. I have really learned a lot during my time at EMBL.
I would also like to thank the other members of my TAC committee, Jochen Wittbrodt and Walter Wittke and my second “Gutachter” from the university of Heidelberg Günther Schütz for constructive discussions of my project.

I would like to thank all past and present members of the Treier lab; Vitor, Catherine, Katrin, Anna Corinna, Uli, Eve, Sandra, Dirk, Maria, Henry and Thomas for making many of the long working days entertaining through discussions about most things imaginable including science. A special thanks to Katrin for helping with the ES cell tissue culture, Sandra for helping with immunohistochemistry and Henry for helping with the Genespring analysis of the microarray data.
A big thanks must go to everybody at the animal house for taking care of our mice and for always being helpful even when I was late with requests. I would also like to thanks the people past and present in the transgenic facility, without whom my mouse would still be a model only.

Thanks to all the friends I have made at EMBL that have made these years some of the best of my life. EMBL is a truly international place and I feel very fortunate to have been given the chance to make friends from so many countries of the world.
I would also like to thank my parents who have always supported me whatever decision I have made right or wrong.

Finally the biggest thanks must go to Rebecca, for always being there to support me and cheer me up. I dedicate this these to you

Summary

The pituitary gland is a key regulator of growth, metabolism and sexual development. The pituitary gland integrates signals from the hypothalamus and from peripheral endocrine glands and responds to changing physiological needs by secreting a series of hormones that regulate the activity of various endocrine glands as well as acting directly on many tissues. Tumours of the pituitary gland are relatively frequent possibly due to the plasticity of the gland. Pituitary gland tumours occur both sporadically and as part of inherited multiple endocrine neoplasia (MEN) syndromes. MEN1 is one of these inherited syndromes. People suffering from MEN1 develop tumours of the pituitary gland, the parathyroid glands, the pancreatic islets and the adrenal glands. MEN1 is caused by a loss of function mutation in the tumour suppressor gene *MEN1*. *Men1* expression is found in all tissues in the mouse and not only in the endocrine system. Menin the protein encoded by *Men1*, shares no homology with any known proteins and contains no recognisable protein domains. Menin is believed to function as a regulator of transcription through binding to several specific transcription factors. These include Smad transcription factors, JunD and members of the NF-kB family of proteins.

To investigate the phenotype of *Men1* deficiency and to elucidate the mechanism of MEN1 tumourigenesis I have generated a conditional *Men1* mouse model that enables me to specifically delete *Men1* in the pituitary gland. *Men1* deficient pituitary glands are hyperplastic as early as 7 weeks of age. The hyperplasia often develops into massive adenomas by 40 weeks of age. Both hyperplasia and adenoma formation shows a gender difference and is more pronounced in female mice. Analysis of the *Men1* deficient pituitary glands revealed pituitary gland overproliferation by 12 weeks of age before the development of adenomas. Microarray analysis of the *Men1* deficient pituitaries identified two growth factors that were significantly overexpressed in *Men1* deficient pituitary glands. Both of these factors also showed a clear gender difference in their expression levels. The overexpression of these growth factors in the *Men1* deficient pituitaries was confirmed by *in situ* hybridisation.

1 Introduction

1.1 Growth control in the pituitary gland

1.1.1 The pituitary gland

The pituitary gland is the master gland of the endocrine system. It integrates signals from the hypothalamus, to which it is connected to by the pituitary stalk and regulates the activity of the thyroid gland, the adrenal gland and the gonads.

The pituitary gland has three anatomical and functional parts, the posterior pituitary gland, which is of neuroectodermal origin, and the intermediate and anterior pituitary gland, which derives from the oral ectoderm. The posterior pituitary gland contains axons from neurons in the hypothalamus that secrete Vasopressin and Oxytoxin. The intermediate gland (which is not present in humans) secretes Melanocyte Stimulating Hormone (MSH). The anterior pituitary gland consists of five major cell types, the lactotropes (10-25 percent), corticotropes (15-20 percent), thyrotropes (3-5 percent), gonadotropes (10-15 percent) and somatotropes (40-50 percent). In response to specific releasing hormones secreted from the hypothalamus each cell type secretes their distinct hormone. Thyrotropin Releasing Hormone (TRH) stimulates Thyroid Stimulating Hormone (TSH) release from the thyrotropes. Gonadotropin Releasing Hormone (GnRH) stimulates release of Luteinising Hormone (LH) and Follicle-Stimulating Hormone (FSH) from gonadotropes. Growth hormone releasing hormone (GHRH) stimulates Growth Hormone (GH) release from the somatotropes and finally Corticotropin Releasing Hormone (CRH) stimulates Adrenocorticotropin (ACTH) release from the corticotropes. A hypothalamic Prolactin Releasing Hormone (PRRH) has been characterised that binds to the G-protein coupled receptor hGR3 (Hinuma *et al.*, 1998), although subsequent studies have suggested that PRRH is only functional in females and only at high concentrations (Samson *et al.*, 1998) and that much of its function may be mediated by the hypothalamus (Seal *et al.*, 2000).

TSH, LH, FSH and ACTH exert their effects through peripheral endocrine organs whereas Prolactin and GH act directly on their target organs to regulate reproduction and growth respectively.

During adult life, the activity and size of the pituitary gland changes with age and in response to certain physiological events such as pregnancy. Accordingly the pituitary gland is subjected to a very complex regulation consisting of hormonal regulation from the hypothalamus, as

well as feedback control from the peripheral target glands and other endocrine glands that regulate the activity and growth of the pituitary gland directly and indirectly through the hypothalamus. This plasticity of the pituitary gland, which is a consequence of the necessity to adapt to changing physiological needs, may be the reason why pituitary gland neoplasias are more frequent than tumours of other tissues. To elucidate the mechanism of pituitary gland tumourigenesis in both sporadic cases and in the context of inherited tumour syndromes like MEN1, I will in the following sections discuss the development of the pituitary gland and the factors that control its growth as well as what is known about factors contributing to tumourigenesis of the pituitary gland and other endocrine glands.

1.1.2 Development of the pituitary gland

A schematic representation of the development of the pituitary gland is shown on **Figure 1.1**. The pituitary gland and the hypothalamus develop from a close association between two embryonic tissues, the neural ectoderm and the oral roof ectoderm. At embryonic day E8.5 of mouse development, the oral ectoderm comes into contact with the neural ectoderm from which it receives inductive signals, mainly BMP4. These signals induce the onset of pituitary gland organogenesis (Treier *et al.*, 1996)(Dasen *et al.*, 1999). *Shh* and *Hnf3ß*, a winged helix transcription factor, which were previously uniformly expressed in the oral ectoderm, are now excluded from the contact region with the ventral diencephalon. This creates a molecular compartment within the oral ectoderm, which later becomes the anterior pituitary gland. At the same time, *Lhx3*, a member of the LIM homeodomain family of transcription factors, is expressed in this molecular compartment and commits the oral ectoderm to the pituitary gland fate. Subsequently at E9.0, the oral ectoderm invaginates to form a structure called Rathke's pouch which is the pituitary gland primordium (**Figure 1.1 A**). The formation of Rathke's pouch is followed by proliferation of cells from the ventral part of the pituitary gland. This proliferation is blocked in the absence of *Lhx3* or FGF8 from the ventral diencephalon. In the definitive Rathke's pouch, *BMP2* is induced at the boundary between Rathke's pouch and the oral ectoderm and a ventral to dorsal BMP2 activity gradient is created. Concomitant with the invagination of the oral ectoderm, a portion of the ventral diencephalon (the infundibulum) evaginates and contacts the dorsal portion of Rathke's pouch directly. FGF8 originating from the infundibulum establishes a dorsal to ventral activity gradient that functions antagonistically to the opposing ventral to dorsal BMP2 gradient (**Figure 1.1 B**) (Treier *et al.*, 1998). These two transient gradients establish patterns of overlapping expression of several

transcription factors in Rathke's pouch. Many of these transcription factors exhibit temporally and spatially restricted domains of expression within the developing pituitary gland resulting in the appearance of the different hormone secreting cell types (**Figure 1.1 C**) (Treier *et al.*, 1998).

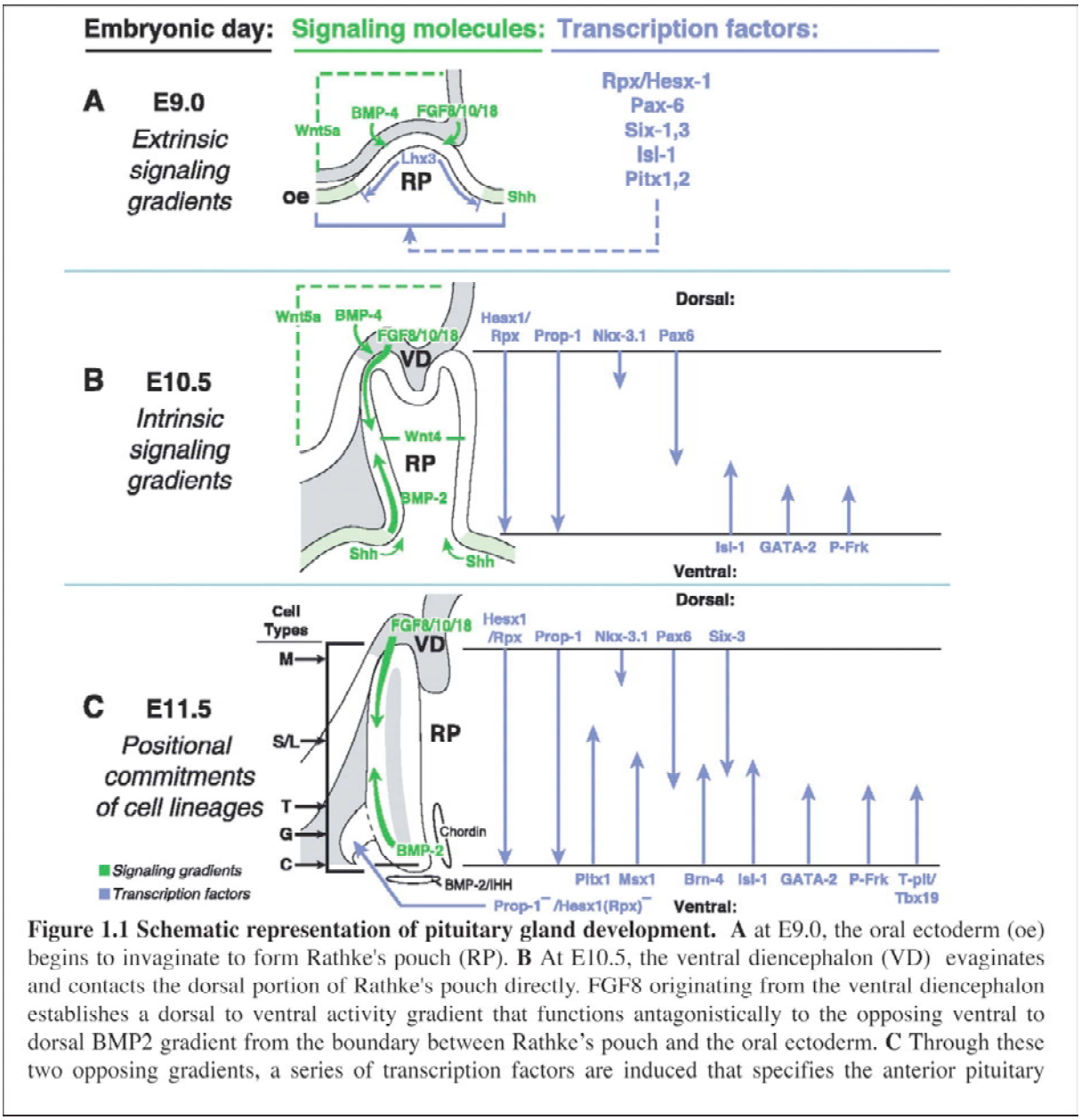

Figure 1.1 Schematic representation of pituitary gland development. **A** at E9.0, the oral ectoderm (oe) begins to invaginate to form Rathke's pouch (RP). **B** At E10.5, the ventral diencephalon (VD) evaginates and contacts the dorsal portion of Rathke's pouch directly. FGF8 originating from the ventral diencephalon establishes a dorsal to ventral activity gradient that functions antagonistically to the opposing ventral to dorsal BMP2 gradient from the boundary between Rathke's pouch and the oral ectoderm. **C** Through these two opposing gradients, a series of transcription factors are induced that specifies the anterior pituitary

A series of mice with pituitary gland phenotypes have contributed to the identification of factors involved in specifying the different pituitary gland cell types. The Ames dwarf mouse has a hypoplastic pituitary gland. In the Ames mouse, somatotropes, lactotropes and thyrotropes are specified but fail to proliferate. Accordingly the number of these cell types is less than 1 percent of wildtype numbers (Sornson *et al.*, 1996). The gene responsible for this phenotype was cloned by positional cloning and named *Prop-1*. *Prop-1* is a homeodomain transcription factor that is exclusively expressed in the pituitary. Its expression can be

detected from E10.5 on in a dorsal to ventral gradient. The phenotype of the Ames mouse is associated with an absence of expression of the transcription factor *Pit-1* which is the reason for the name *Prop-1* (Prophet of Pit). Prop-1 binds directly to the *Pit-1* promoter to initiate transcription (Sornson *et al.*, 1996). Pit-1 was originally isolated as a transcription factor binding to elements in both the *GH* and *Prolactin* promoters (Nelson *et al.*, 1988) and was subsequently identified as the gene responsible for the phenotype of the Snell and Jackson dwarf mice, which completely lack three lineages of pituitary gland cell types, the somatotropes, the lactotropes and the thyrotropes. *Pit-1* expression begins at E13.5 and drives differentiation and maintenance of these three lineages. The *Gata-2* transcription factor on the other hand is necessary for the deveolpment of the thyrotrope and gonadotrope lineages (Dasen *et al.*, 1999).

1.1.3 Control of pituitary gland growth

Once the different pituitary gland cell types have been specified at E16 in the mouse, they proliferate until 7 to 8 weeks after birth to form the adult pituitary gland. The proliferation of the differentiated pituitary gland cell types is under the control of hypothalamic hormone releasing hormones. This has been best illustrated by the regulation of somatotrope growth.

The “little” dwarf mouse is characterised by anterior pituitary gland hypoplasia and significantly decreased GH secretion associated with a dramatic reduction in the number of somatotropes. The "little” mouse carries a mutation in the GHRH receptor, which renders the receptor unable to bind GHRH (Lin *et al.*, 1993). Conversely, overexpression of GHRH leads to somatotrope hyperplasia (Mayo *et al.*, 1988). These findings suggest that the activity of GHRH not only regulates the secretion of GH, but also the proliferation of the GH secreting cells. Likewise it has been shown that CRH, TRH and GnRH are also able to stimulate proliferation of their target cells (Ezzat, 2001) and importantly, that disruption of the gene encoding TRH leads to a significant reduction in TSH positive cells of the pituitary gland (Yamada *et al.*, 1997). Furthermore, in the absence of GnRH, gonadotropes are specified but fail to proliferate (Mason *et al.*, 1986). In contrast corticotropes develop normally in the pituitary gland of CRH deficient mice (Muglia *et al.*, 1995), possibly suggesting the existence of other Corticotropin Releasing Hormones.

The action of GHRH on hormone secretion from and proliferation of somatotropes is counteracted by Somatostatin secreted from the hypothalamus. Likewise the growth of lactotropes is repressed by dopamine secreted from the hypothalamus. On the other hand the secretion of ACTH, TSH, LH and FSH and the proliferation of corticotropes, thyrotropes and

gonadotropes is blocked by Cortisol, Thyroid Hormone and Sex Hormones respectively, secreted from the peripheral endocrine glands, constituting negative feedback mechanisms (Melmed, 2003).

The GHRH receptor is a G-protein coupled receptor that couples to the adenylate cyclase activating G-protein Gαs (Mayo, 1992). The same is true for the other hypothalamic releasing hormone receptors.

The striking effect of cAMP on pituitary gland cell proliferation has been illustrated by two examples. Ectopic expression of a dominant negative form of the Cyclic AMP Binding Element (CREB) in somatotropes results in pituitary gland hypoplasia and a GH deficiency caused by a significant reductions in cell number. Thus disruption of the cAMP responsive pathway blocks proliferation of somatotropes. (Struthers *et al.*, 1991). Conversely activating mutations to the Gαs subunit induces hyperproliferation of somatotropes (Landis *et al.*, 1989).

After normal growth ceases, the pituitary gland recedes somewhat in size. The largest pituitary glands are thus found in adolescent females where they measure up to 9 mm in height in humans (Chanson *et al.*, 2001). There is however one significant exception and that is pregnancy. In pregnant women the pituitary gland more than doubles in size. Interestingly, after pregnancy and lactation the pituitary gland reverts to near normal size within 6 months (Dinc *et al.*, 1998). Expansion of the lactotrope population is responsible for most of the gain in size of the pituitary gland, but there is also evidence that somatotropes can be induced into secreting Prolactin (Melmed, 2003). The proliferation of the lactotrope lineage is induced by Estrogen, a very potent mitogen for lactotropes (Heaney *et al.*, 1999). The dramatic regression of pituitary gland size upon normalisation of Estrogen levels illustrates the very strict growth control normally active in the pituitary gland.

1.1.4 Pituitary gland tumours

Tumours are the result of failed growth control. The development of a tumour is a dynamic process that involves sequential acquisition of tumourigenic traits driven by selectional pressure. Accordingly tumour development often involves a series of changes to pathways providing growth signals or mediating growth inhibitory signals as well as controlling cell survival. Advanced tumour progression also requires increased angiogenesis and the acquisition of limitless replicative potential (Hanahan *et al.*, 2000).

In the pituitary gland, tumour development is often a gradual progression from hyperplasia, which is a general increase tissue size due to higher cell numbers, to neoplasia, which can be

defined as an abnormal mass of cells produced by an autonomous growth of a tissue. Neoplasias can be benign or malignant depending on their growth rate and invasiveness. A benign tumour which originates from glandular epithelium is called an adenoma, whereas a malignant tumour of the same origin is termed a carcinoma.

Pituitary gland tumours are very common. Unselected autopsies have revealed that up to 25 percent of the population may develop pituitary gland adenomas, however most tumours are never diagnosed (Burrow *et al.*, 1981). The vast majority of pituitary gland tumours are sporadic. Pituitary gland tumours are almost inevitably benign, but can nevertheless lead to death due to of their localisation under the brain (Melmed, 2003). Pathology from pituitary gland tumours normally arises from an excess of hormone secretion. The most frequent pituitary gland tumour is a prolactinoma, but GH secreting, ACTH secreting and non-secreting tumours also occur with high incidence (Melmed, 2003).

It has traditionally been debated whether pituitary gland tumours arise because of an intrinsic pituitary gland defect or because of aberrant hormonal stimulation. It is now apparent, that most tumours are of clonal origin, which would favour the intrinsic pituitary gland defect, but it is very likely that external factors also play a role (Melmed, 2003).

Considering that the proliferation of the pituitary gland cells as well as hormone secretion from the pituitary gland is regulated by releasing factors secreted by the hypothalamus, as well as by feedback regulation from peripheral endocrine glands, it is perhaps not surprising that some of these hormones have been implicated in pituitary gland tumourigenesis.

In humans, long lasting hypothyroidism, hypogonadism or hypoadrenalism leads to loss of hormonal feedback inhibition and to pituitary gland hyperplasia caused by expansion of thyrotropes, corticotropes or gonadotropes respectively (Melmed, 2003). Likewise, hyper-secretion of GHRH, CRH or TRH from the hypothalamus is associated with hyper-proliferation of gonadotropes, corticotropes and thyrotropes respectively in humans (Ezzat, 2001). Also high Estrogen levels or too low Dopamine levels induce lactotrope proliferation (Ezzat, 2001). Activating mutations of the pituitary gland cell growth factor receptors are rarely seen in human pituitary gland tumours. Interestingly, there appears to be no correlation between multiple births and increased prolactinoma formation in women despite the dramatic pituitary gland hyperplasia induced by pregnancy (Coogan *et al.*, 1995).

In rodent models, prolonged overexpression of *GHRH* (Mayo *et al.*, 1988)(Asa *et al.*, 1992a), CRH (Asa *et al.*, 1992b), *Estrogen* (Heaney *et al.*, 1999) or disruption of the *Dopamine D2 receptor* (Asa *et al.*, 1999) leads to pituitary gland hyperplasia and eventually to adenomas. Overexpression of other growth factors such as *FGF-β (*Heaney *et al.*, 1999) *FGF4* (Gonsky

et al., 1991), *TGF-α (*McAndrew *et al.*, 1995), and *NGF* (Borrelli *et al.*, 1992) has also been implicated in hyperplasia and prolactinoma formation in mouse models and in human tumours. While these growth factors are sufficient to induce hyperplasias and may increase the likelihood of adenomas, the clonal nature of most adenomas suggests that additional mutations have to occur for progression from hyperplasias (Melmed, 2003). For GH secreting tumours, activation of cAMP responsive pathways appears to be important for pituitary gland tumourigenesis since 30 percent of sporadic tumours carry activating mutations to one of the alpha subunits of the trimeric G proteins, *Gαs* (Vallar *et al.*, 1987). The association between high hypothalamic releasing hormone levels and hyperproliferation in corticotropes, thyrotropes and gonadotropes in both mouse models and in humans suggests that deregulated cAMP signalling can contribute to the formation of all pituitary gland tumours.

A series of mouse models have implicated genes involved in the Retinoblastoma (Rb) pathway in pituitary gland hyperplasia and adenoma formation. The Rb pathway mediates growth repressive signals and controls the onset of S-phase (Hanahan *et al.*, 2000). These mouse models include mice heterozygous for *Rb* itself (Jacks *et al.*, 1992) as well as mice homozygous for the disruption of the cyclin dependent kinase inhibitors, *p18Ink4C* (Franklin *et al.*, 1998), and *p27Kip1* (Kiyokawa *et al.*, 1996). These mice all develop adenomas specifically of the pituitary gland. Disruption of the Rb pathway is generally associated with tumour formation in all tissues (Hanahan *et al.*, 2000), and the preferantial development of pituitary gland tumours in these mouse models is not understood. Studies of human patients have only found p27KIPI1 downregulated in tumours (Lidhar *et al.*, 1999). The down regulation of p27KIP1 is observed in most adenomas and appears to be mediated by protein degradation (Melmed, 2003). Additionally, p16INK4A, another Cdk inhibitor, is very often found downregulated or missing in pituitary gland tumours (Woloschak *et al.*, 1996). This downregulation may be caused by promoter methylation (Woloschak *et al.*, 1997).

Although much still remains to be learnt it thus appears that pituitary gland tumourigenesis is often initiated by deregulation of growth signals that normally regulate pituitary growth such as hypothalamic releasing hormones, Estrogen or Dopamine and that cell autonomous mutations to the cAMP pathway and possibly to the Rb pathway contribute to adenoma formation.

1.2 Multiple endocrine neoplasia

1.2.1 Multiple endocrine neoplasias

Most endocrine neoplasias are sporadic and not hereditary. All endocrine glands are affected, however to a varying degree. Apart from the pituitary gland neoplasias, the most frequent neoplasias are those of the parathyroid glands, which affect approximately 2 percent of postmenopausal women (Carling, 2001). In contrast, tumours of the pancreatic islets are very rare.

Most endocrine tumours are not life threatening, but a minority may develop into carcinomas. Most symptoms experienced by affected individuals are due to hyper secretion of hormones from the glands affected by the tumours. Indeed most endocrine neoplasias are first recognised as hormone excess syndromes.

The endocrine glands are a heterogeneous group of organs without a common precursor during development. Additionally, the glands are positioned in very different places in the body. Nevertheless, a group of mostly inherited syndromes specifically cause neoplasia and subsequent adenoma formation in several endocrine glands of the affected individuals. Although these inherited tumour syndromes are less frequent than sporadic tumours they are significant as they suggest a common mechanism of growth control in the endocrine system and they may help to elucidate the underlying mechanism of tumourigenesis.

The name multiple endocrine neoplasias (MEN) refers to the development of tumours in several different endocrine tissues at the same time. Five hereditary MEN syndromes have been identified based on their characteristic pattern of neoplasias (Hoff, 2000).

MEN1:	Pituitary gland, parathyroid gland, pancreatic islets, adrenal cortex, cutaneous angiofibromas
MEN2A:	medullary thyroid, adrenal medulla, parathyroid gland
MEN2B:	medullary thyroid, adrenal medulla, gastrointestinal tract
FMTC:	medullary thyroid
Carney complex:	pituitary gland, thyroid, testicular, adrenal cortex

Over the last decade, the genes responsible for these syndromes have been cloned. Interestingly it was found that germline mutations to the *RET* proto-oncogene was responsible for MEN2A, MEN2B and FMTC (Mulligan *et al.*, 1993)(Hofstra *et al.*, 1994)(Donis-Keller *et*

al., 1993). RET is a receptor tyrosine kinase. For each of the *RET* associated MEN syndromes, a distinct set of gain of function mutations have been characterised. RET signals though the Ras pathway to the MAP Kinases ERK1 and ERK2 and through the RHO family of GTPases to JNK driving proliferation (Hoff, 2000). The endocrine specific pattern of tumour formation associated with activating mutations to *RET* most likely reflects the expression pattern of *RET,* rather than an endocrine specific mechanism of tumourigenesis as *RET* expression is restricted to the neuronal and the endocrine system (Pachnis *et al.*, 1993).

Loss of function mutations to *PRKAR1A*, a regulatory subunit of the cAMP dependent protein kinase PKA, has been shown to be responsible for the Carney complex. People affected by the Carney complex inherit one disrupted allele of *PRKAR1A* and subsequent loss of the wildtype allele promotes tumour formation (Kirschner *et al.*, 2000). These are the classic characteristics of a tumour suppressor. The concept of tumour suppressors was proposed by Knudson while studying the eye tumour Retinoblastoma. Knudson observed that his patients fell in two categories. One group of patients developed retinoblastoma in one eye only, the average age of onset for these patients was 32 months. The other group of patients developed bilateral tumours and the average age of onset in these patients was only 15 months. Knudson proposed that the latter group had inherited one non-functional tumour suppressor allele in the germline and that the relatively frequent loss of the second allele would initiate the tumour growth. Thus the characteristics of cancer caused by the inheritance of a disrupted tumour suppressor is that tumours arise earlier and more frequently than sporadic tumours of the same organ and that tumours have lost both wildtype tumour suppressor alleles (Knudson, 1971).

In contrast to *RET,* the expression of *PRKAR1A* is not limited to the endocrine system (Barradeau *et al.*, 2000). PKA is the cAMP dependent protein kinase responsible for mediating most of the proliferative effect of cAMP (Stork *et al.*, 2002) The loss of function mutation to PRKAR1A leads to increased PKA activity (Kirschner *et al.*, 2000), which mimics activation of Gαs by ligands binding to G-protein coupled receptors. That activation of the cAMP pathway can lead to adenoma formation in the testis, adrenal and thyroid gland as well as the pituitary gland illustrates one of the common themes in regulation of proliferation in the endocrine system; many cells in the endocrine system normally respond to growth factors, which signal through G-protein-coupled receptors. That cAMP is a mitotic signal for many cells of the endocrine system is also supported by the observation that activating mutations to *Gαs* are frequently found in sporadic thyroid and pituitary gland tumours and Leydig cell tumours of the testis (Lania *et al.*, 2001). Moreover, mutations of

Gαs early in development give rise to the so-called McCune Albright syndrome, which causes hyper activity of the pituitary gland, thyroid, adrenal cortex and gonads, which can develop into cancer. Gαs mutations do not pass through the germline suggesting that a general deregulation of cAMP signalling is not compatible with life (Lania *et al.*, 2001)(Stratakis, 2001).

In many non endocrine tissues cAMP mediates growth arrest. It has been suggested that the ability of cAMP to activate the MAP Kinase pathway is the primary factor that determines if cAMP acts as a mitotic signal or as a growth arrest signal (Stork *et al.*, 2002). The stimulatory effects of cAMP on the MAP kinase pathway appear to be mediated through Rap1 and B-Raf, whereas Raf-1 activation by Ras is blocked by cAMP. Thus the expression of B-Raf is an important factor in the proliferative outcome of cAMP signalling (Stork *et al.*, 2002).

Other hereditary tumour syndromes that can cause endocrine as well as other types of neoplasias have been characterised. These include Peutz-Jeghers syndrome caused by inactivating mutations of the serine threonine kinase *LKB1*, Cowdens disease caused by inactivation of the tumour suppressor *PTEN* (Stratakis, 2001) and Von Hippel-Lindau disease caused by loss of function mutations of the *VHL* E3 ubiquitin ligase, which leads to overexpression of TGF-α and VEGF (Alexander, 2001).

1.2.2 Multiple Endocrine Neoplasia type 1 (MEN1)

MEN1 has an estimated prevalence of 0.02-0.2 per 1000 (Verges *et al.*, 2002). Clinical diagnosis of MEN1 can be made when a patient presents with tumours in at least two of the following organs: parathyroid gland, pancreatic islets (gastrinomas) or anterior pituitary gland (prolactinomas) (Schussheim *et al.*, 2001). MEN1 patients also develop other symptoms namely, adrenocortical tumours, foregut carcinoid tumours of the bronchus, thymus and stomach as well as fascial angifibromas albeit with lower frequency (Schussheim *et al.*, 2001). The prevalence of tumours in the individual endocrine organs varies depending on the study. In one big multi-centre report 95 percent of MEN1 patients had developed parathyroid tumours, 54 percent tumours of the pancreatic islets (48 percent gastrinomas, 14 percent insulinomas, 5 percent glucagomas) and 42 percent pituitary gland tumours (62 percent prolactinomas, 9 percent GH secreting, 4 percent Prolactin and GH secreting, 6 percent ACTH, 15 percent non-secreting) (Verges *et al.*, 2002). 15 percent of gastrinomas progress to aggressive malignancy, which is the primary cause of death from MEN1 (Schussheim *et al.*, 2001).

The average age of onset was 38 years for pituitary gland tumours, 39 years for parathyroid tumours and 41 years for pancreatic islet tumours (Verges *et al.*, 2002). For tumours of the parathyroid gland and pancreatic islets this is at least 10 years before the average onset of sporadic tumours (Schussheim *et al.*, 2001), but this is not the case for pituitary gland tumours, where the average age of onset of sporadic and MEN1 tumours is identical (Verges *et al.*, 2002).

It was also observed that MEN1 pituitary gland tumours were more aggressive than sporadic tumours, 85 percent being macro-adenomas compared to only 42 percent of sporadic pituitary gland tumours. Additionally MEN1 tumours respond less well to treatment. Both of these observations suggest that MEN1 pituitary gland tumours arise through a different mechanism than sporadic pituitary gland tumours (Verges *et al.*, 2002).

Finally MEN1 pituitary gland tumours showed a gender bias with females being more likely than males to develop pituitary gland tumours (50 percent compared to 31 percent) (Verges *et al.*, 2002).

1.2.3 *MEN1*

The gene responsible for Multiple Endocrine Neoplasias was cloned by linkage analysis of MEN1 families and by studying loss of heterozygosity in tumours from patients. Unlike the other multiple endocrine neoplasia genes, this gene had not previously been characterised. The gene was thus named *MEN1*. *MEN1* maps to chromosome 11q13 (Chandrasekharappa *et al.*, 1997). Subsequent analysis found that 85 percent of MEN1 patients have germline mutations of the open reading frame of *MEN1* and that tumours from MEN1 patients showed additional loss of heterozygosity at the *MEN1* locus (Verges *et al.*, 2002). As noted these are the characteristics of a tumour suppressor (Knudson, 1971).

Mutations of *MEN1* found in patients are spread over the entire reading frame but there is no known connection between genotype and phenotype (Verges *et al.*, 2002). Interestingly, while *MEN1* has been found mutated in a significant fraction of sporadic parathyroid and pancreatic islet tumours (Heppner *et al.*, 1997)(Zhuang *et al.*, 1997), *MEN1* inactivation does not appear to play a major role in sporadic pituitary gland tumours (Prezant *et al.*, 1998)(Farrell *et al.*, 1999)

The *MEN1* gene is encoded by ten exons that give rise to two alternatively spliced mRNA containing the same open reading frame (Stewart *et al.*, 1998)(Guru *et al.*, 1999). The *Men1* transcript can be detected as early as embryonic day 7 in the mouse. At embryonic day 14

there is high expression in all tissues and at embryonic day 17 there is widespread expression with the highest signal from the muscles and central nervous system. In the adult mouse, there is a clear expression in all tissues examined, with the highest expression in the liver, brain and testis (Stewart *et al.*, 1998)(Guru *et al.*, 1999).

1.2.4 MENIN

The protein encoded by *MEN1* has been named MENIN. Human MENIN comprises 610 amino acids and mouse Menin 611 amino acids. The protein is 97 % conserved between the two species and most of the difference is concentrated in 40 amino acids at the C-terminus of the protein (Guru *et al.*, 1999)(Stewart *et al.*, 1998). The Drosophila homologue is 46 % identical to human MENIN (Guru *et al.*, 2001).

Interestingly, Menin has no homology to any other protein and no known functional domains. The protein does contain 2 nuclear localisation signals (Chandrasekharappa *et al.*, 1997) and it has been shown to be localised to the nucleus (Guru *et al.*, 1998) and specifically to telomeres during meiosis (Suphapeetiporn *et al.*, 2002).

As there are no known domains, the structure of the protein does not suggest any function of Menin. The level of Menin protein has been suggested to vary during the cell cycle in some reports (Kaji *et al.*, 1999) and to be invariant in others (Guru *et al.*, 1999).

Surprisingly, considering the lack of significant homology to any known protein including characterised GTPases, Menin binds to GTP and has GTP hydrolysis activity (Yaguchi *et al.*, 2002). Classical GTPases, which include Ras family proteins, small G-proteins and elongation factor Tu (EF-Tu), all have a conserved structure that can be recognised from the bacterial EF-Tu to mammalian Ras (Jurnak, 1985). Although Menin contains very vague GTPase consensus motifs, the GTPase function of Menin does not appear to require these regions (Hothorn, personal communication). Menin thus appears to be a novel type of GTPase. Classical GTPases exist in two different conformations depending on whether they are bound to GTP or GDP. It is not known if this is the case for Menin.

The GTPase activity of Menin can be increased many folds by the addition of the nucleoside diphosphate kinase Nm23H1. Thus, Nm23H1 functions as a so-called GAP (GTPase activating protein) for Menin (Yaguchi *et al.*, 2002). No function has yet been established for the GTPase activity of Menin.

1.3 Menin as a regulator of transcription

1.3.1 Menin interacting proteins

The absence of any recognisable domains in Menin has prompted many researchers to look for Menin interacting proteins in the hope that they would provide some clues to the function of Menin. Several factors have been identified through yeast two hybrid screening or immunoprecipitations and sequencing of Menin containing complexes. In agreement with the nuclear localisation of Menin, all of the Menin interacting proteins except for Vimentin and GFAP can translocate to the nucleus.

As of April 2004 the unabridged list of interaction partners is:

Gene	**type**	**Ref.**
JunD	Transcription factor	(Agarwal *et al.*, 1999)
Nm23H1	Multifunction	(Ohkura *et al.*, 2001)
NF-κB	Transcription factor	(Heppner *et al.*, 2001)
Smad3	Transcription factor	(Kaji *et al.*, 2001)
Smad1/Smad5	Transcription factor	(Sowa *et al.*, 2003)
Pem	Transcription factor	(Lemmens *et al.*, 2001)
GFAP	Structural	(Lopez-Egido *et al.*, 2002)
Vimentin	Structural	(Lopez-Egido *et al.*, 2002)
Replication Protein A	DNA replication	(Sukhodolets *et al.*, 2003)
FANCD2	DNA repair	(Jin *et al.*, 2003)
Myosin II-A	Structural	(Obungu *et al.*, 2003)
mSin3A	Transcriptional Co-repressor	(Kim *et al.*, 2003)
Mll2 complex	Histone Methylase	(Hughes *et al.*, 2004)
Mll complex	Histone Methylase	(Yokoyama *et al.*, 2004)

From the first Menin interaction partners to be identified (JunD, NF-κB, Smad3 and Pem), a picture emerged of Menin as a regulator of gene expression. This notion has been strengthened by the subsequent identification of mSin3a, Mll and Mll2 as Menin interacting proteins. Menin is not believed to interact with DNA directly, but rather to regulate transcription by binding to specific transcription factors. I will in the following discuss the evidence that Menin is involved in transcriptional control by discussing three families of

transcription factors, that have be shown to interact with Menin. I will also discuss the transcriptional corepresser mSin3A and the Histone methylases Mll and Mll2, as these proteins may be involved in mediating the effect of Menin on transcription. Finally I will discuss the genes whose expression has been published to be modified by Menin.

1.3.2 Menin and JunD

JunD was the first Menin interacting protein to be identified. JunD was initially isolated in a yeast two hybrid screen with Menin as bait, and the interaction was subsequently confirmed by immunoprecipitation and pull down experiments using *in vitro* translated protein (Agarwal *et al.*, 1999). JunD is a member of the Jun family of proteins. In mammals, two other Jun proteins exist, c-Jun the founding member (Angel *et al.*, 1988) and JunB. The Jun proteins can form homodimers or heterodimers with the Fos family of proteins or the ATF proteins (Angel *et al.*, 1991). These dimers make up the transcription factor AP-1 that binds to the TPA response element (TRE) TGA(C/G)TCA. AP-1, consisting of c-Jun or JunB, has been shown to have growth promoting activity in most tissues (Pfarr *et al.*, 1994). This proliferative effect of c-Jun and JunB is caused both by the direct upregulation of genes required for tissue proliferation and indirectly by an inhibitory association of the Jun proteins with transcription factors that stimulate differentiation, such as the Glucocorticoid receptor (Schule *et al.*, 1990), Estrogen and Vitamin D receptor (Doucas *et al.*, 1991)(Schule *et al.*, 1990). Conversely, *JunD* appears to be expressed in differentiated and postmitotic cells (Pfarr *et al.*, 1994) and *JunD* has been shown to be able to inhibit Ras mediated transformation of NIH3T3 fibroblasts whereas c-Jun supports transformation (Pfarr *et al.*, 1994).

The binding of Menin to JunD has been reported to repress the transcriptional activity of JunD, both in the context of the AP-1 complex and when JunD was fused to the Gal4 DNA binding domain (Agarwal *et al.*, 1999). Given the anti-proliferative effect of JunD, this observation makes little sense in the context of the tumour-suppressor activity of Menin. This apparent paradox was to some extent solved when Agarwal and co-workers subsequently showed that JunD can promote transformation in *Men1* deficient immortalised fibroblasts whereas JunD expression in *Men1* expressing fibroblast had a negative effect on growth (Agarwal *et al.*, 2003). In this cell line, Menin would thus appear to change JunD from a growth promoter to a growth suppressor.

The activity of the Jun family of transcription factors is regulated on a post-transcriptional level through phosphorylation by the Jnk kinases. Jun phosphorylation may regulate interaction with transcriptional cofactors such as CBP/p300 (Davis, 2000).
The mechanism by which Menin exerts its effect on JunD is under debate. In one report it was suggested that Menin prevents JunD and c-Jun phosphorylation by Jnk as well as JunD and Elk1 phosphorylation by Erk2 (Gallo *et al.*, 2002) whereas another study showed that Menin can repress Ap-1 transcriptional activity without affecting the phosphorylation state of the complex (Yumita *et al.*, 2003). Both groups agreed that Menin can repress transcriptional activation of the *c-Fos* gene (Yumita *et al.*, 2003)(Gallo *et al.*, 2002).
Menin mediated suppression of JunD driven transcription can be inhibited by trichostatin A, a Histone deacetylase inhibitor (Gobl *et al.*, 1999), suggesting that Menin may recruit Histone deacetylases to JunD. Histone acetylation is generally believed to loosen the chromatin structure and facilitate transcription. Histone acetylation is carried out by 14 mammalian Histone acetyl transferases (HATs) such as CBP and p300. Conversely, Histone deacetylation is believed to repress transcription. Nine mammalian Histone deacetylases (HDAC) have been characterised (Marks *et al.*, 2001). Both HATs and HDACs associate with the chromatin through transcription factors. The recent finding that Menin binds to the HDAC containing mSin3A complex and that this complex associates with JunD suggests one mechanism through which Menin can modify the activity of the transcription factors it binds.

1.3.3 mSin3A and Menin

In vitro translated Menin can immunoprecipitate mSin3A. Furthermore, Menin can immunoprecipitate mSin3A from Jurkat cells. mSin3A and mSin3B are the mammalian homologues of the yeast transcriptional co-repressor Sin3p (Ayer *et al.*, 1995)(Schreiber-Agus *et al.*, 1995). mSin3A is widely expressed and its transcript is found in all tissues examined (Halleck *et al.*, 1995). mSin3A was originally identified as a transcriptional co-repressor for the MAD transcriptional repressors. MAD inhibits the function of c-Myc by binding to the Myc binding partner Max (Ayer *et al.*, 1995)(Schreiber-Agus *et al.*, 1995). mSin3A binds to a so-called SID (Sin Interaction Domain) domain, which is found in all MAD proteins (Schreiber-Agus *et al.*, 1995). The binding of mSin3A to transcription factors recruits a multi-protein repression complex to the promoter. This complex contains HDAC1 (Hassig *et al.*, 1997) and HDAC2 (Laherty *et al.*, 1997). The Histone deactetylase (HDAC) activity is necessary for transcriptional repression (Hassig *et al.*, 1997). mSin3A has been shown to be

involved in transcriptional repression mediated by several transcription factors apart from MAD, among these are p53 (Murphy *et al.*, 1999) and Pit-1 (Xu *et al.*, 1998).

Menin can also immunoprecipitate deacetylase activity and HDAC1 and HDAC2, which are part of the mSin3A transcriptional repression complex. The mSin3A interaction domain of Menin was mapped to amino acids 295-450. This domain contains a putative SID - a 16 amino acid domain, which may form an amphiphatic helix. These 16 amino acids of Menin can repress transcription when fused to a Gal4-DNA binding domain. Moreover mutation of two residues in the putative SID, is sufficient to reduce repression of JunD by Menin (Kim *et al.*, 2003). The interaction of Menin with mSin3A may thus provide a mechanism for Menin mediated transcriptional repression of JunD. Menin has been shown to function as a transcriptional repressor for other transcription factors than JunD. These transcription factors are the NF-κB family of transcription factors.

1.3.4 Menin and NF-κB

Menin can co-immunoprecipitate NF-κB1 (p50), NF-κB2 (p52) and RelA from 293 cell extracts. Furthermore purified Menin binds recombinant NF-κB1 (p50), NF-κB2 (p52) and RelA (Heppner *et al.*, 2001).

RelA (p65), NF-κB1 (p50), NF-κB2 (p52) are members of the NF–κB family of proteins that in mammals consists of five structurally and functionally related proteins. NF-kB binds to DNA as dimers and the NF-κB family members can combine to form all combinations of homo and heterodimers. p50, p52 dimers lack a transactivation domain and are believed to function as transcriptional suppressors. All the family members contain a Rel homology domain that is responsible for both DNA binding and dimerisation (Ghosh *et al.*, 2002). Recombinant GST fusions of 40 amino acids of the Rel homology domains from NF-κB1, NF-κB2 and RelA can pull down purified Menin. Conversely, deletion of this domain from the NF-kB family members abolished the interaction, suggesting that this domain is responsible for the interaction between NF-κB and Menin. (Heppner *et al.*, 2001).

In unstimulated cells, NF-κB dimers are cytosolic, being bound to members of the I-κB family of proteins. Extra-cellular signals, which include TNFα, CD40L, Interleukin-1 and lipopolysaccharide (LPS) leads to the activation of IKK kinase that phosphorylates I-κB, which is then ubiquitinated and targeted for degradation by the proteasome. The released NF-κB translocates to the nucleus to regulate transcription (Ghosh *et al.*, 2002)(Karin *et al.*,

2002). NF-κB recognises the so-called κB site GGGRNNYYCC, where N is any base, R is Purine and Y is Pyrimidine (Kucharczak *et al.*, 2003).

In cell culture experiments Menin overexpression can block RelA mediated transcription of a reporter plasmid in Cos7 cells, HeLa cells and Ntera-2, a human embryonic carcinoma cell line. Furthermore, overexpression of Menin can reduce phorbol-12-myristate-13-acetate (PMA) induced transcription from a κB site driven reporter in HeLa cells (Heppner *et al.*, 2001).

The inhibition of RelA must be subsequent to RelA translocation to the nucleus since Menin overexpression did not affect the subcellular localisation of RelA thus suggesting that Menin affects the interaction of NF-κB with transcriptional cofactors (Heppner *et al.*, 2001).

NF-κB has been shown to regulate many genes involved in control of proliferation and apoptosis. These genes include *CyclinD1* (Hinz *et al.*, 1999), *c-Myc* (Duyao *et al.*, 1990), *IL-2* (Verweij *et al.*, 1991), *GM-CSF* (Himes *et al.*, 1993). *cIAP* (Wang *et al.*, 2003), *Bfl-1/A1, BCL-*X_L (Lee *et al.*, 1999), *c-Flip* (Micheau *et al.*, 2001). Accordingly, disruption of *RelA* leads to early embryonic lethality associated with massive TNF-α induced apoptosis of the liver (Beg *et al.*, 1995). Considering the nature of these genes it is not surprising that NF-κB has been implicated in cancer. The product of the oncogene *v-Rel* is a constitutively active transcription factor derived from c-Rel (Karin *et al.*, 2002). Other oncoviruses express genes that constitutively activate the NF-κB pathway such as TAX from the HTLV T-cell leukaemia virus (Karin *et al.*, 2002). Increased NF-κB expression has been found in leukaemias and lymphomas which are both caused by uncontrolled growth of blood cells. In these cases, chromosomal rearrangements of the *c-REL* and *NF-κB2* loci, which lead to their overexpression, have been found. NF-κB may also play a role in carcinomas, especially breast cancer, gastrointestinal cancers and colorectal cancers. Most breast cancers and some colorectal cancers are associated with high NF-κB activity (Karin *et al.*, 2002).

Many of the NF-κB regulated genes could potentially be involved in control of growth and apoptosis in the pituitary gland and other endocrine glands affected by MEN1. Specifically *c-Myc,* that when overexpressed induces pancreatic islets tumours in animal models (Pelengaris *et al.*, 2002), and *CYCLIN D1*. *CYCLIN D1* is also known as *PRAD1* (parathyroid adenoma 1) because it was identified at the breakpoint of a chromosomal rearrangement found in parathyroid gland adenomas. These rearrangement leads to overexpression of *CYCLIN D1* and the gene has subsequently been found overexpressed in 18 percent of human parathyroid gland adenomas (Carling, 2001).

Both the effect of Menin on JunD and NF-κB mediated transcription and the interaction of Menin with mSin3A would suggest that Menin functions as a transcriptional repressor. Moreover the similarity between the effect of Menin binding to JunD and RelA suggests a common mechanism, whereby Menin mediates recruitment of mSin3A to the trancription factors. There is, however, also evidence that Menin can function as a transcriptional activator when interacting with other transcription factors. This is the case with the Smad family of proteins.

1.3.5 Smad transcription factors and Menin

Smad3 but not Smad2 or Smad4 can interact with Menin as demonstrated by the co-immunoprecipitation of Menin by Smad3 from COS cells ectopically expressing the Smad transcription factors and Menin (Kaji *et al.*, 2001). Similarly Smad1 and Smad5 can co-immunoprecipitate with Menin from COS7 cells (Sowa *et al.*, 2003).

Smad transcription factors are the main intercellular mediators of signalling by the TGF-β superfamily. The TGF-β superfamily consists of TGF-β1, TGF-β2, TGF-β3, the Bone morphogenic proteins (BMPs), and Activins (Derynck *et al.*, 2003). Upon ligand binding to the TGF-β superfamily of receptor serine/threonine kinases, the Smads are recruited to the receptor and activated by phosphorylation. Smad2 and Smad3 are recruited by TGF-β receptors, whereas Smad1, Smad5, and Smad8 bind to receptors activated by BMPs and Activins. Smad4 functions as a common Smad that can interact with the other Smads (Derynck *et al.*, 2003). Phosphorylated Smads homodimerise and subsequently bind to Smad4. The resulting trimer then translocates to the nucleus and regulates transcription.

Transfection of an antisense *Men1* construct into the rat pituitary gland cell line GH4-C1 inhibits TGF-β mediated growth suppression as well as TGF-β1 induced transcription from the *Pai-1* (Plasminogen activator inhibitor type 1) promoter (Kaji *et al.*, 2001). Furthermore, depletion of Menin also inhibits TGF-β mediated growth repression in a parathyroid cell line and TGF-β mediated reduction of Parathyroid Hormone expression (Sowa *et al.*, 2004). Also TGF-β induced growth arrest in the rat duodenal cell line IEC-17 is blocked by Menin depletion (Ratineau *et al.*, 2004).

Depletion of Menin by antisense transfection in the mesenchymal stem cell lines 10T1/2, ST2 and PA6 inhibits BMP2 induced differentiation into the osteoblast lineage and BMP mediated activation of a reporter shown to be Smad 1 and Smad5 dependent (Sowa *et al.*, 2003).

It would thus appear that Menin not only binds to Smad1, Smad3 and Smad5 but also that the binding of Menin to these transcription factors is required for their transcriptional activity.

The mechanism by which Menin regulates the transcriptional activity of the Smad transcription factors has not been firmly established. Smad trimer formation and the translocation of Smad3 complexes from the cytosol into the nucleus was not affected by the loss of Menin, however in bandshift assays using cell extracts, Smad3 was unable to bind to DNA when Menin levels in the extracts had been reduced by antisense *Men1* (Kaji *et al.*, 2001). However, the binding of Smad3 to Menin was mediated by the MH2 transactivation domain of Smad3 and not by the DNA binding domain MH1 (Kaji *et al.*, 2001).

Smad trimers bind to their cognate binding site SBE (CAGAC) with an affinity that is 100 fold lower than that of high affinity transcription factor DNA complexes. Smads are thus normally recruited to a specific promoter through complex formation with other transcription factors such as AP-1, Sp1, NF-κB, FAST, OAZ and TFE3 (Derynck *et al.*, 2003)(Massague *et al.*, 2000). Given that Smad complexes often require association with more specific transcription factors to bind DNA, it is tempting to speculate that Menin exerts its function by mediating these interactions rather than directly influencing the interaction of Smad3 with DNA. In this case the activity of Menin would be dependent on the context of the promoter. This model would also be in agreement with the binding of Menin to the transactivation domain of Smad3. There is no evidence that Menin itself can function as a transcriptional activator and until now no transcriptional coactivator has been shown to interact with Menin.

If Menin is required for Smad transcriptional activity then loss of function of Smad1, Smad3 and Smad5 could possibly mimic MEN1. Homozygous *Smad3* null mice are viable but show reduced growth and fertility. Importantly, *Smad3* homozygous null animals develop colorectal cancers with 100% penetrance by the age of 24 weeks. Unlike most other tumours of the colon, the Smad3 null tumours were not associated with loss of APC (Zhu *et al.*, 1998). Smad3 null animals also show accelerated wound healing and an impaired inflammatory response (Ashcroft *et al.*, 1999). Inactivation of Smad3 by the oncogene Evi-1 has been implicated in leukaemia (Kurokawa *et al.*, 1998). Smad3 has also been shown to interact with the products of the oncogenes c-Ski and c-SnoN. The binding of these oncoproteins to the Smad complex represses transcriptional activation, possibly through recruitment of the transcriptional repressor N-CoR and mSin3A (Luo *et al.*, 1999)(Stroschein *et al.*, 1999). Homozygous deletion of *Smad1* or Smad5 causes embryonic lethality at embryonic day 9.5 and 11.5 respectively. Mice heterozygous for *Smad1* or *Smad5* deletion are not prone to developing cancers and they are thus not functioning as tumour suppressors in the mouse

(Tremblay *et al.*, 2001)(Lechleider *et al.*, 2001)(Yang *et al.*, 1999)(Chang *et al.*, 1999; Chang *et al.*, 2000).

1.3.6 TGF-β signalling and growth control

TGF-β can both induce and repress its target genes. Activation is mediated by Smad2 and Smad3 together with Smad4, through binding to SBE in complex with specific transcription factors, whereas repression may be mediated by other factors acting through the TGF-β inhibitory element (TIE), GNNTTGGtGa (Kerr *et al.*, 1990). Recent data suggests that Smad3 can mediate TGF-β repression (Frederick *et al.*, 2004). Depletion of Menin does not only block TGF-β1 induced transcription from the *Pai-1* promoter (Kaji *et al.*, 2001) but also TGF-β repression of Parathyroid Hormone expression (Sowa *et al.*, 2004) suggesting that Menin can regulate both TGF-β mediated transcriptional activation and repression.

TGF-β suppresses proliferation in most tissues by blocking cell cycle progression from G1 (Massague *et al.*, 2000)(Blobe *et al.*, 2000). Accordingly, studies of human cancers suggest that inactivation of TGF-β signalling pathways is an important step in the progression of many cancer types; 100 % of pancreatic tumours and 83 % of colon cancers show mutations of one or more components of this pathway (Blobe *et al.*, 2000).

In the pituitary gland, the effects of TGF-β are more complex. TGF-β1 inhibits proliferation of lactotropes and blocks secretion of Prolactin (Sarkar *et al.*, 1992) and in general TGF-β1 inhibits proliferation of pituitary gland cells possibly through upregulation of *p15Ink4B* (Frost *et al.*, 2001). TGF-β1 is mostly expressed in lactotropes (Hentges *et al.*, 2000). In contrast TGF-β3 is believed to support proliferation of lactotropes in response to Estrogen stimulation (Hentges *et al.*, 2000).

Several well-characterised TGF-β targets are relevant for regulation of growth and tumourigenesis. Most of these are activated by TGF-β and these include *p15Ink4B* (Hannon *et al.*, 1994)(Rich *et al.*, 1999), *p21Cip1* (Datto *et al.*, 1995), *p27Kip1,* (Qian *et al.*, 1996), *c-Jun* (Wong *et al.*, 1999), *Pai1* Dennler *et al.*, 1998),*Vegf* (Renner *et al.*, 2002). A few genes are repressed by TGF-β and these include *c-Myc*, (Frederick *et al.*, 2004), *Cdc25* (Iavarone *et al.*, 1997), and *Transin/Stromelysin* (Kerr *et al.*, 1990).

To what extent these genes are regulated *in vivo* by Menin is not known. But genes like *p15Ink4B*, *p21Cip1* and *p27Kip1*, which all encode cyclin dependent kinase inhibitors involved in mediating growth inhibitory signals impinging on the retinoblastoma protein are

potential gowth regulatory genes in the pituitary gland. As noted previously, mutations to factors in the Rb pathway have been implicated in pituitary gland tumourigenesis. Furthermore, as noted previously, c-Myc overexpression induces pancreatic islets tumours in animal models (Pelengaris *et al.*, 2002).

1.3.7 MLL2 Histone methylation complex and Menin

Menin can co-immunoprecipitate with complexes consisting of MLL2, ASH2, RBBp5, WDR5 and hDPY-30 from HeLa cells. (Hughes *et al.*, 2004) and MLL, ASH2, RBBp5, WDR5 and HCF-2 (Yokoyama *et al.*, 2004). These complexes are the mammalian homologues of the yeast SET1 complex (Roguev *et al.*, 2001). *Set1* is the yeast homologue of the Drosophila *trithorax* gene. In mammals, three *trithorax* homologues *Mll, Mll2* and *Mll3* have been characterised (Djabali *et al.*, 1992)(Huntsman *et al.*, 1999). Both *Mll* and *Mll2* are ubiquitously expressed (FitzGerald *et al.*, 1999).

The trithorax group of proteins are involved in maintenance of transcriptionally active genes, enabling expression patterns to exist even after the expression of the transcription factors, that have established these patterns, has ceased. Although first identified by their involvement in maintaining the transcriptional state of homeotic genes, they are also involved in the regulation of other genes. The trithorax group of genes is large and heterogeneous but their phenotypes in Drosophila are comparable (Francis *et al.*, 2001). The Trithorax family of proteins functions a Histone methyl transferase that can methylate Histone3 on lysine-4 (Roguev *et al.*, 2001), which is thought to activate transcription (Noma *et al.*, 2001).

The Histone methyl transferase activity associated with the complex immunoprecipitated by Menin can methylate Histone3 on lysine-4. Like SET1 in yeast, the protein complex can also interact with RNA polymerase II (Hughes *et al.*, 2004). Point mutants of Menin from human MEN1 patients, cannot co-precipitate with the MLL2 complex nor any Histone methyl transferase activity (Hughes *et al.*, 2004).

Both MLL1 and MLL2 have been implicated in cancer. *MLL* was originally cloned as a gene at the breakpoint in chromosomal rearrangements in acute leukaemia and the chromosomal region of *MLL2* has been found amplified in pancreatic carcinomas and in glioblastoma cell lines (Djabali *et al.*, 1992)(Huntsman *et al.*, 1999). Interestingly upregulation of *Hoxa7* and *Hoxa9* was implicated in the immortalisation process caused by expression of an oncogenic *Mll-Enl* fusion gene in mice (Zeisig *et al.*, 2004).

Mll heterozygous null mice are growth retarded and show a homeotic transformation and changed expression pattern of several hox genes including *Hoxa7* and *Hoxc9*. Homozygous animals are not viable and show no expression of *Hoxa7* and *Hoxc9* (Yu *et al.*, 1995).
Men1 deficient MEFs showed a significant down-regulation of the hox genes *Hoxc6* and *Hoxc8* compared to wildtype MEFs (Hughes *et al.*, 2004). Likewise transfection of *Men1* siRNA into HeLa cells reduced the expression of *Hoxa9* (Yokoyama *et al.*, 2004).
Hox genes are important regulators of patterning during development. In addition control of cell proliferation has been suggested to be an important mechanism through which *Hox* genes regulate patterning in vertebrates (Deboule, 1995). In adults, the expression of *Hox* genes is restricted to stem or progenitor cells of highly proliferating cell populations like those of the hematopoietic system (Sauvageau *et al.*, 1995) and disruption of *Hox* gene expression decreases proliferation of these cell types (Lawrence *et al.*, 1997). Aberrant *Hox* gene expression has mostly been associated with cancers of the hematopoietic system. Furthermore, as Menin appears to be involved in maintaining rather than repressing *Hox* gene expression, a direct involvement of *Hox* genes in MEN1 tumourigenesis seems unlikely. However the interaction of Menin with the Mll proteins does suggest one mechanism through which Menin could mediate transcriptional activation.

1.3.8 Menin regulation of telomerase activity

Men1 was isolated in a genetic screen for proteins that when overexpressed in HeLa and MCF-7 cells, can suppress the expression of the human telomerase protein subunit *hTERT* (Lin *et al.*, 2003). Cell lines expressing GFP from the hTERT promoter were infected with a retrovirus that integrates randomly in the genome and drives overexpression of nearby genes. Clones were isolated that showed reduced GFP expression. Apart from *Men1*, genes involved in the c-Myc and TGF-β pathways were isolated (Lin *et al.*, 2003). Depletion of *Men1* from U2OS cells that normally do not express *hTERT* resulted in upregulation of *hTERT*. The influence of Menin on the expression of hTERT appeared to be mediated by direct binding of Menin to the hTERT promoter as judged by chromatin immunoprecipitations. The transcription factors through which Menin bound the hTERT promoter were not identified (Lin *et al.*, 2003).
In humans, hTERT is not expressed in most somatic tissues. In the absence of telomerase activity, the number of cell divisions of proliferating cells is limited by the shortening of the telomers, which eventually induces proliferative senescence. Without telomerase activity, 60

to 70 cell divisions are possible. In theory, this number should be sufficient for even the biggest tumour to develop. In practise, however, most advanced tumours have gone through successive rounds of apoptosis and clonal expansion that may have cost many cell divisions without any gain in tumour size. 70 cell divisions may thus not be sufficient for most cancers to develop as the replicative potential of the cancer cells eventually may be exhausted in the absence of telomerase activity (Hanahan *et al.*, 2000). Upregulation of *hTERT* is therefore believed to be an important step in human cancer and it is found in up to 90 percent of advanced tumours (Hanahan *et al.*, 2000).

1.3.9 Menin regulated transcription and MEN1

There is overwhelming evidence that Menin functions as a transcriptional regulater. Menin interacts with several transcription factors and can modify their transcriptional activity in cell culture experiments. Interestingly, Menin appears to function as a transcriptional corepressor in the case of JunD and the NF-κB family of transcription factors and as a transcriptional coactivator in the case of the Smad family of proteins. How these different effects of Menin on transcription is regulated is not known. The transcriptional repression of Menin may in part be mediated by the interaction of Menin with the transcriptional repressor mSin3A. Likewise the interaction of Menin with the Mll proteins suggest a mechanism by which Menin can be involved in maintaining patterns of gene expression.

None of the transcription factors that have been published to bind Menin provide a satisfactory model for MEN1 tumourigenesis alone. JunD, Smad3 and NF-κB have all been implicated in growth control or tumourigenesis and many of their direct target genes notably the CDK inhibitors, *c-Myc* and *Cyclin D1*, could potentially be mediators of MEN1 tumourigenesis. However none of these genes would appear to explain the endocrine specific development of tumours. Futhermore none of these genes have been shown to be regulated by Menin *in vitro* or *in vivo*.

Loss of Smad3 does lead to loss of growth control and cancer but it does not affect any of the tissues involved in MEN1. Likewise overexpression of NF-kB has primarily been associated with leukaemeias.

It seems reasonable to assume that the binding of a combination of these transcription factors or other as yet unidentified Menin interacting proteins, to a set of promoters render these promoters Menin responsive. Either, this combination of transcription factors occurs on the critical genes only in the tissues affected by MEN1 or the Menin regulated genes specifically

regulate growth of the endocrine system. Thus none of the published Menin responsive genes appear to fit this role.

Alternatively Menin may interact with and regulate other as yet unidentified proteins that are expressed only in the tissues affected by MEN1, or regulate genes that are relevant only for growth control in the endocrine system.

1.4 Aim of Study.

Although the *Men1* gene has been the subject of intense research since its identification in 1997, the molecular mechanisms and cause of the tumourigenesis in patients suffering from MEN1 is still largely unknown. The expression pattern of *Men1* does not offer any clues to the answer since most tissues that express *Men1* do not develop tumours. The sequence of the protein and the distribution of the human mutations also offers little information, since the protein does not contain any recognisable domains and the mutations are distributed over most of the open reading frame. Menin, the protein encoded by the *Men1* gene, has been shown to interact with several other proteins but none of them suggest any model that would explain the potent tumour suppressor activity of *Men1*, nor the tissue specific development of tumours in the endocrine system, although they do suggest that Menin functions as a transcriptional cofactor. Some transcriptional targets of Menin have been published but none of them appears likely to be the prime cause of tumour formation in the absence of *Men1*.

The ubiquitous expression of *Men1* combined with the tissue specific development of tumours in MEN1 suggested to us that *Men1* could regulate a pathway common to most endocrine cells. It would therefore be interesting to establish a mouse model that would allows us to analyse the molecular mechanism and possibly identify genes that may be deregulated in *Men1* deficient cells.

Men1 functions as a classical tumour suppressor as all affected individuals inherit one non-functional allele and subsequent loss of the second allele induces tumourigenesis. Therefore a heterozygous mouse model would be a relevant model of MEN1. However, the stochastic nature of the mechanism that leads to the loss of the wild type tumour suppressor allele meant that it would be impossible to predict when the second *Men1* allele would be lost before the appearance of macroscopic adenomas. This made a heterozygous model problematic for certain types of molecular analysis such as gene expression profiling using microarray analysis, which requires a well defined genetic system.

The published early and widespread expression of *Men1* during mouse development suggested to us that it would be likely that a homozygous deletion of *Men1* in the entire mouse would lead to an early lethal phenotype.

In the light of this, I decided to establish a mouse model of the MEN1 syndrome that would allow me to investigate the molecular changes associated with homozygous loss of *Men1* in a well defined system and at an age where secondary genetic changes would be unlikely. To this end I wanted to generate a conditional knockout model that would allow homozygous

deletion of *Men1* in a significant part of the pituitary gland, a tissue relevant for the study of MEN1

Although the published Menin interacting proteins do link Menin to the regulation of transcription, none of them suggest a model that could explain the tissue specific development of tumours in MEN1. To gain further insights into the molecular function of Menin, I also wanted to undertake a yeast two hybrid screening for novel Menin interacting proteins using a pituitary cDNA library.

2 Results

2.1 Generation of Men1 deficient pituitary glands

2.1.1 Construction of the *Men1* conditional knockout vector

To investigate the role of *Men1* in tumourigenesis, I wanted to generate a mouse model of the MEN1 disease. As mentioned, the published widespread expression pattern of *Men1* (Guru *et al*., 1999) in the mouse suggested to us that the biological function of *Men1* may not be restricted to the endocrine tissue. I thus reasoned that *Men1* may be required for the development of the mouse and decided to pursue a conditional knockout strategy that would enable us to delete *Men1* only in specific tissues.

The conditional knock out approach was based on the bacterial Cre recombinase that recognises a specific 34 bp palindromic sequence called a LoxP site (Hoess *et al*., 1982). Cre recombines out any sequence between a direct repeat of LoxP sites and inverts any sequence between inverted repeats of LoxP. An allele of a gene with inserted LoxP sites is called a floxed allele.

I screened a chromosomal mouse BAC library with a *Men1* exon 2 probe and identified 4 BAC clones that contained the *Men1* genomic region. The genomic organisation of *Men1* has been previously published (Guru *et al*., 1999). *Men1* is encoded by 10 exons. The open reading frame begins in exon 2 and terminates in exon 10. Taking advantage of an HpaI site in intron 2 and a BstEII site in intron 6, I generated a *Men1* conditional knockout vector with LoxP sites in these two introns as outlined in **Figure 2.1.1 A-B** which should allow Cre mediated deletion of exons 3 to 6. The knockout vector contained a positive selection cassette encoding neomycin resistance flanked by Frt sites, a negative selection marker encoding diphtheria toxin, to select against random integration events, a 3498 bp 5' arm and a 2869 bp 3' arm, to enable homologous recombination. The Frt sites flanking the positive selection marker should enable subsequent deletion of the cassette leaving only one Frt site and two LoxP sites, restoring the integrity of the *Men1* locus.

Inactivating mutations of Menin have been reported to be distributed over the entire open reading frame of the protein with no particular hotspots or obvious correlation between mutation and phenotype (Verges *et al*., 2002). I therefore reasoned that deletion of exons 3 to 6, which encode amino acids 150 to 304 of Menin would constitute a null allele. Furthermore possible splicing of exon 2 to exon 7 was predicted to cause a shift in the reading frame.

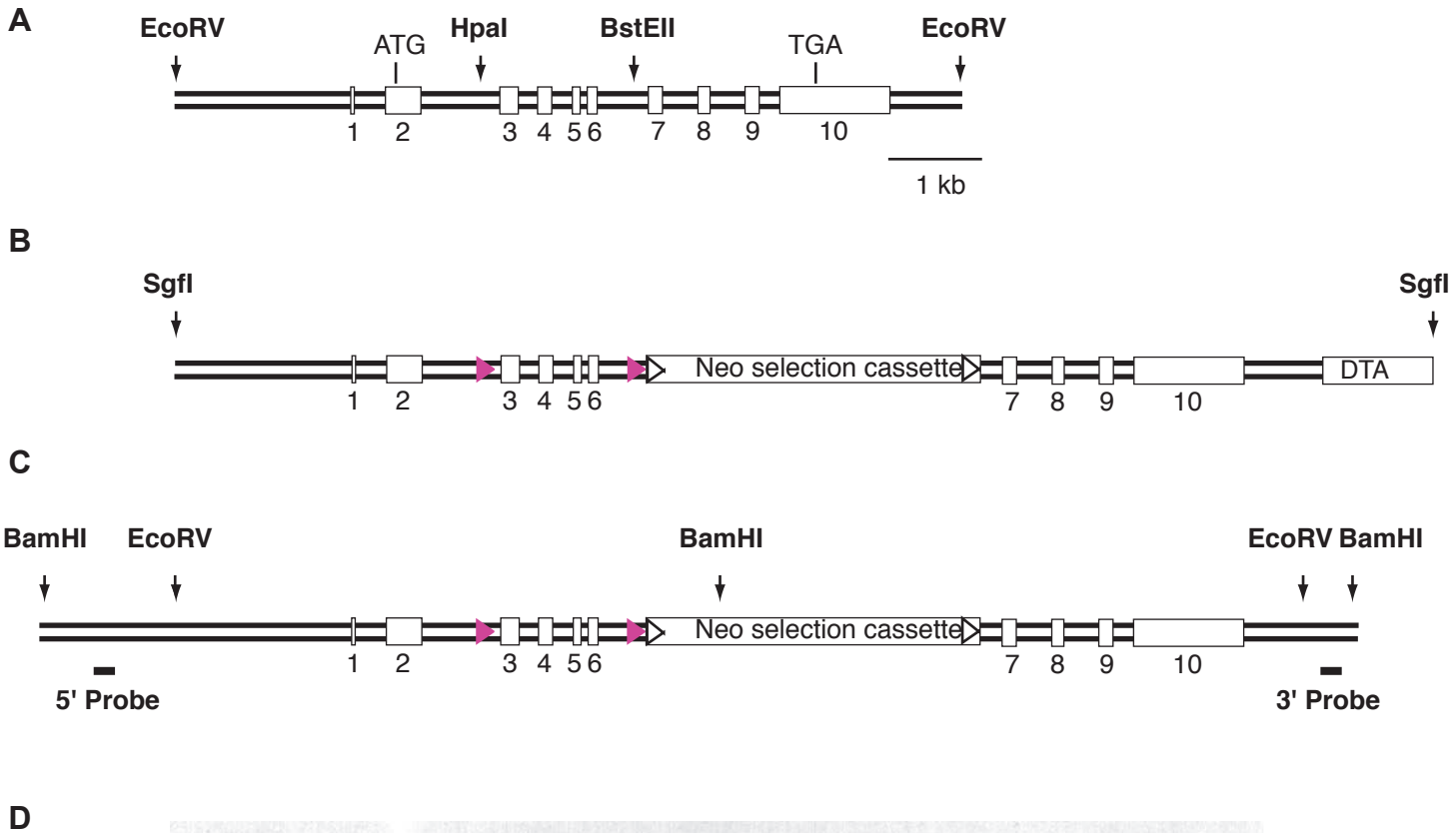

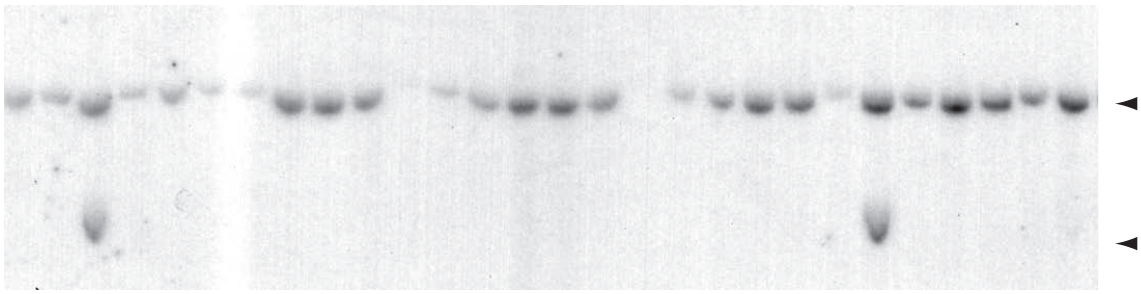

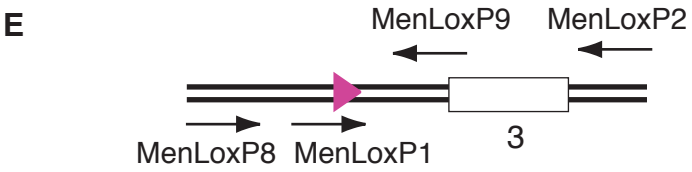

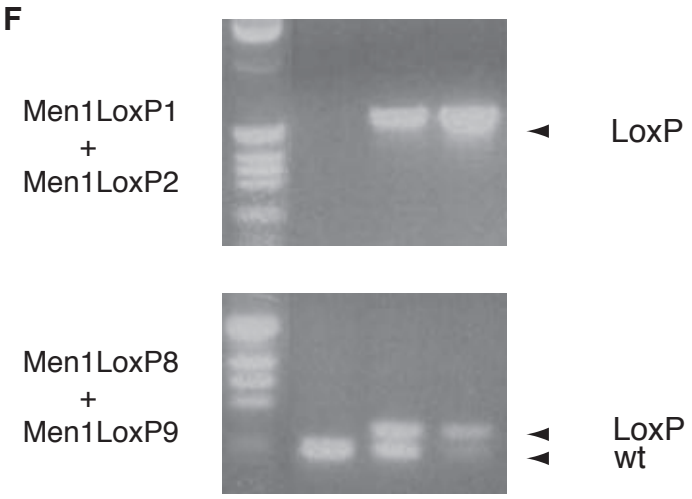

Figure 2.1.1 Generation of conditional *Men1* knockout allele. A Genomic organisation of the *Men1* locus. Restriction sites are indicated with an arrow. The start of the open reading frame is indicated with ATG and the end with TGA. **B** Outline of the *Men1* knock out vector. LoxP sites are indicated with red triangles and Frt sites with open triangles. Sgf1 sites for linealisation of the vector are indicated with arrows. **C** Southern blot strategy. Restriction sites are indicated with arrows. The external probes are indicated with thick black lines. **D** Southern blot with BamHI digested ES-cell DNA. The blot was probed with the 3'probe. **E** PCR strategy for screening for 5' LoxP site. **F** PCR screening for 5' LoxP site. The same ES-cell DNA samples were used for both PCR reactions. The primers used and the identity of the bands are indicated. PCR reactions were analysed on a 2 % agarose gel.

2.1.2 Establishment of *Men1*$^{LoxP\text{-}Neo}$ allele

The knockout vector was electroporated into IB10 ES-cells. G418 resistant clones, which had incorporated the knockout vector, were picked and cultured. To screen the ES-cell clones for homologous recombination at the *Men1* locus, a Southern blot strategy was devised based on a 3' external probe as shown in **Figure 2.1.1 C and D**. A total of 186 ES cell colonies were screened and 23 were positive for homologous recombination at the *Men1* locus.

Homologous recombination to integrate the positive selection marker requires two cross over events; one in the 3' arm and one 5' of the selection cassette. However, since a cross over event between the two LoxP sites would lead to loss of the 5' most LoxP site, it was important to screen the ES-cell clones for the presence of this site. A 96 well plate was thawed and the positive clones were expanded. DNA was extracted and used for Southern blot analysis to confirm the identity of the clones (not shown), and for a PCR based screening for the 5' LoxP site. Two sets of primers were used as shown in **Figure 2.1.1 E**; Men1LoxP1 and Men1LoxP2, which should give rise to a band only in the presence of the 5' LoxP site; and Men1LoxP8 and Men1LoxP9 which should give rise to a slow migrating band as well as a wildtype band if the 5' LoxP site was present. Two positive clones were identified **Figure 2.1.1 F**.

The positive clones were injected into blastocysts by the EMBL transgenic facility and chimeric animals were born with a male to female ratio of 5 to 1 and 12 to 4 for the two clones respectively, reflecting the male origin of the IB10 ES-cells. Male chimeras that were highly chimeric for the ES-cell clone, which is reflected by an a high agouti to black coat colour ratio, were bred to Bl-6 wild type females and their progeny tested for the presence of the 5' LoxP site as in **Figure 1 E and F**. Germline transmission was observed (data not shown). This *Men1* allele was called *Men1*$^{LoxP\text{-}Neo}$ to specify the presence of the positive selection cassette encoding neo resistance.

When *Men1*$^{LoxP\text{-}Neo/wt}$ mice were inter crossed, no homozygous animals were found (40 animals tested), suggesting that the presence of the positive selection disrupted the function of *Men1*, and that *Men1* is essential for development.

2.1.3 FlpE and Cre mediated recombination

The presence of both LoxP sites and Frt sites in the *Men1*$^{LoxP\text{-}Neo}$ allele allows for the generation of several different *Men1* alleles. The names and structures of the different *Men1*

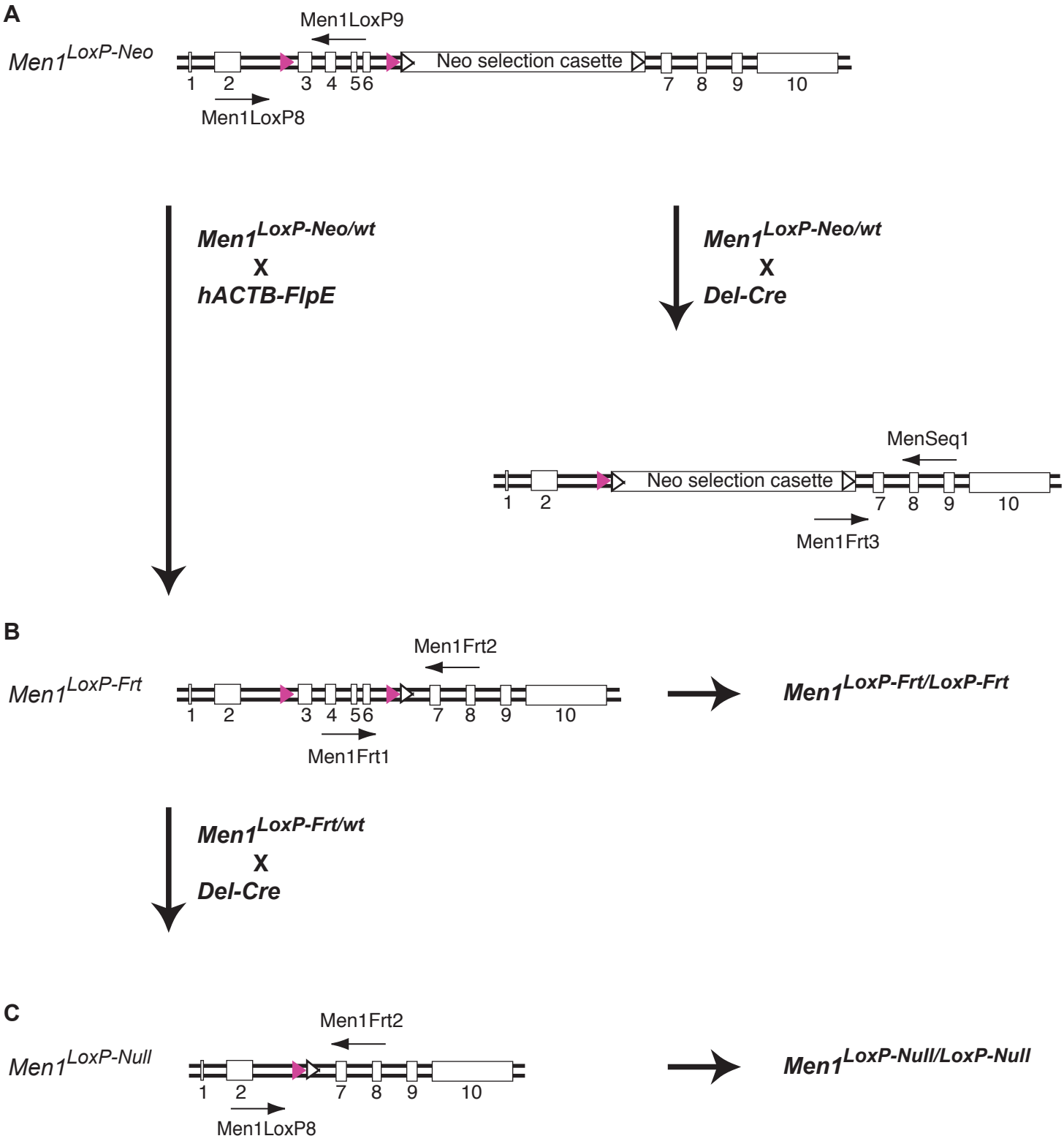

Figure 2.1.2 *Men1*^{LoxP} alleles. Vertical thick black arrows indicate crosses to either Cre of Flp expressing mice as indicated. Horizontal thick black arrows indicate crosses between the same genotypes. Names in bold are genotypes. On all alleles, primer pairs used for genotyping are indicated. **A** Genomic organisation of the *Men1*$^{LoxP\text{-}Neo}$ allele. **B** Genomic organisation of the *Men1*$^{LoxP\text{-}Frt}$ allele.**C** Genomic organisation of the *Men1*$^{LoxP\text{-}Null}$ allele.

alleles and the breeding strategy used to generate them are shown on **Figure 2.1.2**. **Figure 2.1.2** also shows the PCR strategy that was used to genotype the animals. *Men1*$^{LoxP\text{-}Neo}$ males were bred to hACTP-FlpE females to excise the positive selection cassette and restore the function of the floxed allele. hACTP-FlpE mice express the FlpE recombinase throughout the body and importantly also in the germline cells (Rodriguez *et al.*, 2000). The pups were genotyped by PCR as above using the primers Men1LoxP8 and Men1LoxP9 **(Figure 2.1.2 A)**. As **Figure 2.1.3A Left** shows, PCR doublets were observed indicating the presence of the *Men1*$^{LoxP\text{-}Neo}$ allele.

I next wanted to establish if FlpE could mediate excision of the positive selection cassette. **Figure 2.1.3 D** shows the presence of the FlpE allele in the *Men1*$^{LoxP\text{-}Neo}$ positive clones. **Figure 2.1.3 B** shows a PCR with the primers Men1Frt1 and Men1Frt2. It is only in the presence of FlpE that a second, slower migrating PCR band should be seen. This slow migrating band is the product of a PCR over one LoxP site and one Frt site. The fast migrating band is the wildtype band present in all mice. In the absence of FlpE, only the wildtype band can be seen as the 3.500 bp positive selection cassette is too big to be bridged by a standard PCR reaction. Although it appeared that FlpE mediated recombination efficiently deleted the positive selection cassette, subsequent breedings showed that only about 30 percent of the *Men1* alleles passed on through the germline from the *Men1*$^{LoxP\text{-}Neo}$*/FlpE* animals had indeed deleted the cassette.

To test the functionality of the LoxP sites, *Men1*$^{LoxP\text{-}Neo}$ mice were crossed with Deleter Cre animals that express Cre in most somatic cells as well as in the germline (Schwenk *et al.*, 1995). **Figure 2.1.3 A Right** shows the presence of the 5' LoxP site as judged by the primers Men1LoxP8 and Men1LoxP9. However if the Cre recombination is very efficient, this PCR should not generate a doublet as the Men1LoxP9 primer anneals to a sequence between the two LoxP sites. The DNAs that tested negative for the 5' LoxP site were tested for the presence of *Cre* and for the presence of the 3' Frt site. **Figure 2.1.3 E** shows the presence of the *Cre* allele and **Figure 2.1.3 C** the presence of the 3' Frt site using the primers Men1Frt3 and Menseq1. This PCR should indicate the presence of the *Men1*$^{LoxP\text{-}Neo}$ allele and be unaffected by Cre mediated recombination. Samples 8 and 10 show the presence of *Men1*$^{LoxP\text{-}Neo}$ and of *Cre*, but are negative for the presence of the sequence between the LoxP sites (PCR Men1LoxP8 and Men1LoxP9) suggesting that the LoxP sites are capable of Cre mediated recombination. Samples 7 and 8 are positive for *Cre* but negative for the presence of the 3' Frt site suggesting that these animals only carry the wildtype allele.

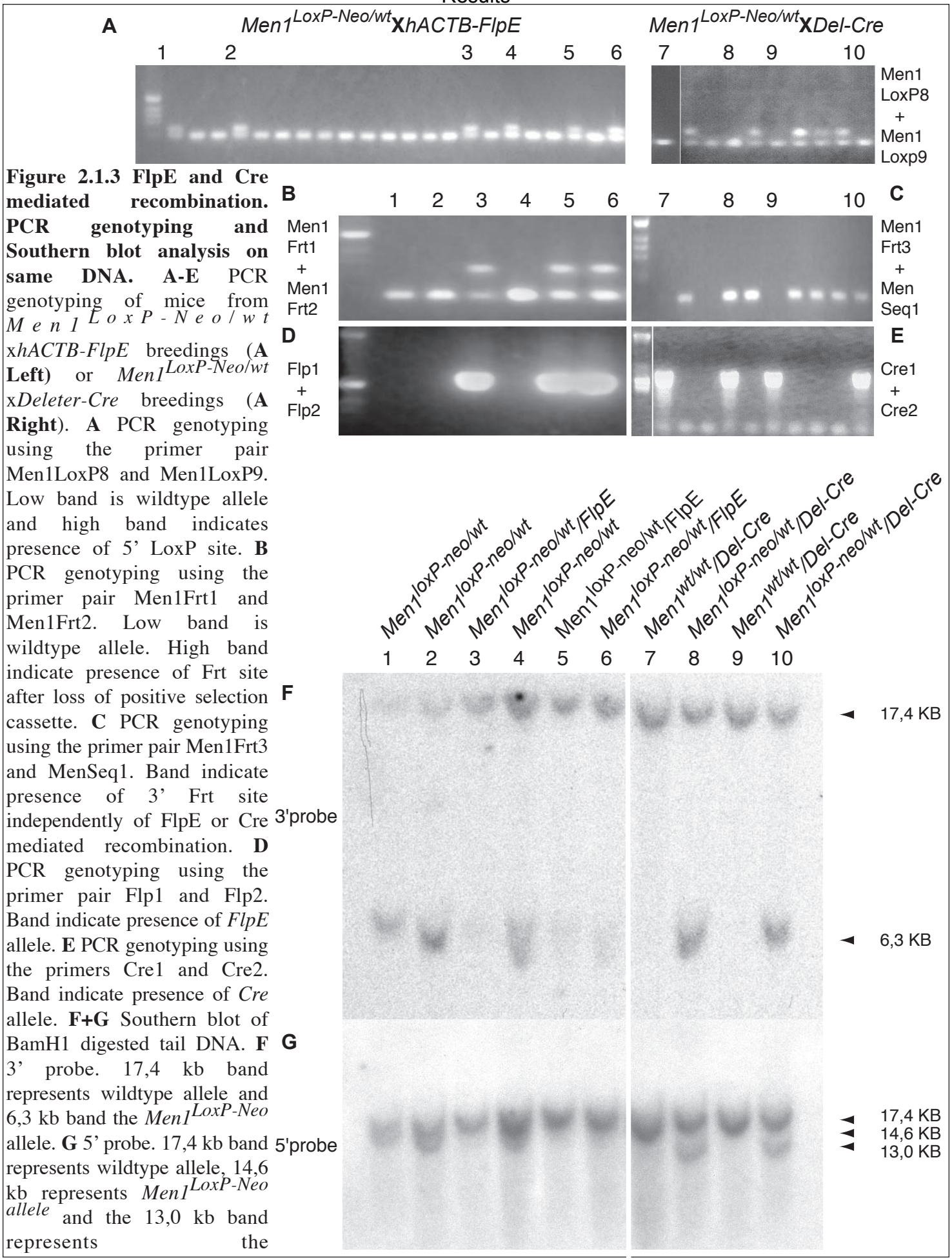

Figure 2.1.3 FlpE and Cre mediated recombination. PCR genotyping and Southern blot analysis on same DNA. A-E PCR genotyping of mice from *Men1*$^{LoxP\text{-}Neo/wt}$ x*hACTB-FlpE* breedings (**A Left)** or *Men1*$^{LoxP\text{-}Neo/wt}$ x*Deleter-Cre* breedings (**A Right**). **A** PCR genotyping using the primer pair Men1LoxP8 and Men1LoxP9. Low band is wildtype allele and high band indicates presence of 5' LoxP site. **B** PCR genotyping using the primer pair Men1Frt1 and Men1Frt2. Low band is wildtype allele. High band indicate presence of Frt site after loss of positive selection cassette. **C** PCR genotyping using the primer pair Men1Frt3 and MenSeq1. Band indicate presence of 3' Frt site independently of FlpE or Cre mediated recombination. **D** PCR genotyping using the primer pair Flp1 and Flp2. Band indicate presence of *FlpE* allele. **E** PCR genotyping using the primers Cre1 and Cre2. Band indicate presence of *Cre* allele. **F+G** Southern blot of BamH1 digested tail DNA. **F** 3' probe. 17,4 kb band represents wildtype allele and 6,3 kb band the *Men1*$^{LoxP\text{-}Neo}$ allele. **G** 5' probe. 17,4 kb band represents wildtype allele, 14,6 kb represents *Men1*$^{LoxP\text{-}Neo\ allele}$ and the 13,0 kb band represents the

To verify the PCR results, Southern blot analysis was done with the same DNA digested with BamHI, using both a 3' and a 5' probe. **Figure 2.1.3 F** shows a Southern blot, which was probed with the same 3' probe that was used in the ES-cell screening. *Men1*$^{LoxP\text{-}Neo}$ gives rise to a 6,3 kb band (lanes 1, 2, 4, 8 and 10), that is almost completely gone in the *Men1*$^{LoxP\text{-}Neo}$*, FlpE* DNA (lanes 3, 5 and 6). The Cre mediated deletion can not be seen with the 3' probe. **Figure 2.1.3 G** shows the Southern blot probed with the 5'probe. The *Men1*$^{LoxP\text{-}Neo}$ gives rise to a band of 14,6 kb compared to the wildtype band of 17,4 (lanes 1, 2 and 4). The *Men1*$^{LoxP\text{-}Neo}$ shifts down 1577 bp upon Cre mediated recombination (lanes 8 and 10).
In conclusion, both FlpE mediated deletion of the positive selection cassette and Cre mediated deletion of exons 3-6 is efficient.

2.1.4 Viability of *Men1*$^{LoxP\text{-}Frt/Frt}$ mice and absence of Menin in *Men1*$^{LoxP\text{-}Null/Null}$ embryos

Men1$^{LoxP\text{-}Neo/wt}$*/FlpE* animals were bred to wildtype Bl-6 animals and pups that had lost both the positive selection marker as well as *FlpE*, were identified. The allele carried by these mice was called the *Men1*$^{LoxP\text{-}Frt}$ (**Figure 2.1.2 B**). *Men1*$^{LoxP\text{-}Frt/wt}$ mice were interbred and the offspring tested for viable mice, homozygous for the floxed *Men1* allele. As **Figure 2.1.4 A** shows, the homozygous animals (only slow migrating band) were found in the expected mendelian ratio (1:2:1), and I thus concluded that the insertion of the two LoxP sites in the *Men1* locus did not interfere with the normal function of the gene.
Men1$^{LoxP\text{-}Frt/wt}$ were also crossed to *Deleter-Cre* animals to generate a null allele without the positive selection cassette. **Figure 2.1.4 B+C** shows a PCR done using *Cre* primers and the primers Men1LoxP8 and Men1Frt2, which should generate a band of 300 bp when both the positive selection cassette and exons 3-6 have been deleted. The PCR was done on samples that had been previously selected for the presence of the *Men1*$^{LoxP\text{-}Frt}$ allele using the primers Men1Frt3 and Menseq1 (as in **Figure 2.1.3 C**)**.** In all the samples that are positive for *Cre*, a 300 bp band can been seen on the Men1LoxP8 and Men1Frt2 PCR and in all samples negative for *Cre*, a weak 1900 bp non-recombined band is visible. The wildtype allele present should give rise to this band in all samples but it is out competed by the stronger 300 bp band when recombination of the floxed allele has occurred.
Men1$^{LoxP\text{-}Frt/wt}$*/Deleter-Cre* animals were bred to Bl-6 wildtype animals and pups that had lost both *Men1* exons 3-6 and *Cre* were identified. The allele carried by these animals was called

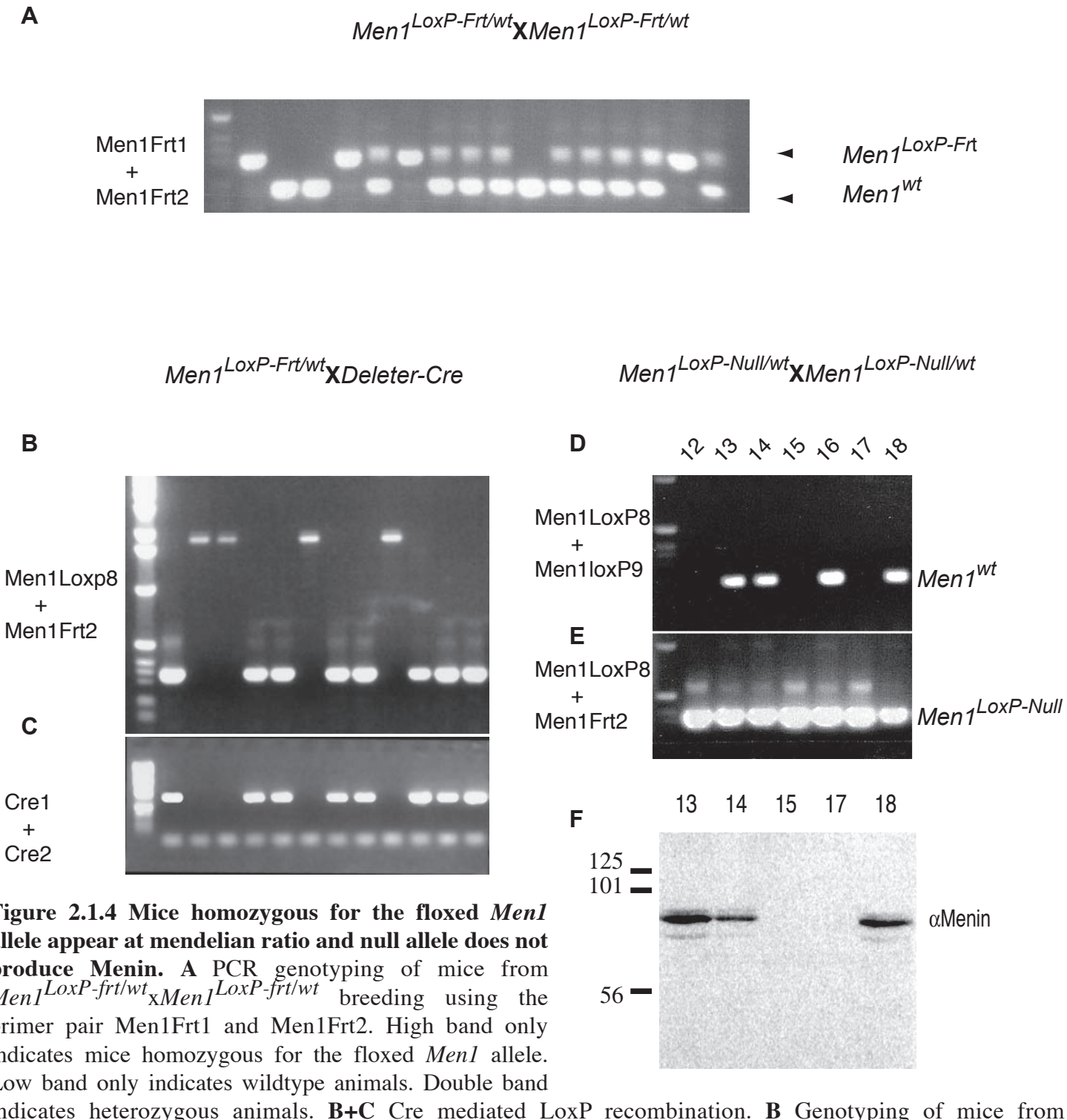

Figure 2.1.4 Mice homozygous for the floxed *Men1* allele appear at mendelian ratio and null allele does not produce Menin. **A** PCR genotyping of mice from $Men1^{LoxP\text{-}frt/wt}xMen1^{LoxP\text{-}frt/wt}$ breeding using the primer pair Men1Frt1 and Men1Frt2. High band only indicates mice homozygous for the floxed *Men1* allele. Low band only indicates wildtype animals. Double band indicates heterozygous animals. **B+C** Cre mediated LoxP recombination. **B** Genotyping of mice from $Men1^{LoxP\text{-}Frt/wt}$x*Deleter-Cre* breedings. Mice were screened for the presence of the floxed allele with primers Men1Frt3 and MenSeq1 (not shown). Positive mice were genotyped with primers Men1LoxP8 and Men1Frt2. Fast migrating band indicate Cre mediated recombination leading to excision of exons 3-6. Slow migrating band is the non-recombined allele. **C** PCR genotyping on the same DNA samples as in **B** using the primers Cre1 and Cre2. All PCR reactions were analysed on 2 % agarose gel. **D+E** Genotyping of E11.5 embryos from a $Men1^{LoxP\text{-}Null/wt}xMen1^{LoxP\text{-}Null/wt}$ breeding **D** PCR genotyping using the primer pair Men1LoxP8 and Men1LoxP9. Bands indicate the presence of the wildtype allele. **E** PCR genotyping on the same DNA samples as in **D** using the primer pair Men1LoxP8 and Men1Frt2. Bands indicate the presence of the Null allele. **F** Western blot of protein extracts from the embryos genotyped in **D+E**. Proteins were separated on 10 % SDS-PAGE, blotted to nitrocellulose and probed with the C19 αMenin antibody.

Men1$^{LoxP\text{-}Null}$ (**Figure 2.1.2 C**). In contrast to hACTP-FlpE mediated deletion, *Deleter-Cre* mediated recombination was very efficiently transmitted through the germline.

To verify that no protein was produced from the null allele, *Men1*$^{LoxP\text{-}Frt/wt}$ animals were interbred and pups were isolated by caesarean section at embryonic day 11.5. The embryos were genotyped **Figure 2.1.4 D+E**, and mouse embryo fibroblasts (MEFs) were established. Protein was extracted from the MEFs and analysed by western blot with a Menin C-terminal antibody **Figure 2.1.4 F**. Cell lines deficient in the wildtype *Men1* allele (**Figure 2.1.4 D+E** samples 15 and 17), were also deficient in Menin protein **Figure 2.1.4 F**.

In summary, this demonstrates that the floxed *Men1* allele is functionally equivalent to the wildtype allele and that the floxed *Men1* allele allows efficient Cre mediated deletion of exons 3-6, leading to Menin ablation.

2.1.5 Pituitary gland specific *cre* mouse lines

I have established and characterised several mouse lines expressing a *Cre* transgene from 14.9 kb of the the *Pit-1* promoter, which should drive expression in lactotropes, somatotropes and thyrotropes (Rhodes *et al.*, 1993). I decided to use the *Pit-1-Cre* line to generate the tissue specific deletion of *Men1* because this line should ensure a widespread and still relatively late (E13-E14) deletion of *Men1* in the pituitary gland (Rhodes *et al.*, 1993). The late expression should prevent any possible developmental abnormalities of the pituitary gland due to *Men1* deletion. The faithful reproduction of the expression pattern of a gene may often require cloning a promoter sequence many thousands of bases upstream from the transcription start. Furthermore, the integration site of the transgene and the copy number may also have a strong effect on the expression pattern of the gene. Because of this it is necessary to characterise the expression pattern of any given mouse line expressing a transgene.

I tested the expression pattern of our mouse lines by crossing them to a Cre reporter line called Z/EG21 (Novak *et al.*, 2000). As depicted in **Figure 2.1.5 A**, this mouse line carries a transgene, driven by the pCAGGS promoter, that ensures ubiquitous expression of *LacZ*. The *LacZ* gene is followed by a strong transcriptional termination sequence and by a gene encoding *EGFP*. The *LacZ* gene and the transcriptional termination sites are flanked by LoxP sites, which allows Cre mediated excision of these elements and expression of *EGFP*. The expression pattern of EGFP thus mimics the expression of Cre.

Figure 2.1.5 B shows the pituitary gland of a Z/EG21 mouse and a Z/EG21/*Pit-1-Cre* mouse in normal light and 488 nm light. In the absence of *Cre*, there is no EGFP signal detectable,

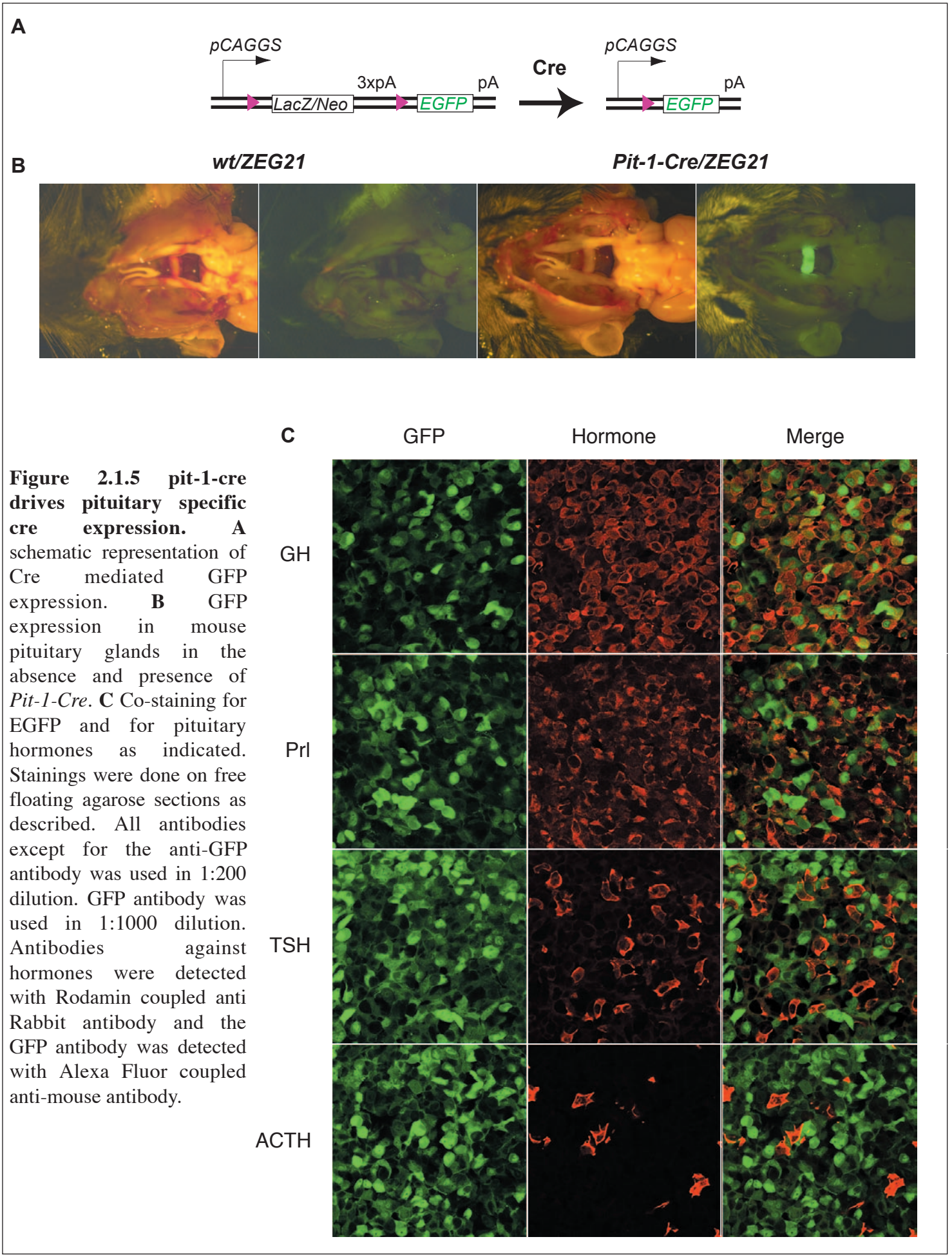

Figure 2.1.5 pit-1-cre drives pituitary specific cre expression. A schematic representation of Cre mediated GFP expression. **B** GFP expression in mouse pituitary glands in the absence and presence of *Pit-1-Cre*. **C** Co-staining for EGFP and for pituitary hormones as indicated. Stainings were done on free floating agarose sections as described. All antibodies except for the anti-GFP antibody was used in 1:200 dilution. GFP antibody was used in 1:1000 dilution. Antibodies against hormones were detected with Rodamin coupled anti Rabbit antibody and the GFP antibody was detected with Alexa Fluor coupled anti-mouse antibody.

but in the presence of *Pit-1-Cre*, there is strong fluorescence from the pituitary gland indicating that there is Cre expression in the pituitary gland. Inspection of the mouse revealed no other fluorescent tissues (data not shown).

To establish the expression pattern of Cre on a cellular level, I stained 50 µm pituitary gland vibrotome sections with anti GFP antibodies and antibodies against the hormones depicted on **Figure 2.1.5 C**. Whereas no expression of GFP in ACTH or TSH expressing cells can be seen, GFP co-localises with GH and Prolactin. Three independent mouse lines expressing *Pit-1-Cre* were characterised and used in *Men1* breedings.

2.1.6 Pituitary gland specific deletion of *Men1*

To ensure an efficient deletion of *Men1*, I decided to set up the experiment to generate mice that would carry a floxed allele over a Null allele of *Men1* in addition to a *Pit-1-Cre* transgene. In these mice, Cre would only have to recombine one allele of *Men1* in each cell to generate a *Men1* deficient cell. To generate these mice I mated $Men1^{LoxP\text{-}Null/wt}$ mice with three independent *Pit-1-Cre* mouse lines. The $Men1^{LoxP\text{-}Null/wt}$/*Pit-1-Cre* mice were subsequently mated with $Men1^{LoxP\text{-}Frt/Frt}$ mice to generate $Men1^{LoxP\text{-}Frt/Null}$/*Pit-1-Cre* mice.

The $Men1^{LoxP\text{-}Frt/Null}$/*Pit-1-Cre* mice were born at the expected mendelian frequency of 25 percent (data not shown). They were phenotypically normal and indistinguishable from their wildtype and heterozygous littermates. Postnatal growth and development of the $Men1^{LoxP\text{-}Frt/Null}$/*Pit-1-Cre* mice was also indistinguishable from that of wildtype mice suggesting that pituitary gland function was intact. Finally, both males and females were fertile indicating that $Men1^{LoxP\text{-}Frt/Null}$/*Pit-1-Cre* mice had a functional pituitary gland. Furthermore immunofluorescence revealed the presence of GH, Prolactin and ACTH expressing cells in the pituitary glands of 8 weeks old $Men1^{LoxP\text{-}Frt/Null}$/*Pit-1-Cre* mice (data not shown).

2.1.7 Pituitary gland phenotype

To characterise the effect of *Men1* deficiency on the pituitary gland, I collected pituitary glands at different times after birth starting at 7 weeks of age for both males and females. **Figure 2.1.6 A** shows examples of pituitary glands from both genders at 7, 10, 13 and 20 weeks of age. Already at 7 weeks the anterior lobe of the *Men1* deficient pituitary glands appeared hyperplastic compared to that of the wildtype pituitary glands. At both 10 and 13 weeks of age the *Men1* deficient pituitary glands were significantly larger than wildtype

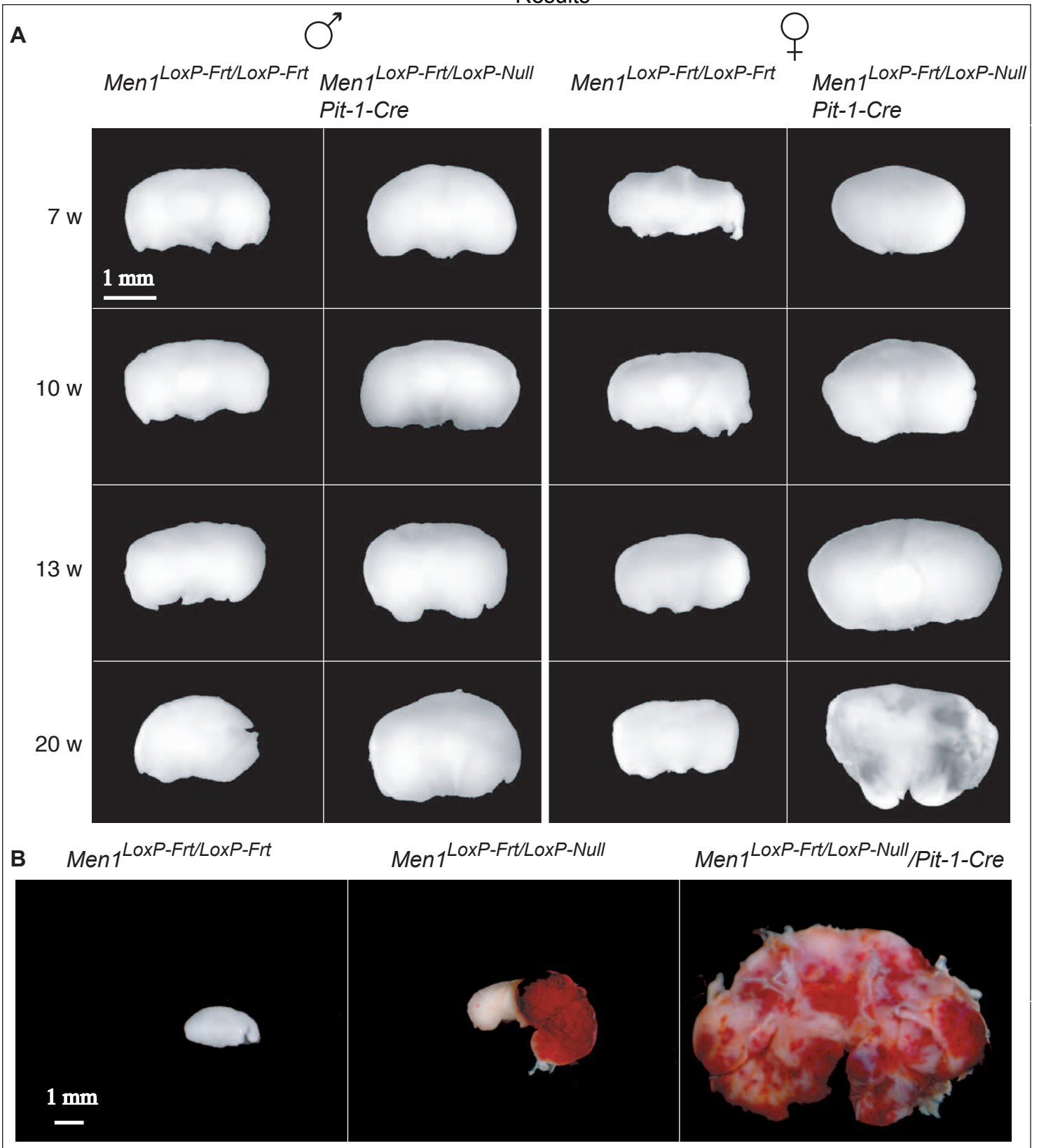

Figure 2.1.6 Pituitary phenotype of *Men1* deletion. Mice were perfused with PBS and 4 % PFA. The pituitaries were removed and photographed. These pituitaries are representative for their gender and genotype. All pictures are taken with Leica MZFLIII microscope.**A** The age, gender and phenotype is indicated. Note that female *Men1* deficient pituitary glands are bigger than their male counterparts. At 20 weeks of age the female, but not the male *Men1* deficient gland has changed morphorlogy **B** Female littermates aged 35 weeks, genotype is indicated. Note that the magnification in panel **B** is different from that in panel **A**. At this age, a hemorrhaging outgrowth can be seen in the heterozygous pituitary gland. The *Men1* deficient pituitary gland is many folds bigger than the wildtype pituitary gland and is clearly hemorrhaging blood.

pituitary glands but were otherwise normal in appearance and morphology. At 20 weeks of age, the wildtype pituitary glands had regressed somewhat and although the *Men1* deficient pituitary glands had not increased in size compared to earlier stages, 2 out of 3 inspected pituitary glands from female *Men1*$^{LoxP\text{-}Frt/Null}$/*Pit-1-Cre* mice had clearly changed their morphology. They appeared to have a less smooth surface and to be haemorrhaging blood from the vessels into the anterior lobe of the pituitary gland, which could not be removed by perfusion. At 20 weeks of age, this phenotype was never observed with pituitary glands from male *Men1*$^{LoxP\text{-}Frt/Null}$/*Pit-1-Cre* mice (0 out of 5 pituitary glands). Heterozygous pituitary glands were indistinguishable from wildtype pituitary glands for both genders at these early stages.

Figure 2.1.6 B shows the pituitary glands from wildtype, heterozygous and *Men1*$^{LoxP\text{-}Frt/Null}$/*Pit-1-Cre* female littermates at 35 weeks of age. The wildtype pituitary gland has reduced somewhat in size compared to 10 and 13 weeks of age but they are otherwise similar in appearance. Interestingly, from one side of the *Men1* heterozygous pituitary gland, a clonal outgrowth, which is clearly haemorrhaging blood, can be observed. This was frequently observed in the pituitary glands from heterozygous animals after 40 weeks of age. This observation suggests that *Men1* heterozygous mice faithfully reproduce MEN1, which is caused by the inheritance of one disrupted *MEN1* allele. By 35 weeks of age, the pituitary gland from the *Men1*$^{LoxP\text{-}Frt/Null}$/*Pit-1-Cre* female is many folds bigger than a normal pituitary gland, and occupies a significant portion of the brain cavity. Although it retains the overall shape of a pituitary gland with two recognisable anterior lobes, the morphology of the pituitary gland is completely different. There is widespread haemorrhaging of blood and the surface of the tissue is completely different from the wildtype pituitary gland. This can no longer be characterised as a hyperplastic pituitary gland but rather as a pituitary gland neoplasm or adenoma.

Although none of the pituitary gland tumours appeared to be invasive, in agreement with the literature on human pituitary gland tumours, some *Men1*$^{LoxP\text{-}Frt/Null}$/*Pit-1-Cre* mice died after 40 weeks of age presumably due to the size of the pituitary gland tumour. To avoid further pathology from these tumours, mice were sacrificed at 45 weeks of age at the latest.

After 45 weeks, 100 percent (13 out of 13) of female *Men1*$^{LoxP\text{-}Frt/Null}$/*Pit-1-Cre* mice had developed adenomas visible to the naked eye. Interestingly, only 40 percent (6 out of 15) of male *Men1*$^{LoxP\text{-}Frt/Null}$/*Pit-1-Cre* mice had developed adenomas and these were generally smaller than those of the female mice. In the remaining cases, the pituitary glands retained the wildtype morphology while still being clearly hyperplastic.

At 45 weeks, heterozygous females, both *Men1*$^{LoxP\text{-}Frt/Null}$ and *Men1*$^{LoxP\text{-}Frt/wt}$/*Pit-1-Cre* mice, had developed pituitary gland adenomas visible to the naked eye in 3 out of 5 mice. These adenomas developed from only one side of the pituitary in all of the cases observed. These adenomas were never found in heterozygous males of 45 weeks of age.

2.1.8 Pituitary gland histology

Pituitary glands from different ages and genders were embedded in paraffin, cut in 7 μm sections and stained with Hematoxyline and Eosin (H&E) (**Figure 2.1.7 A**). In these sections it is apparent that at 7 weeks of age, the entire anterior pituitary gland is significantly enlarged. Already at this stage there is a clear difference between males and females, with the female *Men1* deficient pituitary glands being significantly larger than their male counterparts, with a few exceptions. After 10 weeks of age little gain in pituitary gland size is observed. The posterior and intermediate pituitary gland is clearly compressed by the expanding anterior pituitary gland of the *Men1*$^{LoxP\text{-}Frt/Null}$/*Pit-1-Cre* mice. The overall morphology of the *Men1* deficient pituitary glands does not appear to differ much from that of the wildtype pituitary glands although the anterior gland of the *Men1* deficient pituitary glands does appear to contain larger cavities than wildtype pituitary glands. These cavities are more pronounced in female pituitary glands and they appear to be most prominent in the distal part of the anterior pituitary gland starting at 7 weeks of age. At 20 weeks of age the female pituitary gland has clearly changed morphology and contains large cavities, some of which have been filled with blood from leaking blood vessels.

At 35 weeks the anterior pituitary gland of the *Men1*$^{LoxP\text{-}Frt/Null}$/*Pit-1-Cre* mouse is massively expanded and it contains multiple blood filled vacuoles (**Figure 2.1.7 B**). Despite the massive overgrowth the posterior and intermediate lobe remain intact although they have been severely compressed, suggesting that the tumour is not invasive.

Figure 2.1.8 A shows higher magnification pictures of the anterior and intermediate lobe of the female pituitary glands at 7, 10 and 20 weeks of age. At this magnification it is apparent that the organisation of the cells in the anterior pituitary gland is different in the *Men1*$^{LoxP\text{-}Frt/Null}$/*Pit-1-Cre* mice from the wildtype mice. Most notably the cells appear to be organised into a sort of epithelium surrounding the vacuoles. The vacuoles appear to grow somewhat in size from 7 to 10 weeks. At 20 weeks, haemorrhaging from blood vessels has filled some of the cavities with blood.

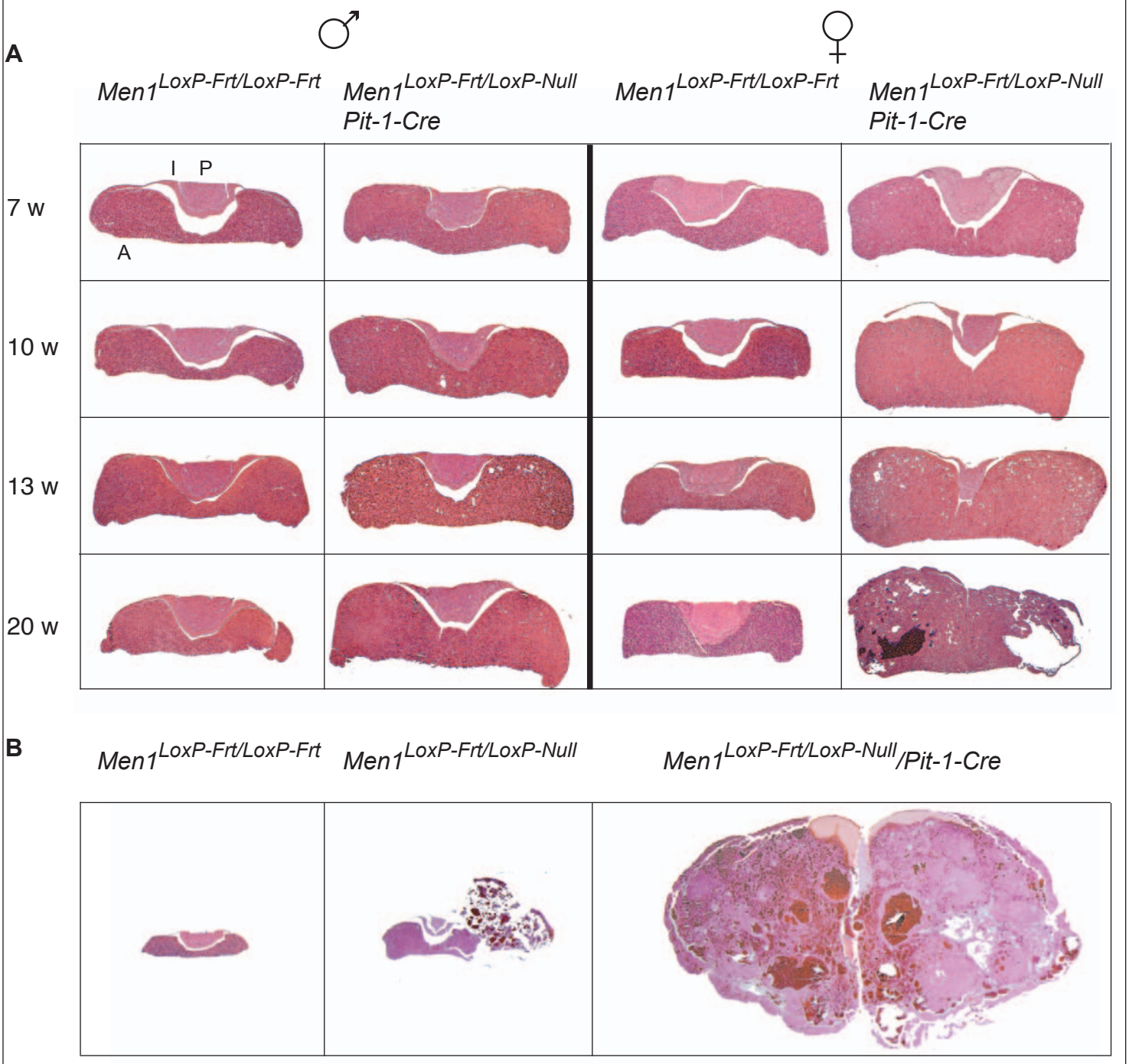

Figure 2.1.7 ***Men1*** **deficient pituitary glands are hyperplastic and develop adenomas by 35 weeks of age.** Hematoxylene and Eosine stained 7µm paraffin sections. **A** The age, gender and phenotype is indicated. On the pituitary gland from the 7 week wildtype male is indicated the positions of the anterior gland (A), the intermediate gland (I) and the posterior gland (P). Note that the female *Men1* deficient pituitary glands are more hyperplastic than their male counterparts at all ages. In the *Men1* deficient pituitary glands, the intermediate and posterior lobes are significantly compressed. Female pituitary glands at 20 weeks of age show a change in morphology, with hemorrhaging of blood into large cavities some of which can be emptied by perfusion. However, there is no major gain in pituitary gland size from 10 to 20 weeks of age. Pictures taken with the Leica Axiophot microscope. These sections are representative for their gender and genotype. **B** Female littermates aged 35 weeks, genotype is indicated. A massive adenoma has developed from the anterior lobe of the *Men1* deficient pituitary gland, which is now many folds bigger than the wildtype pituitary gland and is clearly hemorrhaging blood into multiple large cavities. The intermediate and posterior lobe of the pituitary gland can still be seen although they are severely compressed. Pictures were taken at a Leica MZFLIII microscope.

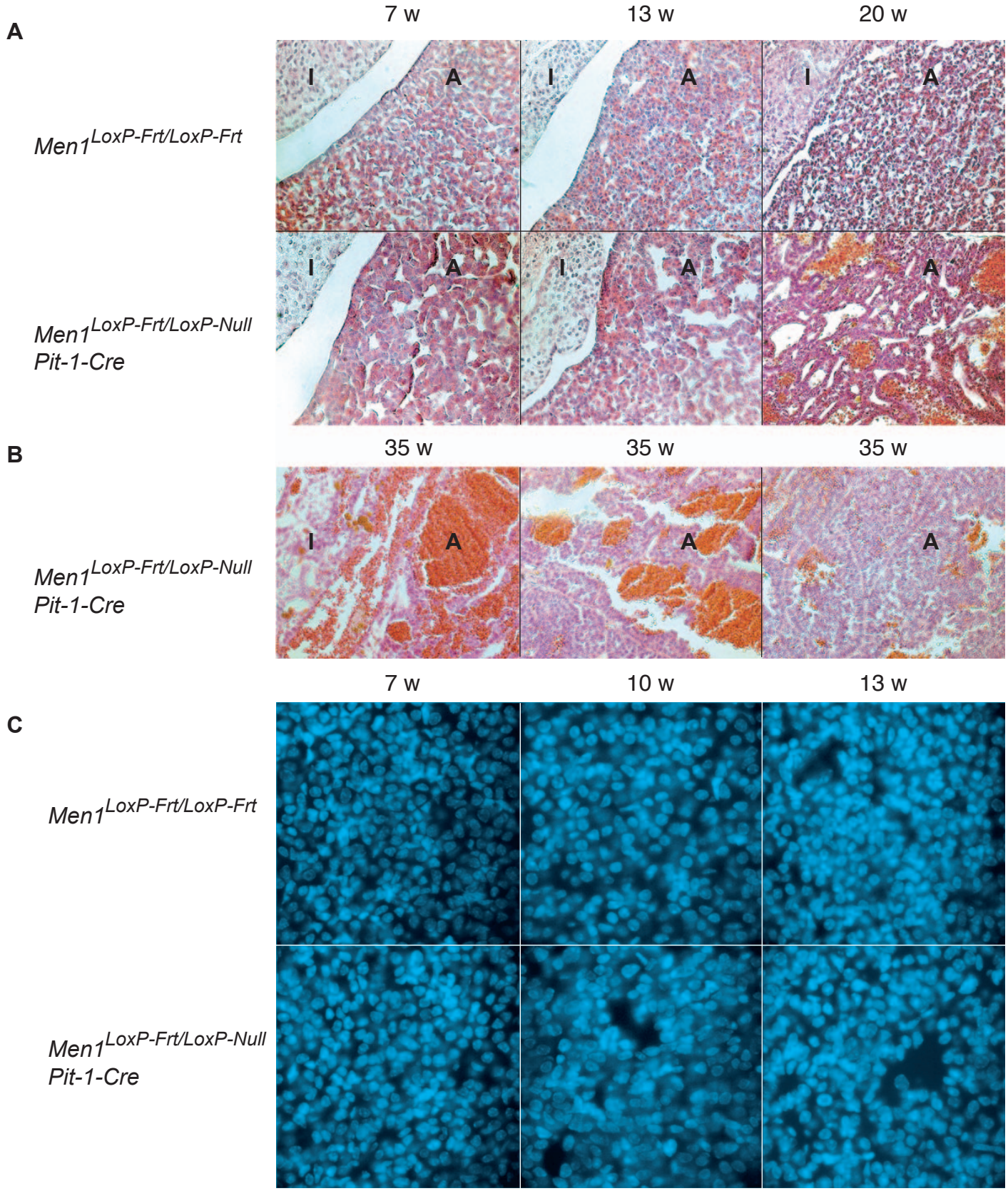

Figure 2.1.8 *Men1* deficient pituitaries develop vacuoles. **A** Higher magnification microscopy of sections from females from Figure 2.1.7. Age and genotypes are indicated. The position of the intermediate and anterior gland is indicated with I and A respectively. **B** Higher magnification microscopy of selected areas of the 35 week old female *Men1* deficient pituitary gland from Figure 2.1.7. Note the intermediate lobe on the left as well as blood filled cavities and epithelial like structures in the anterior lobe. Pictures were taken with on a Leica Axiophot microscope **C Cell density is unaffected by loss of *Men1***. DAPI stained anterior lobes from female pituitaries. Age and genotypes are indicated. Pictures were taken with a Leica DM IRBE microscope.

In the 35 week pituitary gland (**Figure 2.1.8 B**), the cellular organisation is clearly different from that of that of a wildtype pituitary gland. Apart from the multiple large blood filled cavities, other structures such as epithelial like structures can be observed.

The hyperplasia of the *Men1* deficient pituitary glands, apparent as early as 7 weeks of age, would suggest an overproliferation phenotype resulting in an increased number of cells preceding the actual adenoma formation. However, the size of an organ is determined not only by the number of cells but also by the size of the cells. The hyperplasia phenotype of the *Men1* deficient pituitary glands could therefore be caused by an increase in the size of the pituitary gland cells rather than an increase in numbers. As the H&E staining does not allow one to assess the density of the nuclei, which reflects the size of the cells, I stained the 7 μm paraffin sections with DAPI stain which labels DNA (**Figure 2.1.8 C**). High magnification microscopy revealed that the density of nuclei is similar in the wildtype and the *Men1* deficient pituitary glands at 7, 10 and 13 weeks of age suggesting that the hyperplasia of the *Men1* deficient pituitary gland is due to hyperproliferation of the pituitary gland cells.

2.2 Molecular characterisation of Men1 deficient pituitary glands

2.2.1 Analysis of Menin expression in *Men1* deficient pituitary glands

To investigate the extent of Menin depletion in the anterior pituitary gland of *Men1*$^{LoxP\text{-}Frt/Null}$/*Pit-1-Cre* mice compared to wildtype littermates, I performed immunohistochemistry on pituitary gland paraffin sections and immmunofluorescence on free floating agarose sections from 12 weeks old mice, using two commercial and three rat polyclonal antibodies against Menin produced by us. None of these antibodies gave satisfactory results on pituitary gland sections.

Although western blot analysis does not yield information about the pattern of protein expression, it does accurately show the amounts of antigen present in the pituitary. **Figure 2.2.1 A** shows a western blot on pituitary gland protein extracts from 12 weeks old male and 4 and 12 weeks old female *Men1*$^{LoxP\text{-}Frt/Null}$/*Pit-1-Cre* mice and wildtype littermates. At all ages and genders there is a very significant reduction in detectable Menin protein. Moreover, the amount of Menin is reduced in 12 weeks old *Men1*$^{LoxP\text{-}Frt/Null}$/*Pit-1-Cre* mice compared to 4 week old mice, possibly suggesting a proliferative advantage of *Men1* deficient cells. **Figure 2.2.1 B** is a loading control. It shows a probing of the blot with anti Erk1/Erk2 antibodies indicating that the same amount of protein was loaded on the gel. Above the lower band of the doublet a weaker slower migrating band can be seen. This band represents phosphorylated and activated Erk2. No significant difference was seen between wildtype and *Men1* deficient pituitary glands in the amount of activiated Erks. This result was also confirmed with anti phospho-Erk antibodies (data not shown).

I also performed an *in situ* hybridisation experiment using a probe against *Men1* exons 3-6 on sections from 7 week old *Men1*$^{LoxP\text{-}Frt/Frt}$ and *Men1*$^{LoxP\text{-}Frt/Null}$/*Pit-1-Cre* mice and on sections from a 41.5 week old *Men1*$^{LoxP\text{-}Frt/Null}$ mouse (**Figure 2.2.1 C**). At 7 weeks of age, there is clear expression of *Men1* in both the anterior, intermediate and posterior lobe of the pituitary gland of the *Men1*$^{LoxP\text{-}Frt/Frt}$ mice. In contrast, the *Men1* signal is almost absent from the anterior lobe of the *Men1*$^{LoxP\text{-}Frt/Null}$/*Pit-1-Cre* mice, whereas a significant signal is still observed from the posterior and intermediate lobe, confirming the Cre mediated deletion of *Men1* in the Pit-1 lineage. In the 41.5 week old heterozygous pituitary gland, a macroscopic adenoma was observed in the left side of the pituitary gland. This clonal expansion shows the same

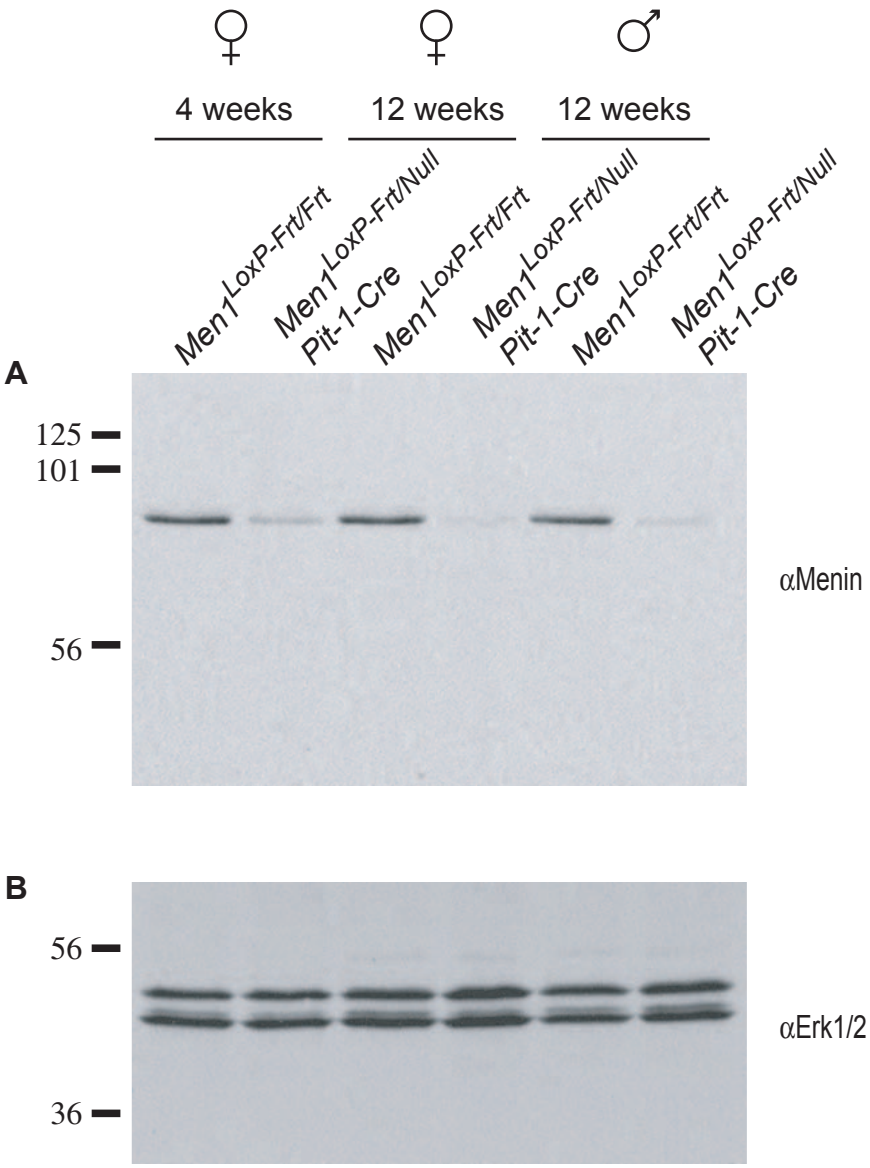

Figure 2.2.1 Menin is almost absent and *Men1* mRNA is significantly reduced in the pituitary glands of *Men1*$^{LoxP\text{-}Frt/Null}$*/Pit-1-Cre* mice. **A+B** Western blot on protein extracts from pituitary glands from mice with the age and gender indicated. Pituitary glands were perfused with PBS and protein was extracted with RIPA buffer. 40 µg of total protein were separated by SDS-PAGE on a 10 percent gel. Protein was blotted to nitrocellulose and probed with antibody. **A** Westernblot was probed C19 anti Menin antibody in 1:1000 dilution in PBS-tween with 1 percent milk powder. 2nd HRP coupled rabbit anti goat antibody was used in 1:5000 dilution in the same buffer. Bound antibody was detected with ECL reagent. **B** Loading control. Westernblot was probed with anti Erk1/Erk2 antibody in 1:1000 dilution in PBS-tween with 1 percent milk powder. 2nd HRP coupled goat anti rabbit antibody was used in 1:5000 dilution in the same buffer. Bound antibody was detected with ECL **C** *In situ* hybridisation of 18 µm cryosections. Sections of female pituitaries from 7 week old *Men1*$^{LoxP\text{-}Frt/Frt}$, *Men1*$^{LoxP\text{-}Frt/Null}$*/Pit-1-Cre* mice and 41.5 week old *Men1*$^{LoxP\text{-}Frt/Null}$ mice were hybridised with a probe against exons 3-6 of *Men1*. Note that the *Men1* signal is almost absent from the anterior lobe of the *Men1*$^{LoxP\text{-}Frt/Null}$*/Pit-1-Cre* pituitary glands but not from the intermediate lobe. In the 41.5 week old heterozygous pituitary gland, a clonal outgrowth in the left side was observed. The *Men1* signal is absent in this outgrowth, suggesting that the wildtype *Men1* allele has been lost by chromosomal rearrangements. The ^{35}S labeled *in situ* probe was visualised by 4 weeks of incubation with Kodak NTB2 and the tissue counterstained with Bisbenzimide. Photographs were made on the Leica MZFLIII microscope.

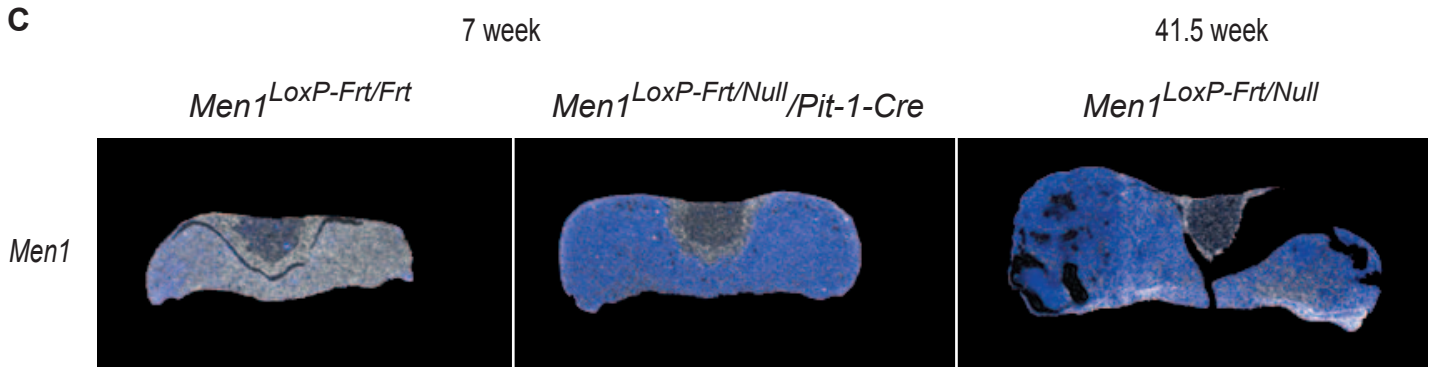

morphology as the adenomas originating from the *Men1*$^{LoxP\text{-}Frt/Null}$/*Pit-1-Cre* mice with large vacuoles and disrupted cellular organisation. The *Men1* signal is absent from the hyperplastic left side of the anterior lobe, although it can be clearly detected in the rest of the anterior lobe of the heterozygous pituitary gland. This observation suggests that the wildtype *Men1* allele has been lost by chromosomal rearrangements in the hyperplastic left side of the heterozygous pituitary gland, and that loss of both alleles of *Men1* is required for tumour formation.

2.2.2 Analysis of growth and apoptosis in *Men1* deficient pituitary glands

The early hyperplasia phenotype of the *Men1* deficient pituitary glands would suggest that there was increased proliferation in these pituitary glands. To investigate the role of Menin in regulating the proliferation rate of the pituitary gland cells, I performed immunohistochemistry on wildtype and *Men1* deficient pituitary gland sections from 12 week female mice using antibodies against two different proliferation markers. **Figure 2.2.2 A** shows a staining with an antibody against KI-67. KI-67 is a nuclear proliferation marker, that is expressed in cells in S-phase, G2-phase and M-phase (Gerdes *et al.*, 1984). It is evident that while few nuclei stain in the wildtype pituitary gland, there is widespread staining in the *Men1* deficient pituitary gland, suggesting that a significant fraction of the cells in the *Men1* deficient pituitary gland are cycling at 12 weeks of age. **Figure 2.2.2 B** shows staining with an antibody against Histone H3 phosphorylated on Serine 10. Phospho-Histone 3 is a nuclear marker for mitosis (Ajiro *et al.*, 1996). In the wildtype pituitary gland very few nuclei stain, and those that do do not display a mitotic appearance. In the *Men1* deficient pituitary gland there is widespread staining, and the stained nuclei have a mitotic appearance, suggesting chromosomal segregation was in progress. A much lower number of cells stain positive for phospho-Histone H3 than do for KI-67. This reflects that mitosis is very short compared to the rest of the cell-cycle.

Increased proliferation caused by aberrant growth signals often leads to apoptosis (Hanahan *et al.*, 2000). To test if this was true for the hyper proliferation induced by the loss of *Men1*, I probed the pituitary gland sections with an antibody against an apoptotic marker, a cleavage product of Caspase3, which is cleaved and activated in apoptosis (Nicholson *et al.*, 1995). As **Figure 2.2.2.C** show, no staining could be detected regardless of the antigen retrieval method used (data not shown).

It thus appears that *Men1* loss leads to hyperplasia caused by hyperproliferation and that this proliferation is not associated with apoptosis.

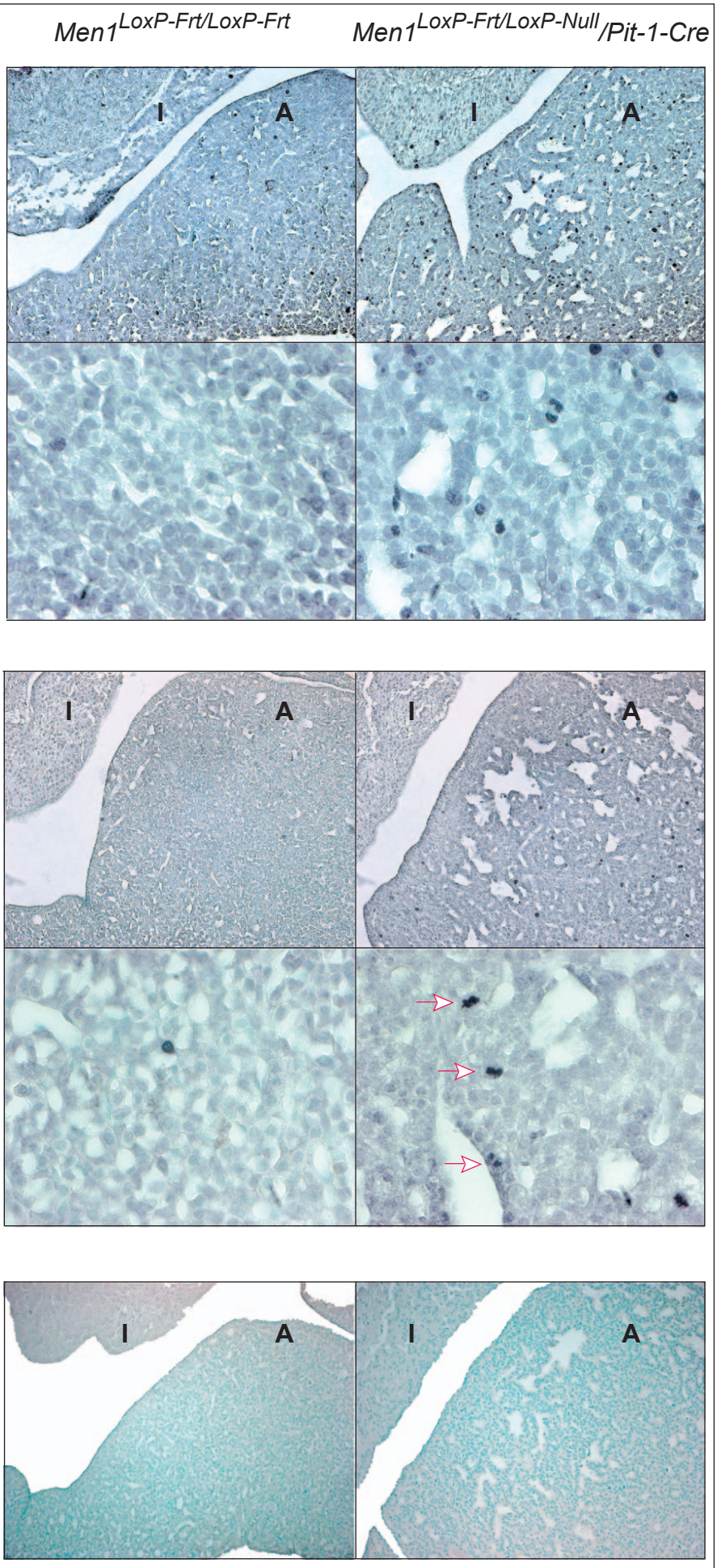

Figure 2.2.2 Increase of proliferation makers in *Men1* deficient pituitaries. Immunohistochemistry on *Men1*$^{LoxP\text{-}Frt/LoxP\text{-}Frt}$ and *Men1*$^{LoxP\text{-}Frt/LoxP\text{-}Null}$*/Pit-1-Cre* mice. 12 week old female mice were perfused with 2 percent PFA and pituitaries were fixed overnight in 2 percent PFA. The pituitaries shown are representative of their age and genotype. **A** Anti KI67 immunohistochemistry. 7 µm paraffin sections were probed with the KI67 antibody from Novocastra in a 1:750 dilution. Antigen was recovered using the microwave method. Bound antibody was detected with HRP coupled 2nd antibody and DAB substrate with nickel. The tissue was counter stained with Methyl Green **B** Anti phospho-Histone H3 immunohistochemistry. 7 µm paraffin sections were probed with the pHistone H3 antibody from Upstate Biotech in a 1:300 dilution. Note the characteristic staining of the dividing nuclei indicated with red arrowheads in the high magnification pictures. Antigen was recovered using the plain method. Bound antibody was detected with HRP coupled 2nd antibody and DAB substrate with nickel. The tissue was counter stained with Methyl Green. **C** Anti Cleaved Caspase 3 immunohistochemistry. 7 µm paraffin sections were probed with the cleaved Caspase 3 antibody from Cell signaling technology in a 1:300 dilution. Antigen was recovered using the plain method. Bound antibody was detected with HRP coupled 2nd antibody and DAB substrate with nickel. The tissue was counter stained with Methyl Green. All pictures were done on the Leica Axiophot microscope.

2.2.3 Microarray analysis of expression pattern in *Men1* deficient pituitary glands

In order to identify genes that may mediate the hyperplastic phenotype of the *Men1* deficient pituitary glands, I decided to analyse the gene expression profile of *Men1* deficient and wildtype pituitary glands. I decided that microarray analysis would be feasible for two reasons. Firstly, even though the *Men1* deficient pituitary glands were hyperplastic, they still retained normal pituitary gland morphology, and the pituitary glands appeared to be functional. Secondly, the Pit-1 lineage constitutes more than 60 percent of the pituitary gland and it would therefore be reasonable to assume that any changes in gene expression caused by *Men1* deficiency would be detectable over the background of *Men1* expressing cells.

As *MEN1* tumourigenesis leads to chromosomal instability with loss and gain of chromosomes, which would make the interpretation of the microarray experiment impossible, I decided to analyse relatively young pituitary glands. Furthermore I decided to analyse RNA from each pituitary gland on separate chips, which would allow me to detect if any gain or loss of chromosomes would have occurred that would lead to a major change in expression profile.

RNA from the pituitary glands of three heterozygous and three $Men1^{LoxP\text{-}Frt/Null}$/*Pit-1-Cre* 12 weeks old males was isolated (four of these animals were littermates). The RNA was used for expression profiling using the Amersham Codelink 20K mouse chip.

For each microarray, the Codelink software calculates a normalised threshold. Genes with intensities below the threshold of the microarray are considered not to be expressed. For all of the microarrays, the thresholds were between 0.275 and 0.338. I defined that only if a gene would be above the threshold in all three of the biological replicates for the heterozygous pituitary glands or all three of the biological replicates for the *Men1* deficient pituitary glands, it would be considered expressed in the pituitary gland. By this definition 10370 genes out of the 20000 genes on the microarray were expressed in the heterozygous pituitary glands, 10018 in the *Men1* deficient pituitary glands and 10962 were expressed in the pituitary glands of either of the two genotypes.

The microarray data was subsequently analysed using Genespring 6.2 (Silicon Genetics). The raw intensity values were normalised to the 50th percentile of the array intensity. **Figure 2.2.3 A** shows a scatterplot of the normalised intensities of the 10370 genes expressed in the heterozygous pituitary glands from the microarray results from two different heterozygous pituitary glands. Most genes align along the diagonal indicating identical expression and 99.1

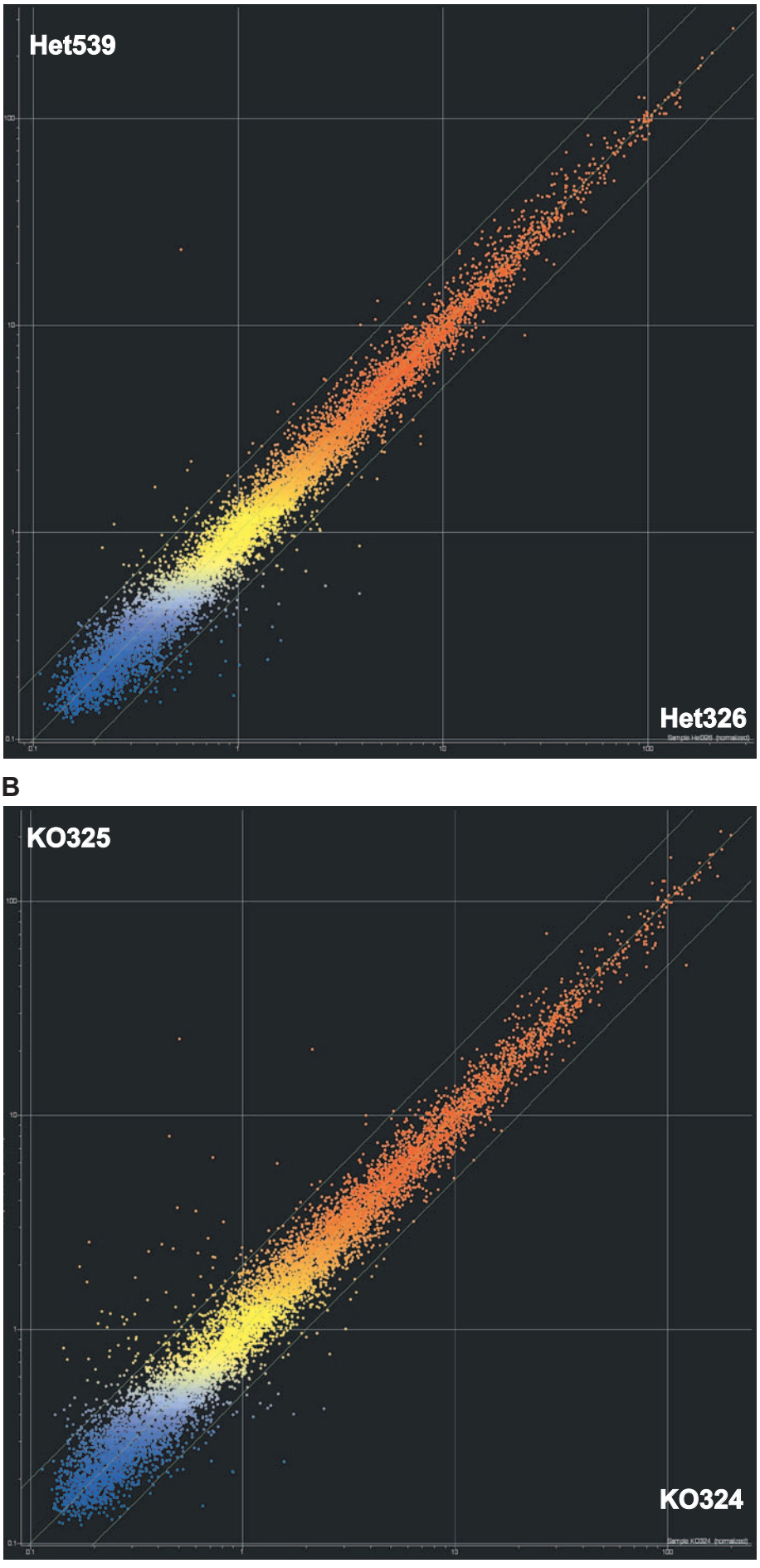

Figure 2.2.3 Gene expression profiling of *Men1* deficient and heterozygous pituitay glands. Scatterplot of biological replicates. More than 98 percent of the genes expressed in the pituitary glands fall within the lines indicating two fold difference. Gene expression profiling was performed on RNA from individual pituitary glands using the Codelink 20K microarrays that contains probes for 20000 individual mouse genes. Three biological replicates were done for both genotypes. The data from the microarrays were imported from the Codelink software into Genespring and normalised to the 50th percentile of all spots on each array (per chip normalisation or scaling) **A** Scatterplot of two heterozygouse biological replicates. 10370 out of 20000 genes were expressed at levels above the threshold value for each microarray in all three biological replicates of the heterozygous pituitary glands. For these genes, the normalised intensity values from the microarray analysis of the pituitary glands of two heterozygous littermates are plotted against each other. Most data points are close to the diagonal indicating identity and 99.1 percent of all datapoints fall within the lines indicating two fold difference. Note that the axis are logarithmic. **B** Scatterplot of two *Men1* deficient biological replicates. As above with the results from two pituitary glands from $Men^{LoxPFrt/Null}$/*Pit-1-Cre* mice. 10018 genes are expressed at levels above the threshold value in all three biological replicates of the *Men1* deficient pituitary glands. 98.4 percent of all datapoints fall within the two lines indicating two fold difference.

percent of all the genes expressed in the heterozygous pituitary glands fall within the two lines indicating a two fold difference. **Figure 2.2.3 B** shows the same representation of two *Men1*$^{LoxP\text{-}Frt/Null}$*/Pit-1-Cre* littermates. As with the heterozygous samples, most genes align along the diagonal and 98.4 percent of the 10018 genes expressed in the *Men1* deficient pituitary glands fall within the two lines indicating a two fold difference. These data suggests that the reproducibility of the experiment is very high and that the pituitary glands are well suited for microarray experiments, but the few datapoints falling well outside the diagonal also emphasises the importance of doing several biological replicates.

Figure 2.2.4 A shows a condition tree of the three heterozygous biological replicates and the three *Men1* deficient biological replicates. The condition tree shows that the three heterozygous and the three *Men1*$^{LoxP\text{-}Frt/Null}$*/Pit-1-Cre* samples cluster together suggesting that the overall differences are biggest between the heterozygous and Men1 deficient pituitary glands, independently of whether the mice were siblings. These data suggests that the predominant gene expression changes are due to *Men1* deficiency in the *Men1*$^{LoxP\text{-}Frt/Null}$*/Pit-1-Cre* mice. **Figure 2.2.4 B** shows that over all genes, the biological replicates are between 97.7 and 98.1 percent identical. For samples of different genotype the identity is between 96.7 and 97.5 percent.

The 20K mouse chip contains probes for all of the published Menin interacting proteins except for *Mll2* and *Fancd2*, thus one can evaluate the expression of these genes in the pituitary gland using the microarray data. All of the Menin interacting *NF-κB* subunits are expressed in the pituitary gland, with *NF-κB1* showing the highest expression. In addition, according to the microarray data *Smad1*, *Smad2* and *Smad4* are expressed in the pituitary gland but not *Smad3* or *Smad5*. Of the other interaction partners present on the chip, only PEM shows no expression.

Many of the genes that have been implicated in growth control and tumour formation in the pituitary gland are present on the microarray. In addition, the genes that have been published to be Menin targets are represented on the microarray as well as many of the TGF-β/Smad3 and NF-κB regulated genes that could be relevant for growth control and tumourigenesis of the endocrine system. **Figure 2.2.5** shows the intensity of these genes in all of the biological replicates. All of these genes are either expressed in the pituitary gland, but not significantly changed in the knockout compared to the heterozygous, or not expressed in the pituitary gland in both the heterozygous and knockout pituitary glands. Among the genes that have previously been implicated in pituitary gland tumourigenesis, genes like *PTTG1*, *bFGF*, *NGF*,

A

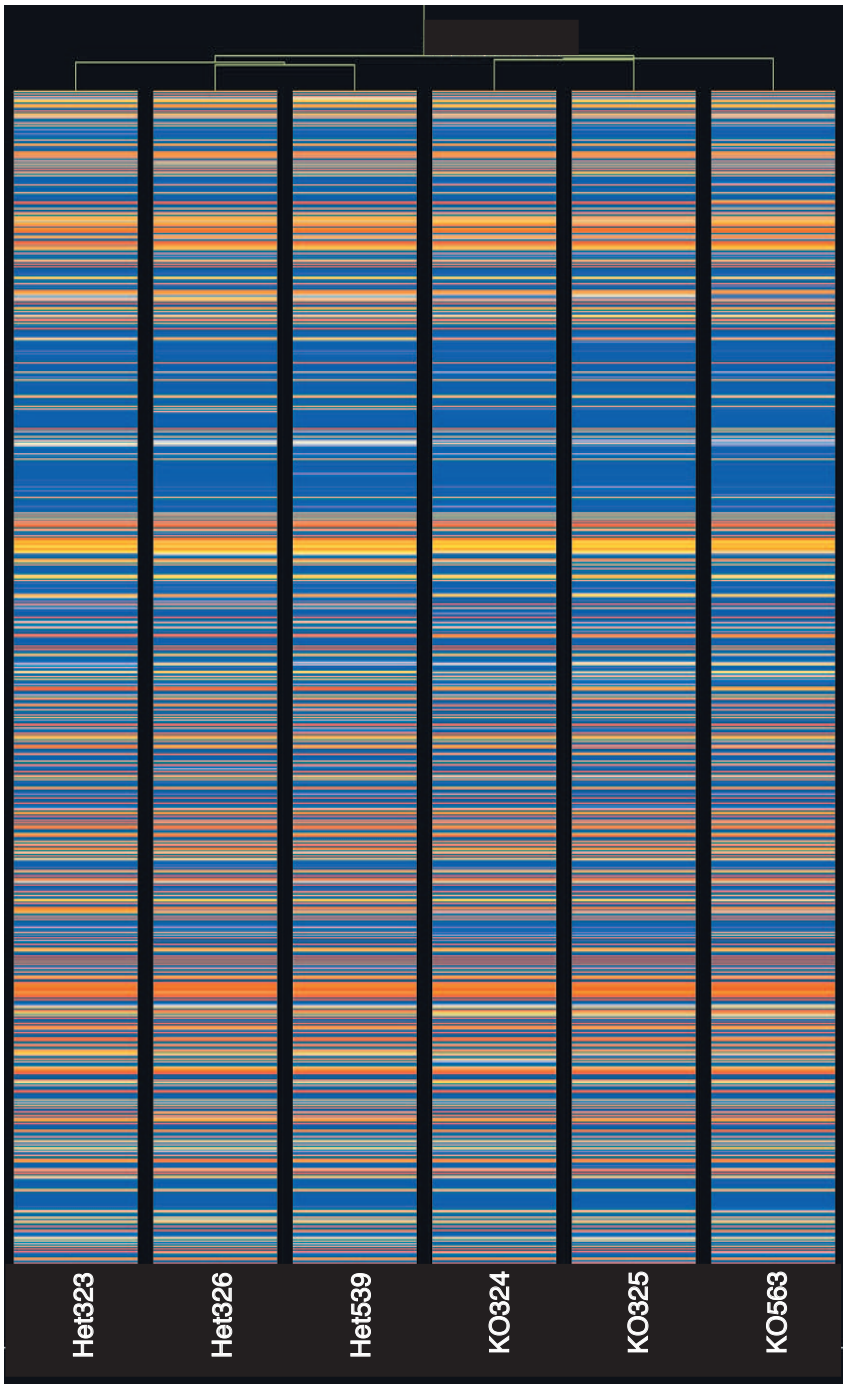

B

	Het323	Het326	Het539	KO324	KO325	KO563
Het323	1	0.978	0.979	0.974	0.971	0.967
Het326	0.978	1	0.981	0.975	0.974	0.972
Het539	0.979	0.981	1	0.975	0.973	0.970
KO324	0.974	0.975	0.975	1	0.978	0.978
KO325	0.971	0.974	0.973	0.978	1	0.978
KO563	0.967	0.972	0.970	0.978	0.977	1

Figure 2.2.4 Gene expression profiling of *Men1* deficient and heterozygous pituitary glands. Biological replicates cluster together, suggesting that loss of *Men1* is the primary cause of change in the gene expression profile. A Condition tree. Three biological replicates were done using RNA from three different pituitary glands from mice of both genotypes. Four of the six animals were littermates (two heterozygous and two *Men1* deficient). The microarray results were analysed in Genespring. All 20000 genes were normalised to the 50th percentile of all spots on each array (per chip normalisation or scaling). The samples were clustered in a condition tree using spearman correlation. Each gene is represented with a bar. The colour of the bar indicates the normalised intensity of the gene on each microarray. Red represents the highest intensity and blue the lowest. The three heterozygous and the three *Men1* deficient samples cluster together, which means that the overall differences are biggest between heterozygous and homozygous animals whether or not they are littermates. This suggests that the main cause of change in gene expression profile is due to loss of *Men1*. **B** Correlation cofficiencies between all six microarrays. All 20000 genes were normalised to the 50th percentile of all spots on each array. The standard correlation between all pairs of microarrays were calculated in Genespring. All biological replicates are between 97.8 and 98.1 percent identical for the heterozygous samples and between 97.7 and 97.8 percent identical for the *Men1* deficient samples. The correlation between all pairs of heterozygous- *Men1* deficient samples is between 96.7 and 97.5 percent.

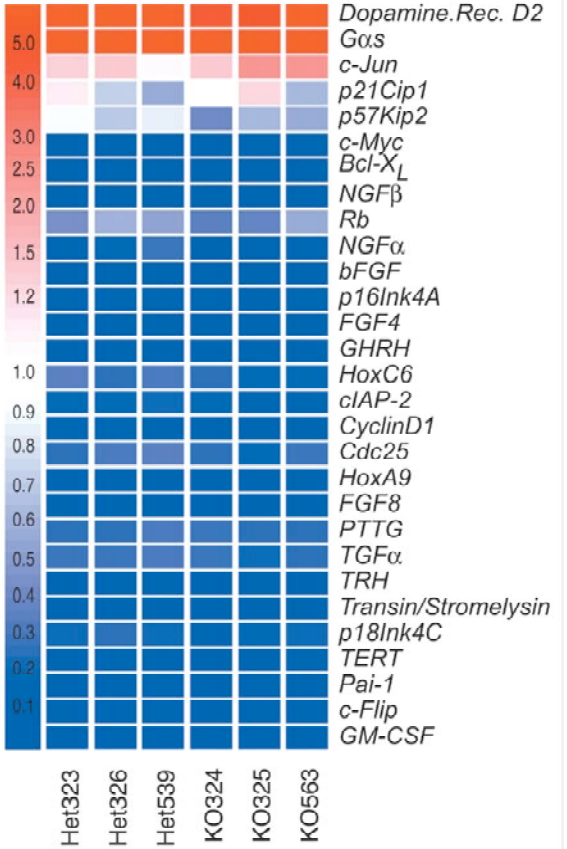

Figure 2.2.5 Genes implicated in pituitary gland growth control, published Menin regulated genes and TGF-β and NF-κB regulated genes are unaffected by *Men1* deletion. Genetree of selected genes. Most of the genes that have been implicated in pituitary gland tumourigenesis, previously published Menin regulated genes as well as several published TGF-β and NF-κB regulated genes are represented by probes on the microarray. None of these show any significant change in expression pattern in *Men1* deficient pituitary glands compared to heterozygous pituitary glands, suggesting that they are not involved in MEN1 tumourigenesis. All intensities were normalised to the 50th percentile of all spots on each array. The intensity of the signal of the indicated genes is shown for each of the biological replicates. Red colour indicates highly expressed genes, white intermediate and blue colour, genes expressed at low levels.

FGF4, *TGF-α, TRH*, *GHRH*, *Dopamine D2 receptor*, *Rb*, *p16Ink4a*, *p18Ink4c* and *Gαs* are present on the microarray but not differentially expressed in the *Men1* deficient pituitary glands. The telomerase gene, which has been reported to be a Menin target, is neither expressed in the heterozygous nor in the knockout pituitary gland. The same is true for *Hoxa9*, whereas *Hoxc6* is expressed in both cases at the same level. Both of these genes have been published to be Menin targets. Among the well characterised TGF-β/Smad3 and NF-κB regulated genes present on the microarray are *p21Cip1*, *Cyclin D1*, *c-Myc, c-Jun*, *Cdc25*, *cIAP*, *Pai-1*, *Transin/Stromelysin*, *GM-CSF*, *BCL-X$_L$* and *c-Flip*. None of these genes show any changes in expression levels in the *Men1* deficient pituitary glands compared to the heterozygous pituitary glands.

These data suggest that the tumour suppressor activity of *Men1* is not mediated by repression or activation of the normal TGF-β or NF-κB targets and that MEN1 tumourigenesis does not involve differential expression of genes that are associated with sporadic tumourigenesis of the pituitary gland. Furthermore, the microarray data suggest that the published Menin responsive genes are not affected by loss of *Men1* in the pituitary gland.

Interestingly, even though the *Men1* probe on the microarray does not hybridise to exons 3 to 6 but rather to exon 10 of the *Men1* mRNA, there is still a 60 percent reduction in the *Men1*

signal in the *Men1*$^{LoxP\text{-}Frt/Null}$/*Pit-1-Cre* pituitary glands compared to the heterozygous pituitary glands. This is most likely the effect of nonsense mediated RNA decay of the *Men1* message due to the disruption of the open reading frame by the Cre mediated recombination.

2.2.4 Genes deregulated in *Men1* deficient pituitary glands

Figure 2.2.6 shows the average expression of the three biological replicates for each individual gene in the heterozygous pituitary glands vs. the knockout pituitary glands for the 10962 genes expressed in the pituitary glands of either of the two genotypes. Along the diagonal, the two lines indicate two fold above and two fold below identity. It is apparent that most genes fall between these two lines. I have defined the 2 fold above or below identity as the cut-off values for deregulated genes. Of the genes that fall outside these lines, most are higher expressed in the heterozygous pituitary glands and these genes are thus normally directly or indirectly activated by Menin. A smaller part of the genes outside the two fold lines are more highly expressed in the knockout pituitary glands than in the wildtype. These genes would normally have been repressed by Menin.

To identify genes that were differentially expressed in the knockout pituitary glands compared to the heterozygous pituitary glands, I generated two sets of genes. One set contained genes whose average expression in the knockout pituitary glands was 2 fold higher than that of the heterozygous pituitary glands, and the other set contained genes whose expression was 2 fold higher in the heterozygous samples. 500 genes were downregulated in the *Men1* deficient pituitary glands compared to the heterozygous pituitary glands and 135 genes were upregulated. To eliminate genes, where a single outlying data point led to an unrepresentative average, a students T-test was performed on the three biological replicates and only genes with a p-value less than 0.05 were considered. This analysis produced two sets of genes that were either more than 2 fold up or 2 fold downregulated in the knockout pituitary glands compared to the heterozygous pituitary glands. The datapoint representing these genes are coloured yellow in **Figure 2.2.6**. In total 199 genes were downregulated and 67 genes were upregulated in the knock out.

Figure 2.2.7 A shows a genetree of the biological replicates for these 266 genes. The intensity of each gene was normalised to median of the intensity of the gene on all the microarrays. The values for the intensities are therefore not comparable to those of **Figure 2.2.6.** It is apparent that the expression of these genes is similar in all of the heterozygous samples and knockout samples respectively. **Figure 2.2.7 B** shows a Venn diagram of the 10370 genes that were

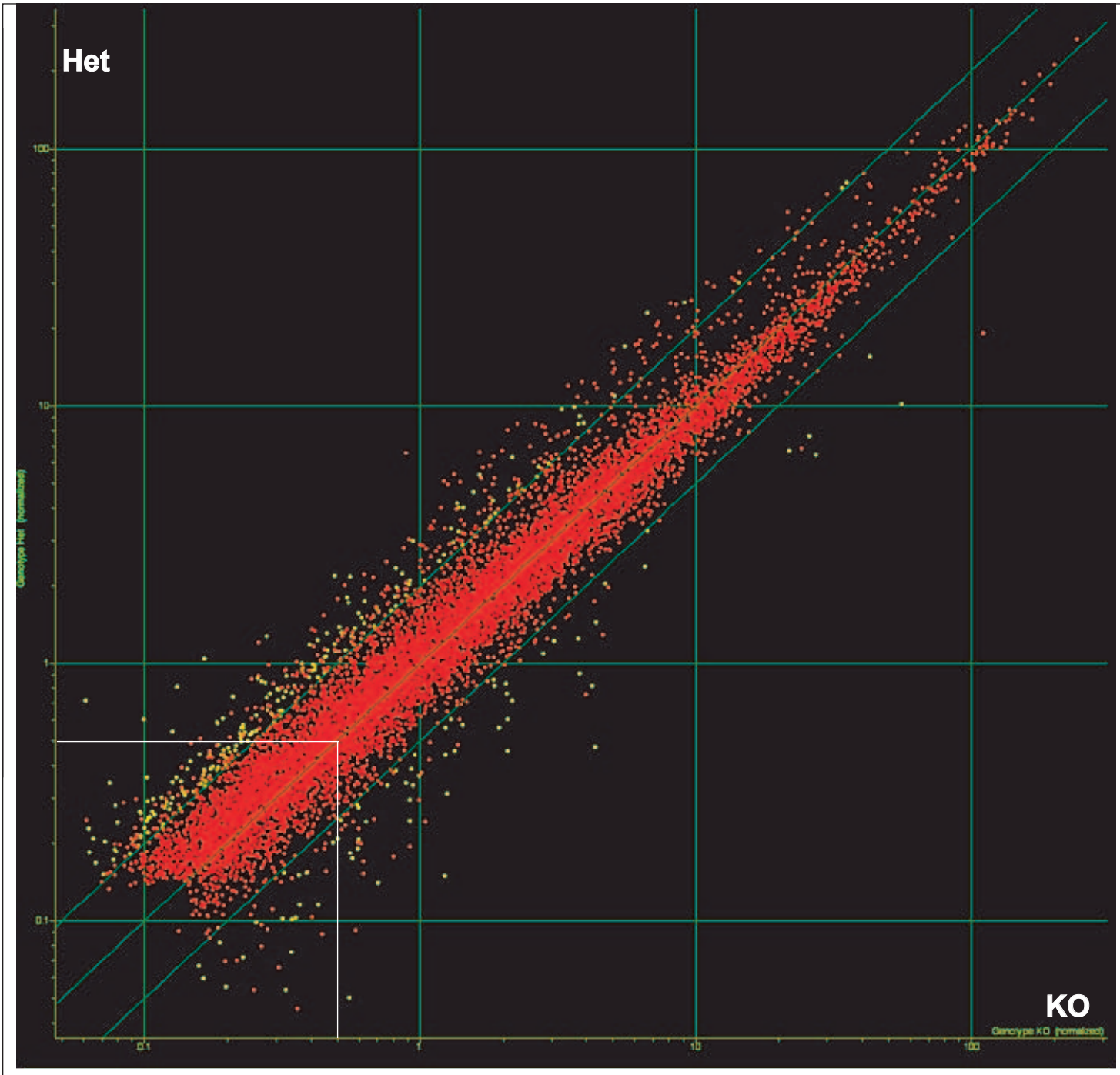

Figure 2.2.6 266 genes are differentially expressed in *Men1* deficient compared to heterozygous pituitary glands. Scatter plot of heterozygous vs. *Men1* deficient pituitary glands. All genes were normalised to the 50th percentile of all spots on each array. Genes that were expressed in either all the heterozygous or in all the *Men1* deficient samples were selected (10962 in total). The average intensity of the gene in the heterozygous pituitary glands is plotted against the average intensity of the gene in the knockout pituitary glands. The middle line along the diagonal indicates identity. The outer lines indicate 2 fold difference. Two sets of genes were generated that showed at least two fold difference in average expression between *Men1* deficient and heterozygous pituitary glands. 500 genes were were downregulated and 135 upregulated in the *Men1* deficient pituitary glands. To eliminate genes, where a single outlying datapoint would lead to an unrepresentative average, a students T-test was performed on the three biological replicates and only genes with a p-value less than 0.05 were considered. By these criteria, 199 genes were downregulated and 67 genes were upregulated more than 2 fold in *Men1* deficient pituitary glands. These genes are indicated with yellow colour on the scatterplot. The white lines indicate a cutoff of 0.5 in normalised intensity, which is common practice to identify meaningful datapoints. 127 downregulated genes and 49 downregulated were above this intensity. The axes are logarithmic.

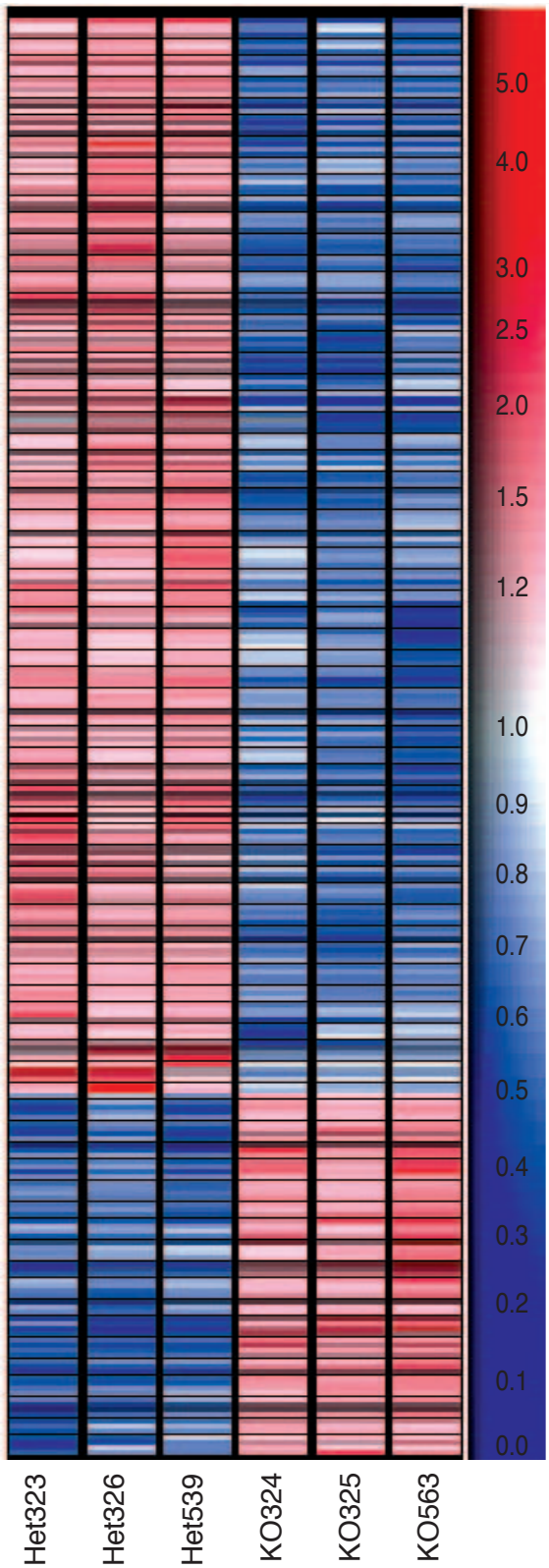

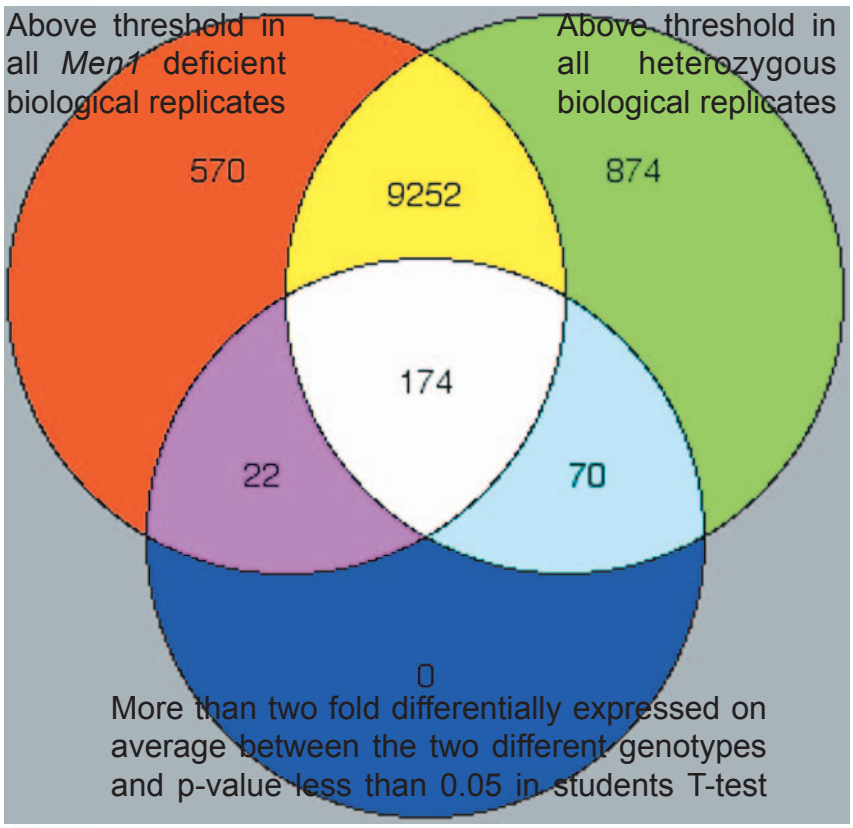

Figure 2.2.7 Expression analysis of deregulated genes. A For the 266 deregulated genes, all biological replicates are similar. Genetree of 266 deregulated genes in *Men1* deficient pituitary glands. Genes that were expressed in either all the heterozygous or in all the *Men1* deficient samples were selected (10962 in total). These genes were normalised to the 50th percentile of all spots on each array. Two sets of genes were generated that showed at least two fold difference in average expression between *Men1* deficient and heterozygous pituitary glands. A students T-test was performed on the three biological replicates and only genes with a p-value less than 0.05 were considered. 199 genes are downregulated and 67 genes are upregulated more than 2 fold in *Men1* deficient pituitary glands. The intensity of each gene on all microarrays was subsequently normalised to the median of the intensity of each gene across all samples. Note that therefore the values for the intensities are not comparable to those from Figure 2.2.6. **B Venn diagram of distribution of 266 genes deregulated in *Men1* deficient pituitary glands.** Venn diagram of 266 deregulated genes, the 10370 genes expressed at levels above the threshold value for each microarray in all three biological replicates of the heterozygous pituitary glands and the 10018 genes are expressed at levels above the threshold value in all three biological replicates of the *Men1* deficient pituitary glands. 70 of the 199 downregulated genes are not expressed at a detectable level in the *Men1* deficient pituitary glands. 22 of the 67 upregulated genes are not expressed at a detectable level in the heterozygous pituitary glands.

expressed in the heterozygous pituitary glands, the 10018 that were expressed in the *Men1* deficient pituitary glands and and the 266 deregulated genes. Of the downregulated genes, 70 cannot be detected in the *Men1* deficient pituitary glands. Conversely, 22 of the upregulated are not expressed in the heterozygous pituitary glands.

Table 2.1 and 2.2 shows the name and description of these genes as well as the fold up or down regulation in the knockout compared to the wildtype.

2.2.7 VIP, Cdc2/cyclin B and IGF1

The analysis of the *Men1* deficient pituitary glands had revealed an early hyperplasia phenotype, that was associated wih hyperproliferation in the pituitary glands of 12 week old *Men1* deficient pituitary glands. To elucidate the cause of this hyperproliferation, I inspected the gene lists for genes that had previously been associated with regulation of proliferation. I identified four genes that were clearly upregulated on the microarrays on the *Men1* deficient pituitary glands. These genes included those encoding *Vasoactive Intestinal Peptide* (*VIP*) 7.4 fold, *Insulin like Growth Factor 1* (*IGF1*) 4.6 fold, *Cdc2A* 3.0 fold and *CyclinB2* 3.7 fold.

VIP is a 28 amino acid peptide originally isolated as a glucagon related vasoactive peptide (Said *et al.*, 1972). It has subsequently been shown to regulate many other physiological activities including embryonic growth, activity of the immune system and neuronal growth and survival (Gozes *et al.*, 1999). In general, VIP causes vasodilation, bronchodilation, immunosuppression, smooth muscle relaxation and increased gastric motility (Gozes *et al.*, 1999). Importantly VIP increases hormonal secretion including Prolactin and GH from the pituitary gland (Gozes *et al.*, 1999) and Insulin from the pancreatic islets (Kato *et al.*, 1994). VIP is a member of a large peptide family whose members include Glucagon, GH Releasing Hormone (GHRH), Secretin and Pituitary gland cyclase activating hormone (PACAP). PACAP and VIP activate the same receptor (Gozes *et al.*, 1999). VIP is expressed from a mRNA that encodes a protein of 170 amino acids. This protein contains two very related peptide hormones VIP and PHI-27. Subsequent cleavage and processing releases the two hormones. Most of the biological activity of the transcript is attributed to VIP (Itoh *et al.*, 1983).VIP is mostly released through nerve terminals (Gozes *et al.*, 1999). VIP binds to two G-protein coupled receptors VPAC1 and VPAC2, that activates adenylate cyclase (Laburthe *et al.*, 1996). The resulting increase in cAMP activates PKA and leads to phosphorylation of

Tabel 2.1

Gene/description	Fold Down KO vs Het
NM_026358	11.1
Crabp1 cellular retinoic acid binding protein	6.4
Cabp2 calcium binding protein 2	6.1
Prostein prostein protein	5.6
Mab21l2 mab-21-like 2	4.7
Cpne7 copine VII	4.6
Clpx caseinolytic protease X	4.6
Trpv2 transient receptor cation channel	4.1
NM_146028	4.0
Pygm muscle glycogen phosphorylase	3.8
BB439385	3.7
Fxyd3 FXYD domain ion transport regulator	3.6
BE690945	3.6
Tm4sf7 transmembrane 4 superfamily	3.5
NM_030069	3.5
Slc7a1 solute carrier family 7	3.5
Rbp4 retinol binding protein 4	3.5
AK003491	3.5
Edr erythroid differentiation regulator	3.3
Col13a1 procollagen, type XIII,	3.2
Nkx2-4 NK2 transcription factor	3.2
BC017634	3.2
AK005465	3.2
AK006636	3.2
Rax retina and anterior neural homeobox	3.2
AK020483	3.2
Dhcr7 7-dehydrocholesterol reductase	3.1
Olfr157 olfactory receptor 157	3.1
Adh6a alcohol dehydrogenase 6A	3.1
NM_025685	3.0
Krt2-6a keratin complex 2-6a	3.0
olfactory receptor MOR171-7	3.0
AK014167	3.0
MOR3-1 olfactory receptor MOR3-1	3.0
Masp1 mannan-binding lectin serine protease	3.0
AK018700	2.9
AI158842	2.9
AK009469	2.9
AK010542	2.9
NM_023546	2.9
atrophin-1 tatorubral pallidoluysian atrophy	2.9
Cst11 cystatin 11	2.8
Mmp14 matrix metalloproteinase 14	2.8
AK004614	2.8
Ehd3 EH-domain containing 3	2.8
Hoxb7 homeo box B7	2.8
Plcd4 phospholipase C, delta 4	2.8
Jph2 junctophilin 2	2.7
Synpo2 synaptopodin 2	2.7
Slc6a3 solute carrier family 6 (dopamine)	2.7
Slitl2 Slit-like 2	2.7
olfactory receptor MOR267-4	2.7
AW492503	2.7
Cpxm2 carboxypeptidase X 2	2.7

Gene/description	Fold Down KO vs Het
BC016427	2.7
NM_028785	2.7
Cthrc1 collagen triple helix repeat	2.7
AK015259	2.6
C1sb complement component C1SB	2.6
Aldh1b1 aldehyde dehydrogenase 1 family	2.6
BC010552	2.6
NM_153158	2.6
Protectin CD59a antigen	2.6
Apbb1ip amyloid beta interacting protein	2.6
Xdh xanthine dehydrogenase	2.6
Slc9a3r1 solute carrier family 9 regulator 1	2.6
AV151664	2.6
Ccnt2 cyclin T2	2.5
AK007819	2.5
BE950979	2.5
Tnk1 tyrosine kinase, non-receptor, 1	2.5
AV328325	2.5
AK008737	2.5
Slc12a4 solute carrier family 12, member 4	2.5
NM_026083	2.5
NM_025749	2.5
AK007198	2.5
BM210487	2.5
BQ032470	2.5
AK009760	2.5
Mlc1 megalencephalic leukoencephalopathy	2.4
BE691581	2.4
AW456706	2.4
Gdf10 growth differentiation factor 10	2.4
Top3a topoisomerase (DNA) III alpha	2.4
Men1 multiple endocrine neoplasia 1	2.4
BB089777	2.4
Pla2g7 phospholipase A2	2.4
Klk6 kallikrein 6	2.4
ARH2 LDL receptor adaptor protein	2.4
IL-17RE Interleukin 17 receptor E	2.4
BB089777	2.4
NM_013737	2.4
NM_026606	2.4
Guca1b guanylate cyclase activator 1B	2.4
Scnn1a sodium channel, nonvoltage-gated	2.4
Ntn3 netrin 3	2.4
Mid1 midline 1	2.4
hypothetical protein 5230400M03	2.4
Traf1 Tnf receptor-associated factor 1	2.4
AK008235	2.4
Pacsin3 PKC and Casein kinase substrate	2.4
Clasp1 CLIP associating protein 1	2.4
Elovl4 elongation of very long chain fatty acids	2.4
Prelp proline arginine-rich, leucine-rich repeat	2.3
BB098221	2.3
NM_145366	2.3
Cklfsf7 chemokine-like factor super family 7	2.3

Tabel 2.1

Gene/description	Fold Down KO vs Het
Kcnc1 potassium voltage gated channel	2.3
Tpit T-box 19	2.3
Mrpl19 mitochondrial ribosomal protein L19	2.3
Rorb RAR-related orphan receptor beta	2.3
Slc38a2; solute carrier family 38, member	2.3
NM_029415	2.3
Kremen kringle containing transmembrane	2.3
NM_133751	2.3
Fbp2 fructose bisphosphatase 2	2.3
AK006490	2.3
olfactory receptor MOR266-1	2.3
taip-2	2.3
NM_146115	2.3
olfactory receptor MOR267-5	2.3
AV290652	2.3
AW048447	2.3
Adh8 alcohol dehydrogenase 8	2.3
AK013762	2.3
Cldn7 claudin 7	2.3
NM_025748	2.3
NM_138654	2.3
P38gamma mitogen-activated protein kinase	2.3
Stk10 serine/threonine kinase 10	2.3
Itpr5 inositol 1,4,5-triphosphate receptor 5	2.3
NM_019631	2.3
Temt thioether S-methyltransferase	2.3
BQ174653	2.3
ORF18 open reading frame 18	2.2
Sh3d4 SH3 domain protein 4	2.2
Ndr2 N-myc downstream regulated 2	2.2
Anxa11 annexin A11	2.2
Sardh sarcosine dehydrogenase	2.2
BM240122	2.2
Lor Mus musculus loricrin	2.2
BB211203	2.2
CD-RAP melanoma inhibitory activity	2.2
BG068423	2.2
NM_023256	2.2
Spp1 secreted phosphoprotein 1	2.2
Mark1 microtubule affinity-regulating kinase	2.2
Fshb follicle stimulating hormone beta	2.2
BC013092	2.2
PRECE-2 kallikrein 26	2.2
NM_028770	2.2
AK005003	2.2
BM198106	2.2
NM_145545	2.2
MLN51 MLN51 protein	2.2
Activin inhibin beta-A	2.2
BB342841	2.2
Ephb3 Eph receptor B3	2.2
AK014475	2.1
APO3L tumour necrosis factor ligand superfam.	2.1
Cited4 Cbp/p300-interacting transactivator	2.1

Gene/description	Fold Down KO vs Het
Tnip1 TNFAIP3 interacting protein 1	2.1
BF019837	2.1
Slc15a2 solute carrier family 15	2.1
Adh1 alcohol dehydrogenase 1	2.1
Stard13 serologically def.colon cancer antigen	2.1
hypothetical protein LOC227699	2.1
AK017526	2.1
Leutropin luteinizing hormone beta	2.1
TWIK-1 potassium channel, subfamily K	2.1
hypothetical protein D330010C22	2.1
AI586049	2.1
Mus musculus otoraplin (Otor), mRNA.	2.1
hesr3 hairy/enhancer-of-split related	2.1
Pet-1 Fev protein	2.1
AK002411	2.1
BC018252	2.1
AK003154	2.1
Bak1 BCL2-antagonist/killer 1	2.1
Gtl2 imprinted maternally expressed mRNA	2.1
AK017115	2.1
Sept9 septin 9	2.1
NM_028139	2.1
Kdt1 kidney cell transcript 1	2.1
Eph1 epoxide hydrolase 1	2.1
Gldc glycine decarboxylase	2.1
PHAS-I eIF4E binding protein 1	2.0
AW556148	2.0
Scya19 chemokine ligand 19	2.0
FBP1 folate receptor 1	2.0
Pcolce procollagen C-proteinase enhan. protein	2.0
AW556148	2.0
Scyb14 chemokine ligand 14	2.0
Gna14 guanine nucleotide binding protein14	2.0
E2f3 E2F transcription factor 3	2.0
Srebf1 sterol regulatory element binding factor	2.0
NM_145470	2.0
NM_172660	2.0

Tabel 2.1 199 genes were downregulated in *Men1* deficient pituitary glands. Genes that were expressed in either all the heterozygous or in all the *Men1* deficient samples were selected (10962 in total). These genes were normalised to the 50th percentile of all spots on each array. Genes were chosen whose average expression in the biological replicates were at least two fold lower in the *Men1* deficient than in the heterozygous pituitary glands . A students T-test was performed on the three biological replicates and only genes with a p-value less than 0.05 were considered. Gene name/description is shown as well as the fold downregulation. Red writing indicate genes that fall below the 0.5 expression threshold indicated in **Figure 2.2.6.**

Tabel 2.2

Gene/description	Fold Up KO vs Het
Plac1 placental specific protein 1	10.6
Scya8 chemokine (C-C motif) ligand 8	8.9
Vip vasoactive intestinal polypeptide	7.4
ribonuclease P 25kDa subunit	6.7
Penk1 preproenkephalin 1	5.2
Hist3h2ba histone 3, H2ba	5.1
Necl1 nectin-lke 1	5.1
AK013779	4.6
Igf1 insulin-like growth factor 1	4.4
Gng3 G protein, gamma 3 subunit	4.2
AK013855	4.0
Pnmt phenylethanolamine-N-methyltransferase	3.9
AK010426	3.7
Stmn2 stathmin-like 2	3.7
CycB2 cyclin B2	3.7
Calca-1 calcitonin/calcitonin-related polypeptide	3.5
C77158	3.4
Ube2c ubiquitin-conjugating enzyme E2C	3.4
Cnil cornichon-like (Drosophila)	3.4
Topk T-LAK cell-originated protein kinase	3.2
NM_026481	3.2
Crtl1 cartilage link protein 1	3.2
AK013867	3.1
NM_172515	3.1
Adcy8 adenylate cyclase 8	3.1
Ryr1 ryanodine receptor 1, skeletal muscle	3.1
Cdc2a cell division cycle 2 homolog A	3.0
Calb1 calbindin-28K	3.0
Atp1a3 ATPase, Na+/K+ transporting, alpha 3	3.0
NM_145967	3.0
AK005765	2.9
Vsnl1 visinin-like 1	2.9
Survivin baculoviral IAP repeat-containing 5	2.9
NM_029703	2.8
Nnmt nicotinamide N-methyltransferase	2.8
Cilp cartilage, nucleotide pyrophosphohydrolase	2.7
AK004470	2.7
AK008943	2.7
Fabp5 fatty acid binding protein 5, epidermal	2.7
Matador Bcl-2-related ovarian killer protein	2.6
AK008577	2.6
AK005178	2.5
Cyca cyclin A2	2.5
Nkd1 naked cuticle 1 homolog	2.5
Myoc myocilin	2.5
Lck lymphocyte protein tyrosine kinase	2.5
Prc1 protein regulator of cytokinesis 1	2.4
AK011241	2.4
NM_020591	2.3
Bmp2 bone morphogenetic protein 2	2.3
NM_172920	2.3
Mill2 MHC I - like leukocyte 2	2.3
Galnt3 N-acetylgalactosaminyltransferase 3	2.3
Padi1 peptidyl arginine deiminase, type I	2.3
NM_023396	2.3
NM_025572	2.3
Cycb-4 cyclin B1	2.2
Zbp1 Z-DNA binding protein 1	2.2
Ubce8 ubiquitin-conjugating enzyme 8	2.2
Cxcl13 chemokine (C-X-C motif) ligand 13	2.1
Fxyd2 FXYD domain ion transport regulator 2	2.1
Bcl11a B-cell CLL/lymphoma 11A	2.1
NM_133851	2.1
Pnma1 paraneoplastic antigen MA1	2.1
AK011311	2.1
Faim2 Fas apoptotic inhibitory molecule 2	2.0
Bscl2 Bernardinelli-Seip congenital lipodystroph	2.0

Tabel 2.1 67 genes were upregulated in *Men1* deficient pituitary glands. Genes that were expressed in either all the heterozygous or in all the *Men1* deficient samples were selected (10962 in total). These genes were normalised to the 50th percentile of all spots on each array. Genes were chosen whose average expression in the biological replicates were at least two fold higher in the *Men1* deficient than in the heterozygous pituitary glands . A students T-test was performed on the three biological replicates and only genes with a p-value less than 0.05 were considered. Gene name/description is shown as well as the fold downregulation. Red writing indicate genes that fall below the 0.5 expression threshold indicated in **Figure 2.2.6.**

CREB. cAMP also activates the mitogen activated protein kinase (MAP kinase) pathway through the GTPase Rap1 (Romano *et al.*, 2003). As mentioned in the introduction, cAMP is a mitotic signal in cells of the endocrine system, which is also reflected by the frequent mutations to *Gαs* and *PRKAR1α* in endocrine cancers (Lania *et al.*, 2001)(Kirschner *et al.*, 2000).

Cdc2 also known as Cdk1, is thought to be the key initiator of mitosis in vertebrate cells (Takizawa *et al.*, 2000). Activated Cdc2/Cdk1 mediates cytosolic events such as centrosome segregation and nuclear events such as nuclear envelope breakdown (Takizawa *et al.*, 2000).
Cdc2/Cdk1 is a cyclin dependent kinase that is dependent on binding to Cyclin B1 or Cyclin B2 for its activity. In addition to the availability of Cyclin B, the activity of the Cdc2/Cdk1 kinase is controlled by many independent mechanisms including inhibitory phosphorylation of Cdc2/Cdk1 by the Wee kinase and activating dephosphorylation through Cdc25. The activity of the Cdc2/Cdk1-Cyclin B complex is also regulated by phosphorylation of Cyclin B and the subcellular localisation of the complex (Takizawa *et al.*, 2000).

IGF1 is a 7 kDa polypeptide highly related to insulin that functions as a growth and survival factor. The main function of IGF1, and the related IGF-2 is thought to be mediating the anabolic and mitogenic effects of GH (Laron, 2001). GH increases systemic IGF1 by stimulating endocrine IGF1 production from the liver. GH also stimulates paracrine production of IGF1 in many other tissues (Laron, 2001). IGF1 stimulates prenatal and postnatal growth and IGF1 deficient mice are 30 percent smaller than their wildtype littermates and show severe postnatal growth retardation (Liu *et al.*, 1993).
IGF1 and the related IGF2 signal through the IGF1R. This receptor tyrosine kinase exists a tetramer composed of two α and two β subunits both encoded by the same gene (Sachdev *et al.*, 2001). Upon IGF binding the receptor autophosphorylates and binds to target proteins that are then phosphorylated. Among these IGF receptor binding proteins are proteins of the IRS family. These proteins function as adaptor proteins that recruit several signal transduction molecules (Sachdev *et al.*, 2001). The most important downstream mediators of IGF signalling are the PI3K, the STAT and the Ras pathways (Sachdev *et al.*, 2001)(Surmacz *et al.*, 2003). Through these effectors the IGF receptor can activate pathways that control proliferation as well as apoptosis. The Ras pathway is one of the most well characterised proliferation promoting signals. Ras activates several kinase cascades that lead to the

activation of several MAP kinases. The PI3K pathway is well characterised as an anti-apoptotic pathway. PI3K phosphorylates inositol phosphates that subsequently activate PKB/AKT. PKB/AKT promotes survival by phosphorylating and inhibiting the proapoptotic protein Bad (del Peso *et al.*, 1997).

2.2.8 Analysis by *in situ* hybridisation of deregulated genes

To verify the microarray results and to investigate the expression pattern of the potential mediators of the hyperplasia and hyperproliferation associated with *Men1* loss, I cloned *in situ* hybridisation probes from a pituitary gland cDNA library or from chromosomal DNA for the genes encoding VIP, IGF1, Cdc2A and Cyclin B2. **Figure 2.2.8** shows the expression of *VIP*, *IGF1* and *Cdc2a* in sections from both male and female mice, either wildtype, heterozygous or homozygous for *Men1* in the Pit-1 lineage. In the 41.5 week old heterozygous pituitary gland, a macroscopic adenoma was observed in the left side of the pituitary gland (not shown), which showed no hybridisation signal with the *Men1* exon 3-6 probe (see **Figure 2.2.1 C** for the *Men1 in situ* hybridisation of sections from the same heterozygous pituitary gland).

As the microarray data suggested, *VIP* is clearly overexpressed in 13 week old male pituitary glands. Moreover the overexpression appears to be concentrated in patchy structures scattered over the posterior lobe. Interestingly however, *VIP* is expressed many folds higher in female *Men1* deficient pituitary glands at both 7 and 13 weeks of age. Although the level of *VIP* expression in the female pituitary glands is many fold higher than in male, *VIP* still appears to be expressed in patchy structures and in some sections *VIP* expression appears to be concentrated along the upper edge of the anterior lobe. Importantly, *VIP* is also many fold overexpressed in the *Men1* deficient outgrowth of the 41.5 week old heterozygous pituitary gland, suggesting that *VIP* overexpression is also associated with the clonal expansion of *Men1* deficient cells occurring during MEN1 tumourigenesis.

The expression of *Cdc2* is similar to that of *VIP*. Again, expression is much higher in *Men1* deficient female pituitary glands than in male pituitary glands. The *Cdc2* signal is concentrated in small punctate structures. Like *VIP*, *Cdc2* is also clearly overexpressed in the *Men1* deficient clonal outgrowth of the heterozygous pituitary gland.

The overexpression of *IGF1* in the male *Men1* deficient pituitary gland is not as apparent as the microarray would suggest. However, in the female *Men1* deficient pituitary gland at 13 weeks, there is a very clear overexpression of *IGF1*. Unlike *VIP* and *Cdc2*, *IGF1* is

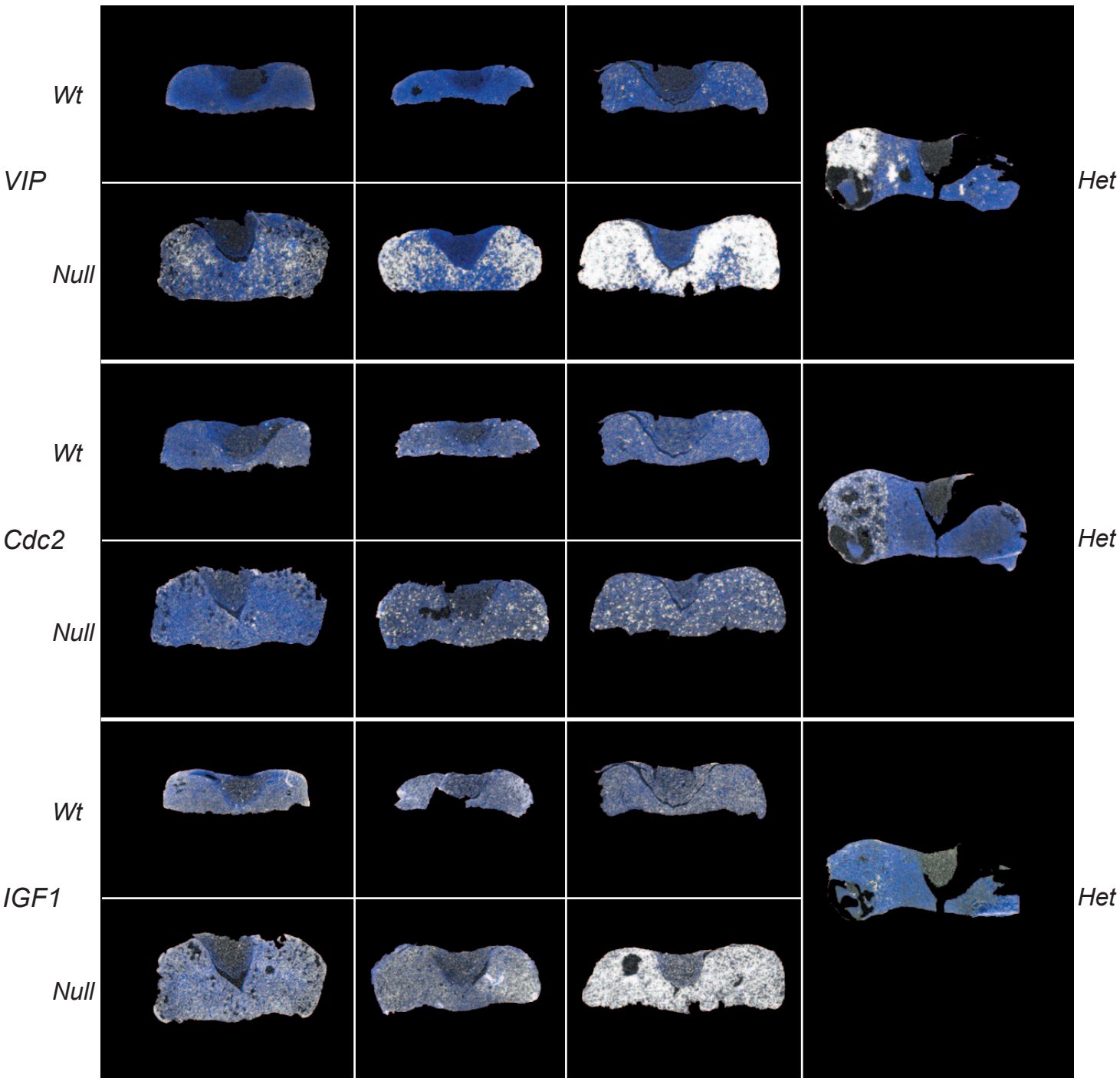

Figure 2.2.8 *VIP*, *Cdc2* and *IGF1* are overexpressed in *Men1* deficient pituitaries. *In situ* hybridisation of 18 µm cryosections. Sections of male and female pituitaries from $Men1^{LoxP\text{-}Frt/Frt}$ *(Wt)*, $Men1^{LoxP\text{-}Frt/Null}$*/Pit-1-Cre (Null)* and $Men1^{LoxP\text{-}Frt/Null}$ *(Het)* mice with the indicated ages were hybridised with the indicated probes. The *VIP* staining shows a patchy expression pattern and is strongest along the upper periphery of the anterior lobe. *Cdc2* signal is concentrated in punctate structures spread over the anterior lobe of the *Men1* deficient pituitary glands. The *IGF1* signal is more homogeneously spread over the anterior lobe. In the heterozygous pituitary glands *VIP*, *Cdc2* and *IGF1* are overexpressed in the clonal outgrowth, which has lost *Men1* expression (see Figure 2.2.1). The ^{35}S labeled *in situ* probe was visualised by 4 weeks of incubation with Kodak NTB2 and the tissue counterstained with Bisbenzimide. Photographs were done on the Leica MZFLIII microscope.

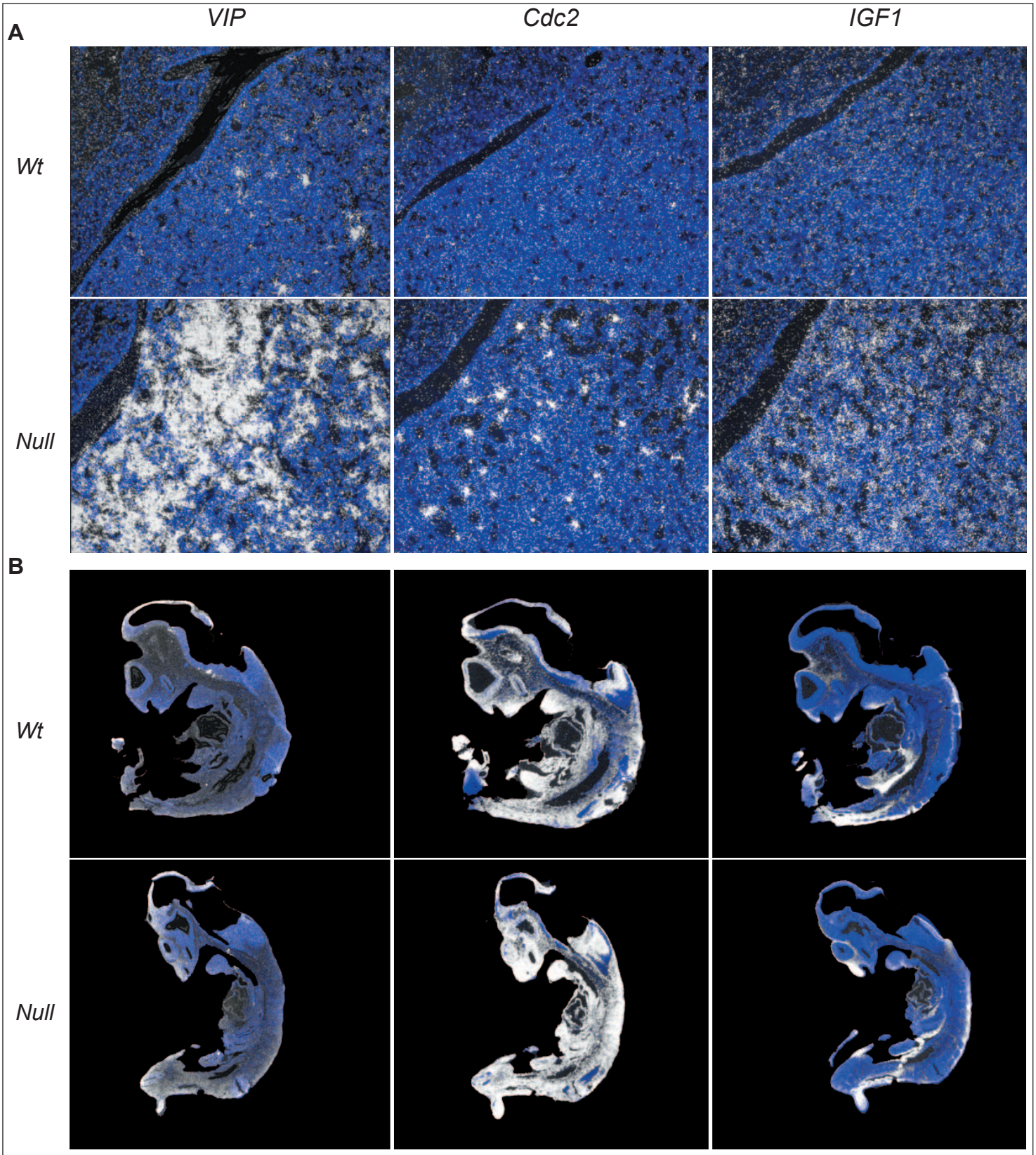

Figure 2.2.9 *VIP*, *Cdc2* and *IGF1* are overexpressed in *Men1* deficient pituitaries but not in *Men1* deficient embryos. *In situ* hybridisation of 18 µm cryosections. The S^{35} labelled *in situ* probe was visualised by 4 weeks of incubation with Kodak NTB2 and the tissue counterstained with Bisbenzimide **A** 13 week female pituitaries from $Men1^{LoxP\text{-}Frt/LoxP\text{-}Frt}$ *(Wt)* and $Men1^{LoxP\text{-}Frt/LoxP\text{-}Null}$*/Pit-1-Cre (Null)* mice were cryosectioned and hybridised with the probes indicated. Photographes were done on the Leica DC500 Axiophot with a 20 times objective. **B** 11.5 day old $Men1^{wt/wt}$ *and* $Men1^{LoxP\text{-}Null/LoxP\text{-}Null}$ embryos were cryosectioned and and hybridised with the indicated probes. Photographes were done on the Leica MZFLIII microscope .

homogenously expressed in the anterior and this may also make the overexpression more difficult to detect in the *in situ* hybridisation experiment. *IGF1* is also overexpressed in the *Men1* deficient part of the heterozygous pituitary gland, although not as clearly as *VIP* and *Cdc2*.

CyclinB expression was not observed in any of the pituitary gland sections (data not shown). This discrepancy between the microarray data and the *in situ* results could be the result of alternative splicing of an exon hybridising to the 30 bp microarray probe .

Figure 2.2.9 A shows higher magnification microscopy of the *in situ* hybridisation of the 13 week female pituitary glands. In this magnification, the patchy expression of *VIP* and *Cdc2* and the more homogenous expression of *IGF1* is clearly visible. As the conditional knockout approach only allowed us to assess the effect on gene expression of *Men1* deletion in the pituitary gland, I also performed *in situ* hybridisation on E11,5 wildtype and $Men1^{LoxP\text{-}Null/Null}$ embryonic sections. As **Figure 2.2.9 B** shows, *Men1* deficient embryos are clearly smaller than their wildtype counterparts at this stage, however there is no major difference in the expression levels of *VIP*, *Cdc2* and *IGF1* in the embryos.

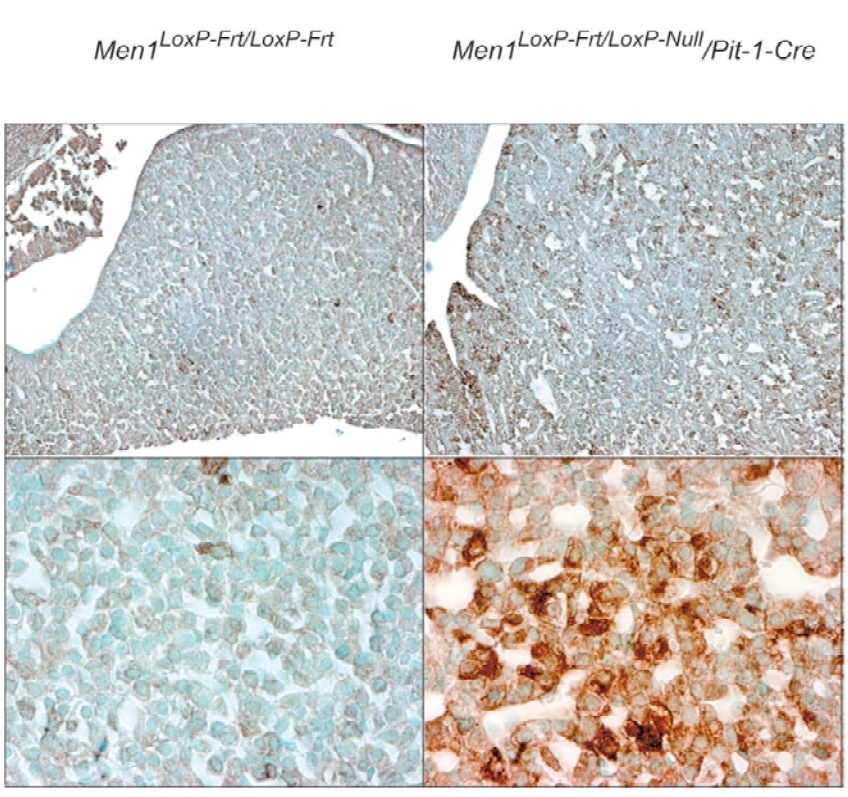

Figure 2.2.10 VIP is upregulated in *Men1* deficient pituitaries. Anti VIP immunohistochemistry on $men1^{LoxP\text{-}Frt/LoxP\text{-}Frt}$ and $men1^{LoxP\text{-}Frt/LoxP\text{-}Null}$/*Pit-1-cre* mice. 12 week old female mice were perfused with 2 percent PFA and pituitaries were fixed overnight in 2 percent PFA. The pituitaries shown are representative of their age and genotype. 7 µm paraffin sections were probed with the VIP antibody from Chemicon in a 1:750 dilution. Antigen was recovered using the plain method. Bound antibody was detected with HRP coupled 2nd antibody and DAB substrate without nickel. The tissue was counter stained with Methyl Green. Pictures were done on the Leica Axiophot microscope

2.2.9 Analysis of VIP expression by immunohistochemistry

To verify that the overexpression of VIP mRNA also results in an overexpression of VIP peptide, I probed pituitary gland sections with an antibody against VIP. **Figure 2.2.10 A**

shows that *Men1* deficient pituitary glands clearly overexpress the VIP protein. The pattern of staining overlaps with that of the mRNA signal. The strongest VIP signal can be seen along the upper edges of the anterior lobe close to the intermediate lobe, but VIP expressing cells can also be found scattered over the entire anterior lobe.

2.3 Screening for novel Menin interaction partners

2.3.1 Yeast two hybrid screening for novel Menin interactors

To identify new interaction partners of Menin, I undertook a yeast two hybrid screening using Menin as a bait. In a first attempt, I used the Cytotrap system from Stratagene with little success. The Cytotrap system is a yeast two hybrid system based on cytosolic interactions. In a second attempt, I used the Matchmaker Gal4 two hybrid system from Clontech. Menin was fused to the Gal4 DNA binding domain (Gal4-DB) and cotransformed into the yeast strain AH109 together with a self-made randomly primed pituitary gland library fused to the activation domain (Gal4-AD) of Gal4. The AH109 strain carries two independent selectable markers encoding the *Ade2* and *His3* genes that are dependent on interaction between bait and target for expression. Approximately $3x10^6$ transformants were assayed for adenine and histidine independent growth and 109 colonies were isolated that grew on medium selecting for both genetic markers. DNA was isolated from the yeast and electroporated into E.coli. Bacterial DNA was then isolated and analysed by restriction digestion to identify the library plasmid.

Isolated plasmids were retransformed into AH109 together with Menin-Gal4-DB or with Gal4-DB. 22 plasmids were identified that promoted growth when cotransformed with Menin-Gal4-DB but not with Gal4-DB alone (**Figure 2.3.1**). These plasmids were sequenced. 9 different genes were identified. **Table 2.3** shows the name, the number of yeast clones and the approximate fragment size and position for each gene.

Among the isolated genes are two genes encoding previously published Menin interacting proteins, JunD and Vimentin, confirming the validity of the system. Trip11/GMAP210 was found most frequently with 10 out of 22 positive clones. All of these clones were identical judged by restriction digest and 5' sequencing. The second most frequent insert encoded a predicted novel gene, referred to as GAD5. This insert was found in 4 positive plasmids. All of these inserts were also identical. JunD was identified with two different fragments each encoding almost the entire reading frame of the protein. All other clones were unique. The growth rate of the yeast on selective plates reflects the strength of the interaction between bait and target protein, as well as the expression level and availability of the target-Gal4 fusion. Judged by growth rate the interaction of Menin with Trip11 was the strongest and the interaction of Menin with Spectrin and Gad27 the weakest. All other interactions were of intermediate strength.

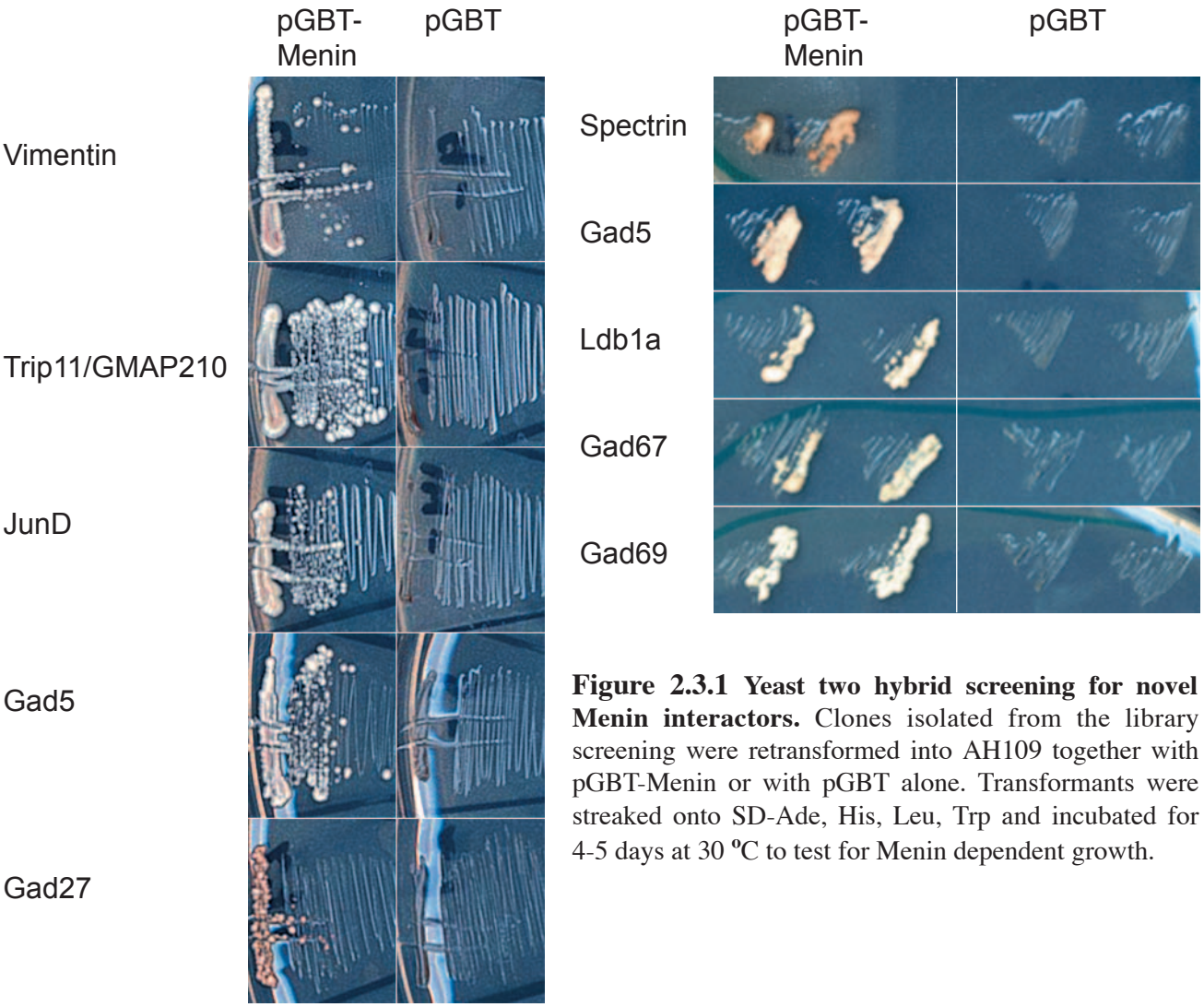

Figure 2.3.1 Yeast two hybrid screening for novel Menin interactors. Clones isolated from the library screening were retransformed into AH109 together with pGBT-Menin or with pGBT alone. Transformants were streaked onto SD-Ade, His, Leu, Trp and incubated for 4-5 days at 30 ºC to test for Menin dependent growth.

Table 2.3

Gene	Number of clones	Size of encoded protein fragment
Trip11/GMAP210	10	aa 732 - 957
Gad5	4	app. 630 aa
JunD	2	aa 23 - 341 aa 1 - 319
Vimentin	1	aa 1 - app.430
Spectrin	1	aa 350 - app.780
Ldb1a	1	aa 1 - app 340
Gad27	1	app. 900 aa
Gad67	1	415 aa
Gad69	1	app. 400 aa

Of the seven novel Menin interaction partners, three have already been cloned and characterised in mammals.

2.3.2 Previously characterised genes as novel Menin interactors

Trip11/GMAP210/Trip230

Trip11/GMAP210 was originally characterised as a Thyroid Hormone Receptor (TR) interacting protein (Lee *et al.*, 1995). The protein encoded by the gene is 1979 amino acids in length. Trip11/GMAP210 has been shown to act as a transcriptional coactivator for TR in a Thyroid Hormone dependent manner (Chang *et al.*, 1997). Furthermore, Trip11/GMAP210 binds to RB and this binding prevents Trip11/GMAP210 from acting as a transcriptional coactivator for TR (Chang *et al.*, 1997).

Surprisingly, Trip11/GMAP210 has also been shown to be a Golgi apparatus associated Protein that binds to the minus end of microtubules (Infante *et al.*, 1999). Furthermore, overexpression of Trip11/GMAP-210 blocks transport between the endoplasmic reticulum and the Golgi apparatus (Pernet-Gallay *et al.*, 2002).

This apparent paradox may be explained by the observation that upon Thyroid Hormone addition Trip11/GMAP210 becomes phosphorylated and then translocates from the Golgi apparatus to the nucleus (Chen *et al.*, 1999).

Spectrin β2/ELF

Spectrin is a tetrameric actin cross-linking complex consisting of two α and two β subunits. In mammals there are five genes encoding β Spectrin (Tang *et al.*, 2002). Spectrin β2 gives rise to at least 3 different isoforms, all encoding proteins of roughly 2000 amino acids. They all share the region encoded by the insert from the yeast two hybrid clone .

Interestingly, the knockout of Spectrin β2 in the mouse gives a phenotype similar to that of double heterozygous Smad2/Smad3 animals (Tang *et al.*, 2003).

Furthermore, Spectrin β2 interacts with Smad3 and Smad4 but not Smad2, and Spectrin β2 translocates to the nucleus upon TGF-β stimulation. Finally TGF-β signalling is disrupted in Spectrin β2 null mouse embryonic fibroblasts (Tang *et al.*, 2003).

Ldb1a

Ldb1a is a transcriptional cofactor that was first characterised as a cofactor for the Lim homeodomain family of transcription factors (Agulnick *et al.*, 1996). In Drosophila it has been shown to interact with several other transcription factors including Bcd, Ftz and SuHw (Matthews *et al.*, 2003). Knockout studies in the mouse have shown that *Ldb1a* is required for normal anterior posterior patterning as well as heart development (Mukhopadhyay M, 2003).

2.3.3 Novel proteins interacting with Menin

Four of the novel Menin interacting proteins had not previously been characterised in mammals. These were referred to Gad5, Gad27, Gad67 and Gad69 from the name of the vector and the number of their respective yeast clone.
The sequences of these yeast two hybrid inserts were blasted against the NCBI nucleotide database. For each of the novel genes, a prediction based on the genomic sequence and/or ESTs was available.

Gad5 is predicted be part of a gene that encodes a protein of 730 amino acids that contains domains homologous to GTPase accelerating proteins for Rab-like GTPases. The accession number of the predicted gene is XM_283964
Gad27 is predicted to be part of a transcript encoding a protein of 1330 amino acids that has homology to Guanine nucleotide exchange factors for Rho like GTPases. The accession number of the predicted gene is XM_147847
Gad67 is predicted to be part of a gene that encodes a Bromodomain containing protein
Gad69 is part of a gene predicted to encode a protein of 542 amino acids with no recognised domains or significant homology to any characterised protein. The accession number of the predicted gene is BC034212

The inserts from the yeast two hybrid library clones were cloned into the Bluescript vector and used as probes in *in situ* hybridisation on embryonic and adult mouse sections.
Gad5, Gad27 and Gad69 did not show any distinct expression at E11.5, E13.5, E17.5 heads or E18,5 heads as well as adult pituitary gland, kidney and adrenal glands (data not shown).

2.3.4 Expression pattern of Gad67 and cloning of cDNA

The *in situ* analysis with the Gad67 probe revealed that the gene showed an expression pattern that suggests an almost ubiquitous expression of Gad67 (**Figure 2.3.2**). At E11,5, the strongest expression was in Rathke's pouch, the precursor to the pituitary gland, and the roof of the midbrain. At E13,5, the strongest expression was in the developing pituitary gland, roof of the neopallial cortex, the gastroduodenal junction, kidney and cartilage of vertebrate. Gad67 expression was distinctly absent from the liver. In E17,5 heads, the strongest signal was from the subventricular zone, olfactory epithelium and pituitary gland. At E18.5 the choroid plexus showed a very specific and strong signal.

To further characterise Gad67, I decided to clone the complete cDNA of the gene.

To this end, I probed a pituitary gland cDNA phage library with the yeast two hybrid library insert. One positive clone was isolated that contained a 3525 bp fragment overlapping 92 bp with the probe. Sequencing revealed that this fragment contained the 5' end of an open reading frame that stretched through the yeast two hybrid clone. ESTs suggested that the open reading frame continued for approximately 1000 bp downstream of the yeast two hybrid clone. To clone this 3' fragment, I performed PCR on a pituitary gland cDNA library with a primer within the yeast two hybrid clone and a primer downstream of the predicted termination codon of the open reading frame. A 1000 bp fragment was cloned and sequenced.

The full length cDNA is 5542 bp. Alignment with the mouse genome revealed that the gene is positioned on the X chromosome where it is encoded by 40 exons. The open reading frame of Gad67 begins in exon1 and stretches 5244 bp. The encoded protein is 1747 amino acids in length. **Figure 2.3.2 B-C** shows the amino acid sequence and predicted structural domains of the protein. Gad67 has two predicted domains. In the N-terminus there is a WD40 repeat region of 322 amino acids and in the C-terminus a double Bromodomain. The yeast two hybrid clone overlaps precisely with the Bromodomain as indicated in **Figure 2.3.2 B**, suggesting that Menin binds to the Bromodomain of Gad67. In mammals two homologous proteins have been identified, WDR9 and WDR11. Orthologues have been predicted but not characterised in *Danio Rerio*, *Gallus Gallus* and *Drosophila*.

WD40 repeat domains, also called WD or transducin repeats, consist of an approximately 40 amino acid core domain that is repeated 4 to 16 times (Li *et al*., 2001). Gad67 contains seven WD40 repeats. The WD40 repeat domain forms a stable β-propeller structure (Wall *et al*., 1995), which is believed to function as a rigid platform for protein complex assembly (Li D, 2001). The mouse genome contains 190 predicted WD40 domain containing proteins. WD40

A

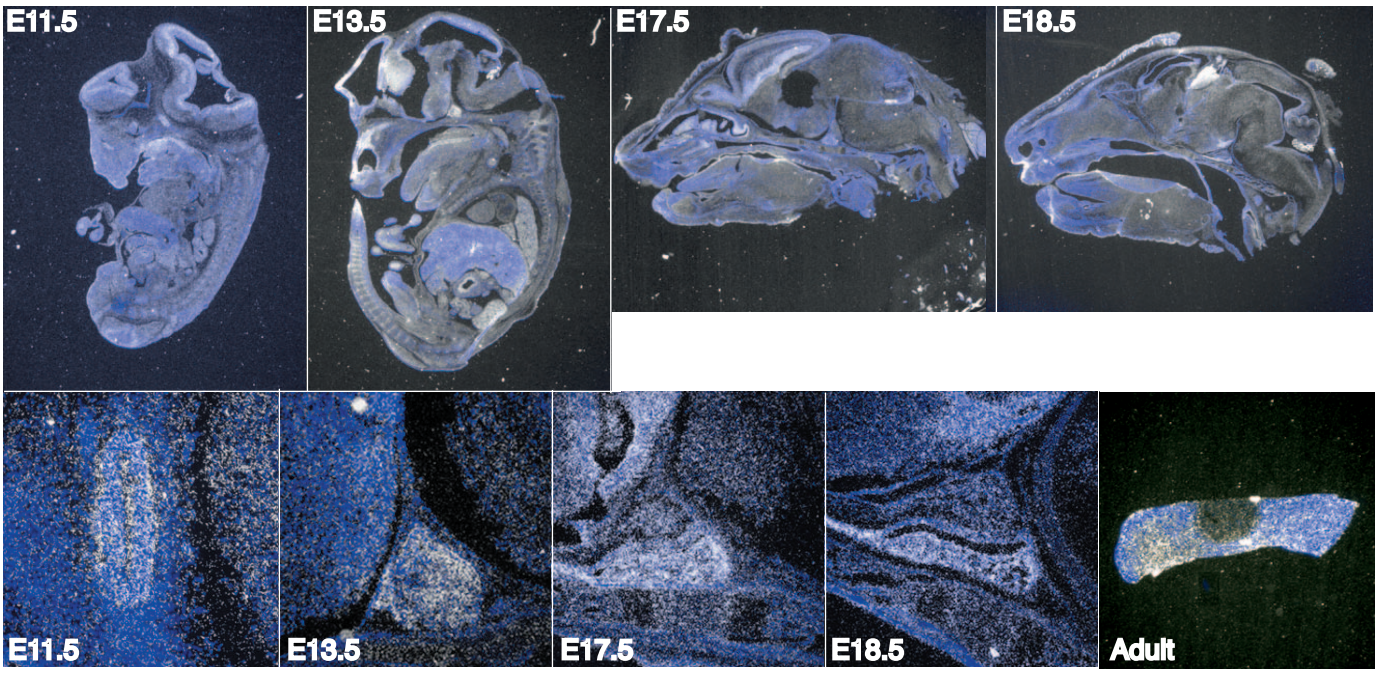

B

MAAAPTQIEAELYYLIARFLQSGPCNKSAQVLVQELEEHQLIPRRLDWEGKEHRRSFEDLVAANAHIPPDYLLKICERIGPL
LDKEIPQSVPGVQTLLGVGRQSLLRDAKDCKSTLWNGSAFAALHRGRPPELPVNYVKPPNVVNITSARQLTGCSRFSHV
FPSSAYQHIKMHKRILGHLSSVYCVAFDRSGRRIFTGSDDCLVKIWATDDGRLLATLRGHSAEISDMAVNYENTLIAAGSC
DKVVRVWCLRTCAPVAVLQGHSASITSIQFCPSTKGTTRYLTSTGADGTICFWQWHVKTMKFRDRPVKFTERSRPGVQI
SCSSFSSGGMFITTGSTDHVIRIYYLGSEIPEKIAELESHTDKVVAVQFCNNGDSLRFVSGSRDGTARIWQYQQQEWKSIV
LDMATKMSGNNLTSAEDKVTKLKVTMVAWDRYDTTVITAVNNFLLKVWNSVTGQLLHTLSGHDDEVFVLEAHPFDQRIILS
AGHDGNIFIWDLDRGTKIRNYFNMIEGQGHGAVFDCKFSPDGNHFACTDSHGHLLLFGFGCSKYYEKIPDQMFFHTDYR
PLIRDANNYVLDEQTQQAPHLMPPPFLVDVDGNPHPTKFQRLVPGRENCKDEQLIPQLGYVANGDGEVVEQVIGQQTND
QEESILDGIIRELQREQDLRLINEGDVPHFPINRSYSVNGALSSPNMDIPSSPNIGLRRSGQIEGVRQMHNNAPRSQMATE
RDLMAWSRRVVVNELNSGVSRVQEECRNAKGDLEVSLYTVEKKKKPSYPIQRNDYQPSCGRSLRRTQRKRQHTYLTRS
NIEHNSQASSQTSGVQEDSDSSSEEDETVGTSDASVEDPVVEWQSESSSSDSSSEYSDWIADAGINLQPPKRQTRQAT
QKIYSSSEDENLKLEDRQKKPKQTKKKKGGLVSMAGEPNEEWLAPQWILDTIPRRSPFVPQMGDELIYFRQGHEAYVRA
VRKSKIYSVNLQKQPWNKMDLREQEFVKIVGIKYEIGPPTLCCLKLAFLDPISGKMTGESFSIKYHDMPDVIDFLVLHQFYN
EAKERNWQIGDRFRSIIDDAWWFGT**VESQQPFQPEYPDSSFQCYSVHWDNNEREKMSPWDMEPIPDGTAFPDEVGAG**
IPVSQEELTALLYKPQEGEWGAHSRDEECERVIQGINNLLSLDFASPFAVPVDLSAYPLYCTVVAYPTDLNTIKQRLENRFY
RRISALMWEVRYIEHNARTFNEPDSPIVKAAKIVTDVLLRFIGDQSCADILDTLQLKSKPEDPDSSDLEEDSEMVDLDSDG
PGTSSGRRAKCRGRRQSLKCNPDAWKKQCEELLSLIYEREDSEPFRQPADPQSYPVQQQQEGESSQSVPPDRQDPSL
SEDYQDGIDTPMDFSTVKETLESGNYDSPLEFYKDVRQIFSNSKAYTSNKKSRIYSMTLRLSALFENHIKNIISDYKSAIQS
QKRRRPRYRKRLRSSSSSLSSSRAPSPKGKQKQMKLQPKNDQNTSVAYARTSSPFSSPDHSLDGPLTNVDGREPRTGA
KRKLLSASEEDESMGGEEKEMKETKEQVHLSSSESGELGSSLSSESTSGSDSDSESTSRTDQDYVDGDHDYSKFIQTR
PKRKLRKQHTNGKRNWKTRGTGGRGRWGRWGRWSRGGRGRGGRGRGGRGRGGGGGRGRGRGRGGRGASRGS
SRAKRARVADDEFDTMFSGRFSRLPRIKTRNQGRRTVLYNDDSDNDNFVSTEDPLNLGTSRSGRVRKMTEKARVSHLM
GWNY

C

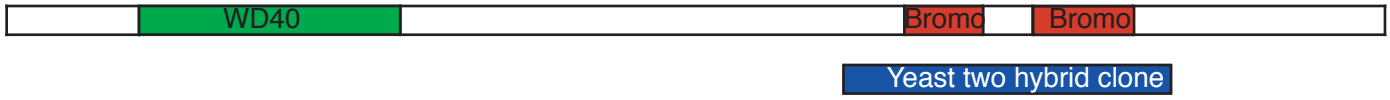

Figure 2.3.2 Cloning and characterisation of *Gad67*. A *Gad67* is expressed in the pituitary gland and many other tissues. *In situ* hybridisation of embryonic and adult cryosections with a 1200 bp *Gad67* probe corresponding to the yeast two hybrid clone. The ^{35}S labeled *in situ* probe was visualised by 4 weeks of incubation with Kodak NTB2 and the tissue counterstained with Bisbenzimide. Photographs were done on the Leica MZFLIII microscope **Top** sagital sections of embryos at E11,5 and E13,5 and sagital head sections of embryos at E17,5 and E18,5 **Bottom** close up of pituitaries from same sections. **B** Complete amino acid sequence of Gad67. The full length cDNA of *Gad67* was cloned by screening of a pituitary gland λ-phage library and by PCR from a pituitary gland cDNA library. The part of the protein encoded by the yeast two hybrid clone is highlighted in blue. **C** Predicted domain structure of protein encoded by the full length cDNA**.** The protein was predicted to contain a WD40 domain and a double Bromodomain by the Conserved Domain Database at NCBI. The yeast two hybrid clone overlaps precisely with the predicted double Bromodomain.

repeat proteins have been shown to be involved in biological processes such as signal transduction (G-protein β-subunit, RACK1 and Stratin), RNA synthesis (most TFIID associated factors – TAFs), chromatin assembly (CAF-1, HIR1 and HIR2), cell cycle regulation (CDC20, Mad2), programmed cell death (Apaf1) (Li *et al.*, 2001) and transcriptional repression (Groucho/TLE1) (Pickles *et al.*, 2002).

The Bromodomain was originally characterised in the Drosophila protein Brahma (Tamkun *et al.*, 1992). Bromodomains specifically recognise acetylated Histones (Dhalluin *et al.*, 1999). Activation of transcription often involves Histone acetylation on specific lysines followed by the remodelling of nucleosomes by ATP dependent chromatin remodelling complexes (Agalioti *et al.*, 2002). Many chromatin associated proteins and nearly all Histone acetyl transferases contain Bromodomains (Jeanmougin *et al.*, 1997). Additionally, all known SWI/SNF like ATP dependent chromatin remodelling complexes contain a Bromodomain protein (Marmorstein *et al.*, 2001). Thus most Bromodomain containing proteins are involved in chromatin remodelling processes.

3 Discussion

3.1 loss of *Men1* leads to pituitary gland hyperplasia and adenoma formation.

To elucidate the role of *Men1* in tumourigenesis of the endocrine system and specifically of the pituitary gland, I established a conditional mouse model of the MEN1 syndrome. Using homologous recombination I replaced the *Men1* coding region with a targeting vector containing two LoxP sites and a positive selection marker flanked by two Frt sites. When intercrossing mice heterozygous for the targeted allele I obtained no homozygous animals, showing that the positive selection cassette disrupted the expression of Menin, and that Menin is required for the embryonic development of the mouse. This has also been reported by two other groups, who found that *Men1*$^{-/-}$ embryos die around embryonic day 11.5 with multiple defects (Crabtree *et al.*, 2001)(Bertolino *et al.*, 2003a).

By crossing to FlpE expressing mice, the Frt site flanked positive selection cassette was successfully excised. The resulting floxed allele was functional and animals homozygous for the floxed *Men1* allele appeared at the expected mendelian ratio. Importantly, the LoxP sites allowed efficient Cre mediated excision of exons 3 to 7 of the *Men1* allele leading to absence of Menin expression.

By crossing the floxed *Men1* allele into *Pit-1-Cre* expressing mice, I specifically deleted *Men1* only in the Pit-1 lineage of the pituitary gland of the mouse. Homozygous deletion of *Men1* in the pituitary gland led to pituitary gland hyperplasia followed in most cases by massive pituitary gland adenoma formation as early as 35 weeks of age. The pituitary glands from heterozygous animals were indistinguishable from those of wildtype animals at early ages but they also developed tumours later showing that the deletion of *Men1* in the mouse is a relevant model for studying MEN1. This is also in agreement with parallel studies using conventional knockout strategies (Crabtree *et al.*, 2001)(Bertolino *et al.*, 2003b). Development of pituitary gland adenomas was much more frequent and more rapid in mice with a homozygous *Men1* deletion in the pituitary gland than it was in heterozygous littermates in agreement with the results from recent conditional knockout models in the pancreatic islets and parathyroid gland (Bertolino *et al.*, 2003c)(Crabtree *et al.*, 2003)(Biondi *et al.*, 2004). All adenomas originated from the anterior pituitary gland. Although many of these tumours grew aggressively, invasion of surrounding tissue like the posterior pituitary gland was never observed.

There was a clear gender difference with respect to the propensity to develop pituitary gland adenomas. By 45 weeks of age, 100 percent of the female mice with a homozygous deletion of *Men1* had developed adenomas visible to the naked eye whereas the corresponding number for males was only 40 percent. This gender difference was also observed in the heterozygous mice, where 3 out of 5 female mice had developed macroadenomas by the age of 45 weeks whereas no males were observed with adenomas visible to the naked eye. In human MEN1 patients there is also a clear gender difference with respect to the frequency of pituitary gland tumours. In one study 50 percent of female MEN1 had been diagnosed with a pituitaty gland tumour compared to 31 percent of Male patients (Verges *et al.* 2002). Interestingly, this gender difference has not been described for other endocrine tumours in MEN1 (Verges *et al.* 2002).

Pituitary gland adenoma formation was preceded by significant pituitary gland hyperplasia in all mice tested as early as 7 weeks of age. At 10 weeks of age, the anterior lobes of pituitary glands from $Men1^{LoxP\text{-}Frt/Null}$/*Pit-1-Cre* mice were more than twice as big as those from wildtype or heterozygous littermates. The extent of hyperplasia formation also showed a gender difference. At all ages, most *Men1* deficient pituitary glands were bigger in females than in males.

At 12 weeks of age a significant fraction of the cells in the *Men1* deficient pituitary gland stained positive for the G1/S/M phase marker KI-67. This staining was not observed in the wildtype pituitary glands of the same age. The presence of KI-67 suggests that in the absence of *Men1* many cells are still actively progressing through the cell cycle. A significant fraction of cells in the *Men1* deficient pituitary gland but not in the wildtype pituitary gland also stain positive for the mitotic marker phospho-Histone3, suggesting that cell division is still taking place in pituitary glands from 12 week old female $Men1^{LoxP\text{-}Frt/Null}$/*Pit-1-Cre* mice but not in those from their wildtype littermates. The lack of staining for the apoptotic marker cleaved Caspase3 in any of the pituitary gland sections suggests that this hyperproliferation is not associated with significant apoptosis. Hyperproliferation caused by the expression of oncogenes is often associated with increased apoptosis, induced by the deregulation of growth promoting pathways (Hanahan *et al.*, 2000). The absence of apoptosis in connection with the hyperproliferation induced by loss of *Men1* may reflect that the loss of *Men1* not only leads to an increase in growth signal but also to a suppression of apoptosis.

The growth of the wildtype and *Men1* deficient pituitary glands at early ages and the subsequent development of adenomas in the *Men1* deficient pituitary glands offer some insight into the mechanism of MEN1 tumourigenesis.

At 7 weeks of age, the wildtype pituitary glands have stopped gaining in size whereas the *Men1* deficient pituitary glands expand significantly until 10 weeks of age. After 10 weeks, the expansion of the *Men1* deficient pituitary glands slows down dramatically and even for female *Men1* deficient pituitary glands there is little gain in size from 10 weeks onwards until adenoma formation sometime after 20 weeks of age. Although there is still some proliferation occurring at 12 weeks of age, which must lead to gain in cell numbers. This suggests that loss of *Men1* leads to significant hyperproliferation after the normal growth of the pituitary gland has started to decrease. Furthermore, after a certain size of the pituitary gland or a certain age has been reached, even *Men1* deficient pituitary glands show a very significant reduction in growth.

The size of the pituitary adenomas present as early 35 weeks of age suggest that in these pituitary glands, rapid proliferations has resumed at some point causing them to gain many folds in size. When this resumption of growth happens and what initiates it remains to be established. Although massive adenomas develop with 100 percent penetrance in the female *Men1* deficient pituitary glands by 45 weeks of age, these adenomas vary significantly in size. In addition, only 40 percent of male *Men1* deficient pituitary glands have developed adenomas by 45 weeks of age. These observations suggest that although loss of *Men1* induces hyperproliferation, it is not sufficient for adenoma formation. This conclusion is also supported by the observation that adenomas in heterozygous *Men1* mouse models show loss and gain of chromosomes, with gain of mouse chromosome 15 being the most frequent (Crabtree *et al.*, 2003). These chromosomal rearrangements may lead to genetic lesions that initiate resumption of rapid growth and adenoma formation. The complete loss of *Men1* signal in the heterozygous adenoma, suggests that it is only *Men1* deficient cells that contributes to adenoma formation. This suggests that the secondary genetic lesions are cell autonomous lesions (not secreted growth factors) that leads to a clonal expansion of *Men1* deficient cells. This is also in agreement with the theory that all pituitary adenomas are of clonal origins (Melmed, 2003).

3.2 Gene expression profiling suggests a novel mechanism for MEN1 tumourigenesis

Although little is known about the function of Menin, most data suggest that the protein functions as a transcriptional regulator. As cancer invariably involves changes in gene expression pattern (Hanahan *et al.*, 2000), I reasoned that the tumourigenesis caused by loss of *Men1* would most likely be associated with changes in the gene expression profile of the pituitary gland cells.

To investigate the molecular mechanism of the tumour suppressor activity of *Men1*, I analysed the expression profile of the *Men1* deficient pituitary glands compared to heterozygous littermates by microarray analysis. Relatively young males (13 weeks) were chosen to minimise the risk of major chromosomal rearrangements or the gain of secondary mutations.

Many of the genes implicated in sporadic pituitary gland tumourigenesis were among the 11500 genes expressed in the pituitary glands. These genes included *PTTG1*, *bFGF*, *NGF*, *FGF4*, *TGF-α, TRH*, *GHRH*, *Dopamine D2 receptor*, *Rb*, *p16Ink4a*, *p18Ink4c* and *Gαs*. None of these genes showed any significant change in expression levels. Furthermore, western blot analysis with anti p27Kip1 antibodies showed no difference between wildtype and *Men1* deficient pituitary glands at 13 weeks of age (data not shown). Down regulation of p27Kip1 on a posttranslational level is associated with pituitary gland tumourigenesis (Melmed, 2003). The clear gender bias in adenoma formation and the enhanced hyperplasia in early female pituitary glands would suggest a hormonal influence. Systemic administration of Estrogen, the female sex hormone, has been shown to cause pituitary gland hyperplasia and subsequently adenoma formation in rats (Heaney *et al.*, 1999). This hyperplasia is associated with increased expression of PTTG1 and bFGF (Heaney *et al.*, 1999). As neither PTTG1 nor bFGF were overexpressed in the *Men1* deficient pituitary glands it appears that a general deregulation of Estrogen signalling is not present in MEN1 tumourigenesis.

The microarray data thus suggests that the mechanism of tumourigenesis associated with loss of *Men1* differs from those previously described for sporadic pituitary gland tumourigenesis. This conclusion is also in agreement with the observation that inactivation of *MEN1* does not appear to play a major role in sporadic pituitary gland tumours (Prezant *et al.*, 1998)(Farrell *et al.*, 1999)

The finding that Menin may regulate transcriptional pathways involving NF-kB and Smads and thus interfere with TGF-β signalling suggests a possible mechanism for tumourigenesis.

Although it does not explain the very tissue specific development of tumours. Many TGF-β and NF-κB target genes have been implicated in growth control, apoptosis and metastasis and they would therefore be potential mediators of MEN1 tumourigenesis. These genes include *p15Ink4B , p21Cip1*, *c-Myc*, *cyclin D1, c-Jun*, *Cdc25*, *cIAP*, *Pai-1*, *Transin/Stromelysin*, *GM-CSF*, *BCL-X_L* and *c-flip*. Interestingly however, none of these genes showed any change in their expression pattern in *Men1* deficient pituitary glands suggesting that they are not involved in MEN1 tumourigenesis.

3.3 VIP, IGF1 and Cdc2 are upregulated in Men1 deficient pituitary glands

The adenoma formation in *Men1* deficient pituitary glands was invariably preceded by hyperplasias and hyperproliferation. It is thus reasonable to conclude that loss of *Men1* leads to deregulation of genes that can provide self-sufficiency in growth signals or alternatively, change the expression level of genes that normally mediate growth inhibitory signals. The absence of apoptosis associated with the hyperproliferation may also reflect changes to genes affecting apoptosis and survival.

Analysis of the microarray experiment yielded two lists of genes that were reproducibly either more than two fold overexpressed or two fold underexpressed in the *Men1* deficient pituitary glands compared to the heterozygous pituitary glands.

Although the majority of the genes that showed differential expression in the *Men1* deficient pituitary glands were downregulated in the absence of *Men1*, I did not identify any genes in this group that were obvious candidates for growth control genes. However, on inspection of the upregulated genes, a number of genes were identified that, according to the literature, could be involved in regulation of growth or apoptosis. These included genes encoding secreted growth factors as well as genes involved in cell cycle control and apoptosis. Of the genes overexpressed in the *Men1* deficient pituitary glands, I decided to further analyse four genes. These were the genes encoding two secreted growth factors, Insulin like Growth Factor 1 (IGF1), 4,6 fold upregulated and Vasoactive Intestinal Peptide (VIP), 7,4 fold upregulated and the genes encoding the cyclin dependent kinase Cdc2/Cdk1 and its ligand Cyclin B2, which were 3,0 and 3,7 fold upregulated respectively. However, it should be noted that there are other genes among the genes upregulated in the *Men1* deficient pituitary glands, which could play a role in MEN1 tumourigenesis. These include *BMP2*, which as noted previously plays a role in the development of the pituitary and the specification of the pituitary gland cell types (Treier *et al.*, 1996)(Dasen *et al.*, 1999), and most notably *Survivin*. Survivin is a

member of the IAP family of apoptosis inihibitory proteins that are believed to suppress apoptosis by blocking activation of caspases. A role for Survivin in regulating chromosome segregation has also been suggested (Reed *et al.*, 2000). *BMP2* and *Survivin* were upregulated 2.3 and 2.9 fold respectively in the microarray experiment. The overexpression of these two factors have not yet been verified by *in situ* hybridisation, but the overexpression of *Survivin* could potentially play a role in the suppression of any apoptosis that may be associated with progression to pituitary adenoma.

In situ hybridisation analysis of male and female pituitary glands at different ages confirmed *VIP*, *IGF1* and *Cdc2* but not *CyclinB2* as being differentially expressed in *Men1* deficient pituitary glands compared to wildtype. *VIP*, *Cdc2* and *IGF1* were all clearly overexpressed in the anterior lobe of the *Men1* deficient female pituitary glands compared to the wildtype pituitary glands at 13 weeks of age. Moreover, all genes showed a clear gender difference in expression levels. At 13 weeks, female *Men1* deficient pituitary glands expressed *VIP*, *Cdc2* and *IGF1* at a level many folds higher than the male pituitary glands. Interestingly, the difference in expression levels between wildtype and the *Men1* deficient pituitary glands increased with the age of the female for all three genes. *CyclinB2* showed no expression at any of the ages and genotypes tested. For both *VIP* and *Cdc2* the expression of the genes was concentrated to patchy structures scattered over the anterior pituitary gland, whereas the expression of *IGF1* was evenly distributed over the entire anterior lobe.

Overexpression of growth factors like VIP and IGF1 are likely to lead to increased signalling through their cognate receptors. However, for a cyclin dependent kinase like Cdc2/Cdk1, the level of Cyclin B as well as the activity of the inhibitory Wee kinase and the activating Cdc25 phosphatase has more influence on the activity of the kinase than the concentration of Cdc2/Cdk1 itself. As I could not confirm the overexpression of *cyclinB* by *in situ* hybridisation under any of the tested conditions, there is no evidence at present to suggest that *Men1* deficient cells have increased Cdc2/Cdk1 activity. I will therefore only discuss the implications of the VIP and IGF1 overexpression for MEN1 here.

The overexpression of *VIP* in the female *Men1* deficient pituitary glands was especially striking. The *in situ* hybridisation does not yield any quantitative data, but if the upregulation in the male pituitary gland was 7 fold as the microarray suggested, then that of the female pituitary glands must be many times higher. Importantly, there was very strong *VIP*

expression in the *Men1* deficient neoplasia present on the 41 week old heterozygous pituitary gland, suggesting that the data obtained from the young pituitary glands are valid for the older heterozygous pituitary glands that resemble the MEN1 syndrome most closely.
In some of the female sections, *VIP* expression was highest along the periphery of the anterior pituitary gland. This is the same region of the Men1 deficient pituitary glands that develops the most prominent vacuoles at 7 weeks of age. To what extent the formation of vacuoles and the subsequent haemorrhaging of blood into them is caused by VIP is not known, but VIP has been shown to be a vasodilating peptide (Gozes *et al.*, 1999).
According to the microarray data, *IGF1* was clearly overexpressed in 13 week old male pituitary glands. Although the *in situ* experiment presented clearly validates the microarray experiment and demonstrated overexpression of *IGF1* in the female 13 week old pituitary gland, the overexpression in the 13 week old male in this experiment was less clear. However, other *in situ* experiments did clearly demonstrate overexpression in the male pituitary glands supporting the microarray data. In the heterozygous pituitary gland, *IGF1* did show overexpression in the *Men1* deficient outgrowth, albeit to a lesser extent than *VIP* or *Cdc2*.
VIP protein was also significantly upregulated in *Men1* deficient pituitary glands. VIP expressing cells were scattered over the entire anterior pituitary gland, although VIP expressing cells appeared to be more concentrated in certain areas such as the edge of the anterior lobe facing the intermediate lobe. As we do not yet have a reliable antibody that detects Menin in pituitary gland sections, I have not yet been able to investigate if VIP is exclusively expressed in *Men1* deficient cells.

The *Pit-1-Cre* transgene should ensure expression of Cre in the lactotrope, somatotrope and thyrotrope lineages (Rhodes *et al.*, 1993), although I could only detect Cre mediated EGFP expression in the lactotrope and somatotrope lineages. The *in situ* hybridisation experiment with the *Men1* probe and the western blot with the anti Menin antibody showed that the deletion of *Men1* was efficient, suggesting that *Men1* has been deleted in the lactotrope and somatotrope lineages, which constitutes more than half of the pituitary cells. It remains to be established which of these two cell lines express the deregulated genes in the *Men1* deficient pituitary glands. There is no evidence that both cell lineages deregulate the same genes in response to the deletion of *Men1*. It may thus be that each of the two lineages only are responsible for a subset of the genes found deregulated in the $Men1^{LoxP\text{-}Frt/Null}$/*Pit-1-Cre* pituitary glands. Intriguingly, for secreted growth factors there even is a possibility that one cell type secretes the growth factor that stimulates the growth of the other. These issues could

be resolved by selectively deleting *Men1* in the somatotrope or lactotrope lineages using the *GH* or *Prolactin* promoter to drive *Cre* expression.

3.4 VIP and pituitary gland proliferation

VIP is a small peptide of the glucagon family, closely related to the GH Releasing Hormone that signals though a G protein coupled receptor. Receptor activation by these peptides leads to increased intracellular cAMP as well as activation of Phospholipase C and intracellular Ca^{2+} release. Among the physiological effects of VIP is the increased secretion of many hormones from the endocrine system. These include Prolactin and GH from the pituitary gland (Gozes *et al.*, 1999) and Insulin from the pancreatic islets (Kato *et al.*, 1994). Indeed, VIP has been proposed to be a physiological Prolactin releasing factor (Abe *et al.*, 1985) and VIP stimulates Prolactin release *in vivo* in response to TRH (Balsa *et al.*,), IGF1 (Lara *et al.*, 1994) and Serotonin (Balsa *et al.*, 1998) or low Thyroid Hormone or Dopamine levels (Balsa *et al.*, 1996). In the endocrine system, factors that induce hormone secretion often additionally stimulate proliferation of the secreting cells. Thus, overproduction of releasing hormones from the hypothalamus leads to pituitary gland hyperplasia that may progress to adenomas (Melmed, 2003). The vast majority of hormone secreting adenomas in human MEN1 patients secrete Prolactin and a smaller fraction secrete GH or ACTH (Verges *et al.*, 2002), whereas only Prolactin and GH secreting tumours were observed in mouse models (Crabtree *et al.*, 2001)(Bertolino *et al.*, 2003), suggesting that *Men1* controls growth of lactotropes and somatotropes.

VIP is a mitogen for lactotropes. It stimulates proliferation of lactotropes *in vitro* (Prysor-Jones *et al.*, 1989)(Fernandez *et al.*, 2003). The VIP induced proliferation of lactotropes is abolished by addition of a PKA inhibitor (Fernandez *et al.*, 2003) indicating that the mitotic signal is mediated by cAMP. Interestingly, the stimulation of lactotrope proliferation by VIP can also be partly blocked by MAP kinase inhibitors (Fernandez *et al.*, 2003) suggesting that VIP can activate the MAP kinase pathway. Indeed it has been shown that in addition to PKA activation, VIP stimulation of Prolactin secretion also involves activation of the small GTPase Rap1, through cAMP responsive exchange factors, and subsequent activation of MAP kinases (Romano *et al.*, 2003). This is in agreement with the observation that cAMP mediated stimulation of lactotrope proliferation requires activation of both PKA and the MAP kinase pathway (Suzuki *et al.*, 1999).

VIP has also been implicated in lactotrope stimulation *in vivo*. Estrogen induced hyperplasia is associated with increased VIP expression, with a correlation between pituitary gland size and the concentration of VIP (Prysor-Jones *et al.*, 1988). Additionally, VIP antagonists have been shown to block Estrogen induced hyperplasia (Gomez *et al.*, 2003)

Prolonged overstimulation with Estrogen can lead to prolactinoma formation (Heaney *et al.*, 1999)(Piroli *et al.*, 2004). Moreover, Estrogen induced pituitary gland prolactinomas show a gender bias both with respect to adenoma size and VIP expression suggesting that VIP could be a mediator of Estrogen induced prolactinoma formation (Piroli *et al.*, 2004).

Intriguingly, overexpression of the VIP related GHRH induces somatotrope hyperplasia and subsequent adenoma formation with exactly the same kinetics as loss of *Men1* does (Kineman *et al.*, 2001). As noted previously, VIP induces hormone secretion in both lactotropes and somatotropes and both cell types recognise cAMP as a mitotic signal. The reason why VIP may preferentially induce prolactinomas is that the VIP receptor is enriched in lactotropes (Wanke *et al.*, 1990).

3.5 IGF and pituitary gland proliferation

IGF1 is a 7 kDa polypeptide related to insulin. IGF1 and the highly related IGF2, signal through IGF1R, a receptor tyrosine kinase. IGF signalling leads to activation of the PI3K pathway, the STAT pathway and the RAS pathway (Sachdev *et al.*, 2001)(Surmacz, 2003). Through these effectors the IGF receptor can activate pathways that control proliferation as well as apoptosis.

IGF1 is normally expressed by cells within the pituitary gland and IGF1 can induce proliferation of pituitary gland lactotropes and corticotropes *in vitro,* but has no effect on the other pituitary gland cell lines (Oomizu *et al.*, 1998)(Fernandez *et al.*, 2003). It may in some cases even attenuate proliferation of somatotropes (Fernandez *et al.*, 2003). The IGF1 induced lactotrope proliferation can be blocked by MAP kinase inhibitors, suggesting that IGF1 stimulates proliferation through activation of Ras and its downstream MAP kinase. Interestingly, the mitogenic effect of IGF1 on cultured lactotropes could also be partially blocked by PKA inhibitors or VIP antagonists, suggesting that part of the mitogenic signal of IGF1 is through an autocrine loop involving VIP (Fernandez *et al.*, 2003). Likewise, VIP has been implicated in IGF1 induction of Prolactin secretion from lactotropes (Lara *et al.*, 1994).

3.6 VIP and IGF1 in Cancer

Both VIP, IGF1 and the related IGF2 have been implicated in cancer. VIP is found overexpressed in some cancers, especially cancers of the pancreatic islets. These tumours of the pancreatic islets are called VIPomas and the disease is also known as Verner-Morrison syndrome. The Verner-Morrison syndrome is extremely rare with only 1 out of 10 million being affected. To what extent VIP expression contributes to the process of tumourigenesis is not known. In rodent models, VIP receptor antagonists have been shown to inhibit mammary gland carcinogenesis (Moody *et al.*, 2004), ovarian cancer (Chatzistamou *et al.*, 2001), prostate cancer (Plonowski *et al.*, 2002) and non-small cell lung cancer (Moody *et al.*, 1993), whereas VIP itself inhibits growth of small cell lung cancer (Maruno *et al.*, 1998). In vitro, VIP has also been shown to stimulate proliferation of HT29 colon adenocarcinoma cells by activating the ERK pathway through Rap1 (Alleaume *et al.*, 2003) and VIP receptor antagonists have been shown to inhibit growth of neuroblastoma cell lines (Lilling *et al.*, 1994-95).

High levels of circulating IGF, within the normal range, leads to an increased risk of breast and prostate cancer, two cancers that are normally considered to be strongly affected by sex hormones. To what extent IGF directly contributes to the tumourigenesis is not known (Renehan *et al.*, 2004).

In an interesting mouse model for pancreatic islet cancer, Christofori et al. overexpressed the SV40 large T antigen, which binds to, and inactivates RB and p53, in the pancreatic islets. Its overexpression led to hyperplasia in 50 percent of the islets followed by adenoma formation in a smaller fraction. The adenoma formation was in all cases associated with a clear overexpression of IGF2. Overexpression of SV40 large T antigen in *igf2*$^{-/-}$ mice led to suppression of tumour growth associated with increased apoptosis *(Christofori et al., 1994).* The association of proliferation with apoptosis was also illustrated by another mouse model where the overexpression of *c-Myc* in the pancreatic islet led to widespread apoptosis. However, when the *c-Myc* expression was combined with expression of the anti apoptotic gene *Bcl*X_L, the suppression of apoptosis led to rapid adenoma formation (Pelengaris *et al.*, 2002).

3.7 Regulation of *VIP* and *IGF* expression

The expression of *VIP* is regulated by many hormones and growth factors. Thus *VIP* expression is stimulated by TRH (Balsa *et al.*, 1996a), IGF1 (Lara *et al.*, 1994), Serotonin

(Balsa *et al.*, 1998), Estrogen (Degerman *et al.*, 2002), TGF-β1, ciliary neutropkic factor (Pitts *et al.*, 2001) and Activin (Symes *et al.*, 2000) and repressed by Thyroid Hormone (Degerman *et al.*, 2002) and Dopamine (Balsa *et al.*, 1996b). VIP expression is normally restricted to specific areas of the brain, the peripheral nervous system and to the anterior pituitary gland.
The *VIP* promoter is regulated by many transcription factors. Of special interest for Menin is the binding of Smad3 and Smad4 in response to TGF-β. Binding of AP-1 and STAT can also activate the *VIP* promoter (Pitts *et al.*, 2001). AP-1 and STAT probably mediate the effect of IGF1 on the VIP promoter (Pitts *et al.*, 2001) as IGF can activate these transcription factors through IRS and through Ras activation. The Activin stimulation of *VIP* is likely to be mediated by Smad1 and Smad5, two other Menin interacting proteins.
Sequence analysis of the mouse and human *VIP* promoter reveals that they contain a Thyroid Hormone Response Element (TCACCCTGACCC in the mouse) within 3000 bp of the transcriptional start as well as AP-1 sites (TGA(C/G)TCA). Moreover, both the mouse and the human promoter contain perfect TGF-β inhibitory elements (TIE). In the mouse there are 3 TIE sites just upstream of the transcriptional start point and in the human 1 TIE site 800 bp downstream of the transcriptional start. Also in both mouse and human consensus NF-κB binding sites can be found 5000 bp upstream of the transcriptional start for the mouse promoter and 1500 bp downstream of the transcriptional start for the human promoter.
The expression of IGF1 is primarily regulated by GH and many of the effects of GH are thought to be mediated by IGF1 (Laron, 2001). Additionally, IGF1 expression can be stimulated by Thyroid Hormone (Fagin *et al.*, 1989) and possibly Estrogen (Umayahara *et al.*, 1994). The regulation of IGF1 expression is complex as it involves 4 different transcriptional start sites giving rise to several alternatively spliced forms (Jansen E, 1991). The *IGF1* promoter contains binding sites for AP-1 (Umayahara *et al.*, 1994), Sp-1 (Zhu *et al.*, 2000) and GATA transcription factors (Wang *et al.*, 2000).

3.8 Menin interacting proteins

Using a yeast two hybrid system, I screened a pituitary gland cDNA library for novel Menin interacting proteins. After screening approximately 3 million transformants, which corresponds to roughly a third of the estimated complexity of the library, I identified 22 plasmids that enabled Menin dependent growth. These plasmids contained fragments from 9 different genes. Of these, JunD and Vimentin had previously been published as Menin interacting proteins, confirming our yeast two hybrid approach. 3 plasmids contained

fragments from known genes that had not previously been published as encoding Menin interacting proteins. These were GMAP210/TRIP11, Ldb1a and Spectrin. Finally 4 plasmids contained fragments from novel genes. *In situ* hybridisation failed to reveal any expression of 3 of these genes, but the fourth, Gad67, showed expression in most tissues except for the liver. I subsequently cloned the full-length cDNA from a phage library. Sequencing revealed that the protein contained two predicted domains. A WD40 repeat domain in the N-terminus and a double Bromodomain in the C-terminal half. The yeast clone overlapped precisely with the Bromodomain.

The isolation of JunD once again confirmed this protein as a Menin interacting protein. Likewise, the identification of Spectrin as a potential Menin interacting protein further strengthened the association between Menin and TGF-β signalling (Tang *et al.*, 2003). Moreover, the finding that Menin can interact with Spectrin in a yeast two hybrid system suggests a mechanism for the regulation of Smad3 by Menin and also provides a mechanism whereby Menin could regulate TGF-β signalling in the absence of Smad3. The binding between Menin and Spectrin remains to be confirmed by an independent method. It also remains to be investigated if Menin, Spectrin and Smad3 all bind to each other directly or indirectly.

It is interesting to note that the proposed functions of Spectrin and GMAP210/Trip11 are similar. Both are structural proteins in the cytosol that may translocate to the nucleus to function as transcriptional cofactors upon stimulation with either TGF-β or Thyroid Hormone (Chen *et al.*, 1999)(Tang *et al.*, 2003). It is also noteworthy that Spectrin, GMAP210/Trip11 and Ldb1a have all been characterised as transcriptional coactivators. Although Menin has previously been shown to interact with transcriptional corepressors, this is the first time that transcriptional coactivators have been suggested to interact with Menin.

The function of Gad67 is unknown. The presence of a WD40 domain suggests that Gad67 can function as an assembly platform for protein complexes (Li *et al.*, 2001). More importantly, the double Bromodomain of Gad67 suggests that the protein is involved in chromatin remodelling. The Bromodomain binds to acetylated lysines, most often in the context of Histone tails (Dhalluin *et al.*, 1999). Furthermore, Bromodomain containing proteins are an integral part of Histone modification and chromatin complexes (Jeanmougin *et al.*, 1997)(Marmorstein *et al.*, 2001). To what extent Gad67 is involved in MEN1 tumourigenesis is yet to be elucidated. It should however be noted that the Bromodomain is one of 11 protein domains that was found significantly overrepresented among 291 characterised cancer genes

compared to their frequency among all genes, in a recent survey of the literature. According to this survey, 10 percent of all bromodomain proteins have been found mutated in human cancers (Futreal *et al.*, 2004).

3.9 VIP and IGF1 as mediators of MEN1 tumourigenesis

There is no evidence that Menin binds DNA directly. Rather it appears to regulate transcription by binding to transcription factors or to transcriptional cofactors. It follows from this that the influence of Menin on a promoter in a given cell is dependent on the transcription factors and cofactors expressed in that cell. Thus, the loss of Menin is likely to effect different genes in different tissues. For the same reasons it seems unlikely that the interaction of Menin with a single transcription factor or cofactor will provide a satisfactory explanation for the endocrine tumourigenesis caused by the loss of Menin. It seems more likely that a complex interplay between several Menin binding factors on a set of promoters will render these promoters Menin responsive.

Menin has been reported to function as a coactivator for some transcription factors and as a corepressor for others. The microarray analysis of *Men1* deficient pituitary glands did not provide any definitive answers regarding the effect of Menin on transcription. While the expression of most genes was unaffected by the deletion of *Men1*, a subset of the genes were either upregulated or downregulated in the *Men1* deficient pituitary glands. To what extent these genes are direct targets of Menin or if the change of expression is an indirect effect, is not known as microarray or *in situ* hybridisation analysis does not distinguish between direct or indirect effects on transcription.

In the microarray experiment *VIP* was one of the genes with the highest fold of deregulation. Moreover, the *in situ* hybridisation analysis of *VIP, Cdc2* and *IGF1* demonstrated that the overexpression of *VIP* in the *Men1* deficient pituitary glands was much more pronounced that that of *Cdc2* or *IGF1*. *VIP* would therefore be an obvious choice for promoter analysis to establish the mechanism of Menin regulation. As noted previously, the *VIP* promoter contains several elements that would allow Menin interaction. The binding of Menin to the *VIP* promoter should be verified experimentally by chromatin immunoprecipitation or bandshift analysis. To elucidate a possible mechanism for Menin dependent regulation, promoter analysis of the *VIP* promoter in a suitable system should yield information about the transcription factors Menin may bind to regulate expression of *VIP*.

The loss of *Men1* in the pituitary gland changes the expression level of a small subset of the genes expressed in the pituitary gland. If the tumour suppressor activity of Menin is related to its role as a transcriptional regulator, it is likely that the mediators of MEN1 tumourigenesis are among these genes. Thus, *VIP* and *IGF1* are the best candidate genes for causing the pituitary gland hyperplasia and hyperproliferation associated with MEN1 tumourigenesis. Both VIP and IGF1 are potent mitogens for lactotropes and possibly also for somatotropes and corticotropes. The combination of VIP and IGF1 should in theory be sufficient to supply growth signals and to suppress possible apoptosis associated with hyperproliferation. According to the theory of Robert Weinberg, these are two of the 6 characteristics acquired by malignant tumours. To what extent VIP and IGF1 are sufficient to induce pituitary gland hyperplasia or even adenoma formation *in vivo* remains to be tested by transgenic overexpression experiments.

The MEN1 syndrome also involves tumour formation in other endocrine organs than the pituitary gland. Though it is not certain, it seems likely that the mechanism of tumourigenesis is similar in all of these organs. It would therefore be interesting to investigate if *VIP* and *IGF1* are overexpressed in *Men1* deficient parathyroid or adrenal glands or in the pancreatic islets. This could be tested by deleting *Men1* specifically in these organs by crossing the floxed *Men1* allele into mice expressing *Cre* in beta cells using the *Insulin* promoter or in the parathyroid gland using the *Parathyroid Hormone* promoter.

Little is known about the effects of VIP and IGF1 on the parathyroid gland. VIP can stimulate Parathyroid Hormone release through stimulation of cAMP production (Joborn *et al.*, 1991) suggesting that the Chief cells of the parathyroid gland are VIP responsive. Likewise, IGF1 has been shown to be able to bind to and stimulate growth of human parathyroid adenoma cells *in vitro* (Tanaka *et al.*, 1994).

Overexpression of VIP alone in the pancreatic islets does not lead to adenoma formation in mouse models although it does increase insulin secretion. Whether the overexpression was associated with hyperplasia was not reported (Kato *et al.*, 1994). The absence of adenoma formation could reflect that cells of the pancreatic islets may not be as responsive to cAMP as a mitotic signal as cells of other endocrine organs. Pancreatic islet tumours are not very frequent in neither the Carney syndrome caused by deregulated PKA signalling, nor the McCune Albright syndrome, caused by an activating mutation to *Gαs*. Alternatively, the expression of *VIP*, like that of *c-Myc* and *SV40 largeT antigen* is not tumourigenic in the absence of a survival signal such as BCL-XL or IGF1 or 2. To verify that VIP and IGF1 can

indeed mediate the MEN1 tumourigenesis, transgenic experiments with the two growth factors should be performed.
In addition, the role of VIP as mediator of MEN1 tumourigenesis can also be investigated by blocking the action of VIP by administering VIP antagonists to *Men1*$^{LoxP\text{-}Frt/Null}$/*Pit-1-Cre* mice. This experiment would establish if VIP overexpression is required for the hyperplasia and subsequent adenoma formation in *Men1* deficient pituitary glands.

In conclusion, I have established a mouse model that faithfully reproduces the MEN1 syndrome in the pituitary gland. Using this mouse model I have begun to elucidate the mechanism of MEN1 tumourigenesis, and identified a number of genes that are deregulated in *Men1* deficient pituitary glands. This work has laid the foundations for the understanding of how Menin regulates proliferation in the pituitary gland. The identification of several growth factors that are overexpressed in *Men1* deficient pituitary glands may explain their hyperproliferation phenotype and subsequent progression to aggressive pituitary adenoma. Transgenic overexpression studies of these growth facors in the pituitary will doubtlessly help to further understand the role of *Men1* in pituitary tumourigenesis.

List of Abbreviations

ACTH	Adrenocorticotropin
BAC	Bacterial Artificial Chromosome
BMP	Bone Morphogenic Protein
cAMP	cyclic Adenosine Mono Phosphate
CREB	cAMP Response Element Binding protein
CRH	Corticotropin Releasing Hormone
EGFP	Enhanced Green Fluorescent Protein
ERK	Extracellula signal Regulated Kinase
FGF	Fibroblast Growth Factor
FMTC	
FSH	Follicle-Stimulating Hormone
g	gram
GH	Growth Hormone
GHRH	Growth hormone releasing hormone
GnRH	Gonadotropin Releasing Hormone
HDAC	Histone Deacetylase
IGF	Insulin Like Growth Factor
L	Litre
MAP kinase	Mitogen Activated kinase
ml	milli litre
µl	micro litre
LH	Luteinising Hormone
M	Molar
MEN1	Multiple Endocrine Neoplasias type 1 (disease)
MEN1	Multiple Endocrine Neoplasias type 1 (human gene)
Men1	Multiple Endocrine Neoplasias type 1 (mouse gene)
mM	milli Molar
µM	micro Molar
MSH	Melanocyte Stimulating Hormone
NGF	Nerve Growth Factor
PKA	Protein kinase A

TGF	Transforming Growth Factor
TR	Thyroid Hormone Receptor
TRH	Thyrotropin Releasing Hormone
TSH	Thyroid Stimulating Hormone
VEGF	
VIP	Vasoactive Intestinal Peptide
wt	wild type

4 Materials and Methods

4.1 Materials

4.1.1 Chemicals

Acrylamide	Biorad
L-Adenine	Sigma
Agar, Bacto	Becton-Dickinson
Agarose	Invitrogen
Ampicillin	Sigma
Amino acids (for yeast) all	Sigma
Except L-Phenyl-Alanin	Merck
Ammonium Chloride	Merck
Ammonium-Persulfate (APS)	Biorad
Bovine Serum Albumin, Fraction V (BSA)	Sigma
Bromophenol blue	Sigma
Calcium Chloride	Merck
Carrier DNA (Herring testis)	Clontech
Chloramphenicol	Sigma
Dextran Sulfate	Amersham Pharmacia
Dextrose	Merck
Dithiothreitol (DTT)	Biomol, Germany
DMSO (Dimethylsulfoxide)	Sigma
DPX	Agar Scientific
EDTA	Merck
Ethanol	Merck
Ethidium Bromide	Sigma
Fetal Calf Serum	Invitrogen
N,N-Dimethylformamide	Sigma
Formalin	Electron Microscopy Sciences
Geneticin-Sulfate	Sigma
L-Glutamine	Invitrogen

Glycine	Merck
HEPES	Invitrogen
Isopropanol	Merck
Kanamycin	Sigma
Lithium Acetate	Sigma
Lithium Chloride	Merck
Magnesium Chloride	Merck
MEM Non-essential amino acids	Invitrogen
β-Mercaptoethanol	Sigma
Methanol	Merck
P^{32}-dCTP	Amersham
Paraformaldehyde (PFA)	Sigma
Penicillin/Streptomycin	Invitrogen
Peptone	Difco
PEG4000	Sigma
Potassium Chloride	Merck
Protease Inhibitors Complete	Roche
^{35}S-UTP	Amersham
Sodium Acetate	Merck
Sodium Hydroxide	Merck
Sodium Pyruvate	Invitrogen
TEMED	Biorad
Triethanolamine	Sigma
Triton X-100	Sigma
Trypsin	Invitrogen
Tween20	Gerbu
L-Uracil	Sigma
Xylene	Sigma
Yeast extract	Difco
Yeast Nitrogen Base without amino acids	Difco

4.1.2 Equipment, plastic ware and other materials

Acid washed beads (0,5 mm)	Sigma

Agilent Bioanalyser	Agilent
Aquamount, Aqueous Mountant	LERNER Laboratories
Bacterial Petri dishes	Greiner Bio-One
High-Density mouse BAC membranes	Research Genetics
Cell counter chamber	(Neubauer improved) BRAND
Cell culture dishes	NalgeNUNC International
Cell incubator Hera cell	KendroLaboratoryProducts
Centricon YM-10	Amicon
Centrifuge 5417C	Eppendorf
Centrifuge RC5C	Sorvall, Instruments
Centrifuge RC-3B	Sorvall, Instruments
Cryotome CM 3050S	Leica Microsystems
Codelink 20K mouse Bioarray	Amersham
Coverslips (24x60 mm)	Superior Marienfeld
Electrophoresis chambers	PeqLab
Electroporation system Gene Pulser II	BIO RAD
Electro-SeparationSystem S&S BIOTRAP	Schleicher & Schuell Bioscience
Filtration bottles STERICUP	MILLIPORE
Fine forceps and scissors	ROBOZ
Gene Pulser , Electroporation cuvettes	BIO RAD
Hybridiser incubator Techne HB-1D	TECHNE
Hybridisation bottles	TECHNE
Hybridisation Transfer Membrane NEN	Life Science Products
Microlance hypodermic needles	Becton Dickinson
Microscope Slides Super Frost ,Plus 25x75mm	ROTH
Microscope Axiovert 25	Zeiss
Mini Protean 3 system	Bio-Rad
Mini Trans-Blot Cell	Bio-Rad
Nitrocellulose Membranes PROTRAN	Schleicher & Schuell
Nylon Membranes Biotrans	ICN Biomedicals Inc.
OCT Coumpound Embedding Medium	Tissue-Tek,
Optical Microscope	Zeiss
Paraffin Microtome RM2165	Leica Microsystems
PCR thermal cycler PTC-200	Biozym

PCR thermal reaction tubes	ABgene
Plastic tubes (50 ml and 15 ml)	FALCON
Power supply Power Pac 300	BioRad
Reaction tubes (1.5 ml)	ROTH
Serological Pipets (25 ml; 10 ml; 5 ml; 2 ml)	FALCON
Spectrophotometer Ultraspec 3000	Pharmacia Biotech
Vibrotome VI 1000S	Leica Microsystems
Ultracentrifuge L8-M	BECKMAN

4.1.3 Enzymes

Proteinase K	MERCK
Hot Star Taq DNA Polymerase	QIAGEN
Restriction endonucleases	New England BIOLABS; Roche, SIBenzyme
Pwo DNA polymerase	Roche
Expand High Fidelity system	Roche
Klenow	New England Biolabs

4.1.4 Molecular weight markers

1kb DNA ladder	Invitrogen
Broad Range protein ladder	Biorad

4.1.5 Oligonucleotides

Targeting vector synthesis

The targeting vector linker was put together by four oligoes:

MenKO1S:

5’ cgcgatcgcgatatcataacttcgtataatgtatgctatacgaagttatgttaacg 3’

MenKO1AS:

5’ gtaccgttaacataacttcgtatagcatacattatacgaagttatgatatcgcgatcgcgagct 3’

MenKO2S:

5’ aacataacttcgtataatgtatgctatacgaagttatggcgcgccggtcaccactagtgcgatcgcg 3’

MenKO2AS:

5’ gtaccgcgatcgcactagtggtgaccggcgcgccataacttcgtatagcatacattatacgaagttatgtt 3’

Cloning of pGad67

Gad67SacI1:	5’ agcagagctcccagtccaaaaggc 3’
Gad67PstI:	5’ aaattccctgcagtagaaggccagtg 3’
Gad67BamHI:	5’ tacgctatgctgcttgaaacttgcca 3’
Gad67AseI:	5’ tgttcaatatagcgtacctcccac 3’
Gad67NotIXhoI:	5’ ggtggcggccgcctcgagatggcggcggcacc 3’
Gad67SacIDn:	5’ ggctgccaccagatcc 3’

Mouse genotyping:

Men1LoxP1:	5’ gttatcataacttcgtataatgtatgc 3’
Men1Loxp3:	5’ agccacaccggcattgac 3’
Men1LoxP8:	5’ gcaagcatctgaggcctcttgtgagc 3’
Men1LoxP9:	5’ caggtccacccagccagaaactgcc 3’
Men1Frt1:	5’ gttagcttgctcattgtggtaggaggc 3’
Men1Frt2:	5’ tactccctcccacctccattccaggc 3’
Men1Frt3:	5’ cggcgcgccggtcaccactcctac 3’
Menseq1:	5’ ctccctgtctctaatactgc 3’
Cre1:	5’ gcctgcattaccggtcgatgcaacga 3’
Cre2:	5’ gtggcagatggcgcggcaacaccatt 3’
FlpE1:	5’ ctaatgttgtgggaaattggagc 3’
FlpE2:	5’ ctcgaggataacttgtttattgc 3’

***In situ* probes**

Men1-Up:	5’ ccagaattcgcaccaaactggacagctcg 3’
Men1-Dn:	5’ ccaaagcttcttgtgataaagggtgagtgg 3’
VIP-Up:	5’ ccagaattcatggaagccagaagcaagc 3’
VIP-Dn:	5’ ccaaagcttccagctcttcaagaaagtctgc 3’
IGF-Up:	5’ ccagaattcatgtcgtcttcacacctc 3’
IGF-Dn:	5’ ccaaagcttgaccacttttgcaaggtgc 3’
Cdc2-Up:	5’ ccagcggccgcgttcatggattcttcactcgcc 3’
Cdc2-Dn:	5’ ccaaagcttcttcagggccattttgccag 3’
CyclinB-Up:	5’ ccagcggccgcgctgtcaagaacaagtatgcc 3’
CyclinB-Dn:	5’ ccaaagctttaagtagatcaatagctttatttttc 3’

4.1.6 Antibodies

Primary antibodies:

αGFP	Mouse	Chemicon
αProlactin	Rabbit	Chemicon
αGrowth Hormone	Rabbit	Chemicon
αTSH	Rabbit	Parlow
αACTH	Rabbit	Parlow
αKI-67	Rabbit	Novacastra
αMenin C19	Goat	Santa Cruz
αphospho-CREB	Rabbit	Cell Signalling Technologies
αphospho-Histone H3	Rabbit	Upstate Biotech
αVasoactive intestinal peptide	Rabbit	Chemicon
αCaspase	Rabbit	Cell Signalling Technologies
αErk1/2	Rabbit	Cell Signalling Technologies
αphospho-Erk1/2	Mouse	Cell Signalling Technologies
αp27Kip	Mouse	Santa Cruz

Secondary antibodies:

HRP-coupled αRabbit (western)	Goat	Chemicon
HRP-coupled αMouse (western)	Goat	Chemicon
HRP-coupled αGoat (western)	Rabbit	DAKO

Rhodamine Red-X-Conjugated αRabbit	Jackson ImmunoReaserch
Fluoroscein-Conjugated αMouse	Jackson ImmunoReaserch

4.1.7 Plasmid vectors

Bacterial vectors:

pBluescript SK	Stratagene
pSP73	Promega

pET-41-a-c	Novagen

Yeast vectors:

pGAD, pGBT	Clontech

Mammalian vectors:

FLPe cassette	Stewart, A.F.
pKS-DTA	Tajbakhsh, S.

Mouse BAC genomic clones	Research Genetics

4.1.8 Commercial kits

ABC kit	Vectastain
Codelink Expression Assay Reagent	Amersham
DAB Peroxidase Substrate System	Vector
Geneclean Spin kit	Q-BIO gene
Lambda mini kit	Qiagen
Large Construct kit	Qiagen
QIAquick Gel Extraction kit	Qiagen
Maxiprep	Qiagen
Prolong Antifade Kit	Molecular Probes
Riboprobe® Combination System-SP6/T7	Promega
RNeasy	Qiagen

4.1.9 Generally used solutions

BAC Church:	7 % SDS, 25 mM Na_2HPO_4 pH 7.2, 1 % BSA, 1 mM EDTA
BAC Wash:	1 % SDS, 20mM Na_2HPO_4, 1mM EDTA
Gel-loading Buffer:	0.25 % bromophenol blue, 15 % Ficoll, in water
PBS:	137 mM NaCl, 2.7 mM KCl, 6.5 mM Na_2HPO_4, 1.5 mM KH_2PO_4
20xSSC:	3M NaCl, 0.3M Na_3citrate•$2H_2O$ (pH to 7.0 with 1M HCl)
50xTAE:	0.04 M Tris-Acetate, 0.001 M EDTA

Tail Buffer:	0.1 M EDTA, 0.1 M NaCl, 1 % SDS, 0.05 M Tris-HCl, pH 7.6, ProteinaseK, 0.5 mg/ml
5xTBE:	45 mM Tris-borate, 1 mM EDTA
TBF1:	30 mM Potassium acetate, 100 mM RbCl, 10 mM $CaCl_2$, 50 mM $MnCl_2$, Glycerol to 15 % (v/v), pH 5.8 with acetic acid
TBF2:	10 mM MOPS, 75 mM $CaCl_2$, 10 mM RbCl, Glycerol 15 % (v/v), pH 6.5 with KOH
TBS:	100 mM Tris-HCl pH 7.5, 150 mM NaCl
TE	10 mM Tris-HCl (pH 8.0), 1 mM EDTA (pH 8.0)

4.1.10 Generally used media for bacteria and yeast

LB: 1 % Bacto-tryptone, 0.5 % Bacto-yeast extract, 0.5 % NaCl

YPD: 2 % Peptone, 1 % Yeast extract, 2 % Dextrose, 2 % Agar (for plates only)

SD: 0.67 % Yeast nitrogen base, 2 % dextrose, 1xDropout solution, 2% Agar (for plates only)

10xDropout solutions: L-Adenine 200 mg/L, L-Arginine-HCl 200 mg/L, L-Histidine 200 mg/L, L-Isoleucine 300 mg/L, L-Leucine 1000 mg/L, L-Lysine-HCL 300 mg/L, L-Methionine 200 mg/L, L-Phenylalanine 500 mg/L, L-Threonine 2000 mg/L, L-Tryptophan 200 mg/L, L-Tyrosine 300 mg/L, L-Uracil 200 mg/L, L-Valine 1500 mg/L.

4.1.11 Cells

Bacterial strains

E.coli XL-10 strain:	Tetr, D(mcrA)183, D(mcrCB-hsdSMR-mrr)173, endA1, supE44, thi-1, recA1, gyrA96, relA1, lac Hte (F' proAB, lacIqZ DM15 Tn10 (Tetr) Amy Camr)a
E.coli Y1090 strain:	F-, D (lacU)169, lon-100, araD139, rpsL, supF, mcrA, trpC22::Tn10/pMC9

BL21 DE3

Yeast strains

AH109:	MATa, trp1-901, leu2-3, 112, ura3-52, his3-200, gal4D,

gal80D, LYS2::GAL1$_{UAS}$-Gal1$_{TATA}$-HIS3, GAL2$_{UAS}$-Gal2$_{TATA}$-ADE2, UAR3:: MEL1$_{UAS}$-MEL1$_{TATA}$-lacZ

ES cells

ES cells used for gene targeting were from the IB10 line. The IB10 is a mycoplasma-free ES cell line rederived at the EMBL Transgenic Service from the E14,1 ES cell line, therefore containing a 129/OLA genetic background.

4.2 Methods

4.2.1 DNA - Plasmids

Preparation of plasmid DNA from bacteria

Mini preparation of plasmid DNA was performed according the following procedure: 1.5 ml of an overnight (O/N) bacterial culture was centrifuged in an eppendorf tube for 1 minute at 14000 rpm and room temperature (RT), the pellet was resuspended in 300 µl of resuspension buffer (50 mM Tris-Cl, pH 8.0, 10 mM EDTA, 100 mg/ml RNAse A), 300 µl of lysis buffer (200 mM NaOH, 1 % SDS) were added, mixed by inversion and incubated at RT for 1 minute, the lysate was mixed with 300 µl of cold neutralization buffer (3.0 M Potassium Acetate, pH 5.5), incubated on ice for 10 minutes and centrifuged for 10 minutes at 14000 rpm and RT, 800 µl of the supernatant were transferred to a new tube and the DNA was precipitated with 500 µl isopropanol, centrifuged for 5 minutes at 14000 rpm and washed with 1 ml of 70% ethanol. The DNA was air dried and resuspended in 50 µl TE. For large scale preparation of plasmid DNA, the QIAGEN Plasmid Maxi Kit was used according to the manufacturer's instructions.

Purification of supercoiled DNA by CsCl gradient centrifugation

For purification of supercoiled plasmids, 4 g Caesium Chloride were dissolved in 3.8 ml of TE containing the DNA to be purified. 0.2 ml of Ethidium Bromide solution (10 mg/ml in water) were added and the mixture was transferred to a 4 ml centrifuge tube (Beckman) for centrifugation in a Beckman vertical Vti65 rotor. After sealing, the tubes were spun O/N at 60000 rpm and 25°C. One visible band at the center of the gradient was collected into a glass tube using a hypodermic needle. Ethidium Bromide was extracted from the DNA by a series of equal volumes of 1-Butanol extractions until no pink colour was detected. The DNA was

centrifuged in a centricon filter device at 4000 rpm (SS34 - Sorvall) and 25°C and washed 3 times with TE to remove CsCl.

Plasmid extraction from yeast

5 ml of SD-Leu were inoculated with one yeast colony and grown for 2 days at 30°C. The yeast culture was spun down 1500 rpm (RC-3B – Sorvall) for 5 minutes, washed once in water and resuspended in 300 µl yeast lysis buffer (2.5 M LiCl, 50 mM Tris-HCl pH 8.0, 4 % triton X-100, 62.5 mM EDTA). 300 µL Phenol/Chloroform (50/50) was added and the suspension was vortexed vigorously for 1 minute with 50 µl acid washed beads. The mixture was spun at 14000 rpm (Eppendorf) for 5 minutes and the top aqueous phase was collected into a new tube. The DNA was precipitated with 600 µl of ice-cold ethanol for 15 minutes at -80°C, spun at 14000 rpm for 10 minutes at 4°C. The pellet was washed in 70 % ethanol and dried. The pellet was resuspended with 40 µl water and precipitated with 4.8 µl Sodium Acetate and 100 µl Ethanol at 14000 rpm for 10 minutes. The pellet was washed in 70 % ethanol, dried and resuspended in 20 µl water. Purified yeast plasmid was transformed into E.coli XL-10 by electroporation.

Spectrophotometric determination of DNA and RNA concentration

Spectrophotometric measurements of DNA solutions were done at wavelengths of 260 nm. An OD=1 at 260 nm corresponds to a concentration of 50 µg/ml for double-stranded DNA and 33 µg/ml for single-stranded oligonucleotides and 40 µg/ml for RNA.

DNA restriction and Klenow treatment

To a solution of DNA the appropriate 10xbuffer and restriction enzyme were added according to the manufacturer's recommendations, mixed in a reaction tube and typically incubated O/N at the appropriate temperature. Klenow treatment was done in accordance with the NEB protocol.

Electrophoresis of DNA

Analysis and preparation of DNA were performed using agarose gels containing 0.5 µg/ml Ethidium Bromide. 1xTAE-buffer was used as gel and electrophoresis buffer. DNA samples were loaded into the gels in 1xDNA loading buffer and run at 5 V/cm of gel. The DNA samples were generally run in parallel to a DNA molecular weight marker (1kb ladder).

Isolation and purification of DNA from preparative agarose gels

DNA was isolated from agarose using two different commercial kits according to the fragment size. For fragments up to 6 kb, the QIAquick® Gel extraction Kit (Qiagen) was used according to the manufacturers instructions. For fragments bigger than 6 kb, the Gene Clean Spin Kit was used according to the manufacturers instructions. For purification of large amounts of DNA from agarose gels, the S&S BIOTRAP Electro-Separation-System for elution and purification of charged molecules was used according to the manufacturer's instructions.

DNA ligation

For ligation of purified DNA fragments into linealised plasmid vectors, an appropriate amount of each DNA species was incubated O/N in a total volume of 10 µl with 1 µl of 10xbuffer and 1U DNA ligase. Ligation reactions were incubated O/N at 16°C.

Preparation of chemocompetent Escherichia coli XL-10 cells

5 ml of LB medium (+tetracycline) were inoculated with a single colony of E.coli XL-10 and incubated with shaking (300 rpm) O/N at 37°C. 250 ml of LB medium were inoculated with 3-4 ml of the overnight culture and incubated with shaking at 37°C until an OD600 of 0.5 to 0.6. The cell suspension was incubated on ice for 5 minutes, poured into 50 ml Falcon tubes and centrifuged at 3000 rpm (GSA - Sorvall) and 4°C for 10 minutes. The supernatant was discarded and the bacterial pellet was resuspended in 20 ml of TBF1 buffer (2/5 volume) and incubated on ice for 5 minutes. The cell suspension was centrifuged at 3000 rpm (RC-3B) and 4°C for 5 minutes, the supernatant was discarded and the bacterial pellet was resuspended in 2 ml TBF2 buffer (1/25 initial volume). After 15 minutes of incubation on ice 200 µl aliquots were frozen in liquid nitrogen and stored at -80°C.

Transformation of chemocompetent Escherichia coli XL-10 cells

100µl of competent E.coli XL-10 cells were added to DNA in an eppendorf tube and incubated on ice for 30 minutes, the mixture was then heat shocked for 90 seconds at 42°C, followed by a 3 minutes incubation on ice. 1 ml of LB medium was added and the cell suspension was incubated for 30 minutes at 37°C. The transformation was then plated on the appropriate selective media and incubated at 37°C overnight.

Preparation and transformation of electrocompetent E.coli XL-10 cells

5 ml of LB medium was inoculated with one colony of XL-10 and grown O/N at 37°C. 500 ml of LB was inoculated from the overnight culture and grown to an OD600 of 0.6. The bacteria were chilled on ice for 10 minutes and spun down at 4000 rpm (GSA) at 4°C for 20 minutes. The supernatant was aspired and the pellet resuspended in 500 ml of ice-cold water and spun as above. This procedure was repeated. After two washes, the bacteria were resuspended in one volume of ice cold water. Up to 0.5 μg plasmid DNA in 1 μl water was mixed with 100-300 μl of competent bacteria and placed in a pre-chilled cuvette. The electroporation apparatus was set at 2.5 kV, 25 mF and 200 ohms and the transformation was subjected to one pulse. The transformation was transferred to 1ml of LB and incubated on a wheel for 30 minutes at 37°C. Finally the bacteria was plated on the appropriate selective plates (LB-ampicilin in the case of pGAD vector recovery)

Transformation of yeast

50 ml YPD was inoculated with one or more yeast colonies and grown 16-18 hours at 30°C (OD600>1.5). The overnight culture was diluted in 300 ml to an OD600 of 0.2 in fresh YPD and the culture was grown until an OD600 of 0.6. The yeast was spun spun down at 1.000 rmp (RC-3B) for 5 minutes at room temperature, the pellet was resuspended and washed in 50 ml of water, spun again and finally resuspended in 1.5 ml of freshly prepared TE-LiAc (10 mM Tris-HCl PH 7.5, 1 mM EDTA, 100 mM LiAc).

For small scale transformations 0.1 μg of plasmid and 100 μg of herring testis carrier DNA were added to an eppendorf tube and 100 μl of competent yeast suspension were added and mixed by vortexing. 600 μl of PEG/LiAc solution (40 % PEG4000, 10 mM Tris-HCl PH 7.5, 1 mM EDTA, 100 mM LiAc) were added and the mixture vortexed again. The transformation was incubated for 30 minutes at 30°C, 70 μl of DMSO were added and the mixture was then heat shocked for 15 minutes at 42°C. After cooling on ice, the yeast was spun down at 14000 rpm, and the supernatant was removed. The pellet was resuspended in 300 μl sterile TE and plated on appropriate selective medium.

4.2.2 DNA - λ phage

Culture and preparation of bacteria for infection with λ-phage

For the preparation of bacteria for infection, a 500 ml Y1090 culture (LB medium supplemented with 0.2 % Maltose and 10 mM $MgCl_2$) was inoculated and incubated O/N at 37°C with agitation. The following day 500 ml of fresh medium were inoculated with the O/N culture and grown until an OD600 of 1.5. The cells were then centrifuged for 15 minutes at 4000 rpm (GSA) and 4°C. The cell pellet was resuspended and washed in the same volume of a 10 mM $MgSO_4$ solution. The cells were again centrifuged at 4000 rpm for 15 minutes, resuspended in 1/4 volume of 10 mM $MgSO_4$ and stored at 4°C up to 4 weeks.

Infection with and plating of λ-phage

To plate λ phage infected bacteria, tenfold serial dilutions of λ-phage stocks were prepared in suspension medium (0.1 M NaCl, 0.01 M $MgSO_4$, 0.05 M Tris-HCl, pH 7.5). For infection, 180 µl of E. coli in $MgSO_4$were added to 10 ml tubes and 10 µl of λ-phage dilution were added and mixed. The mixture was incubated at 37°C for 20 minutes to allow adsorption of the phage particles to the bacteria. 4 ml of molten 0.7 % agarose were added to each tube, mixed with the bacteria and poured onto a pre-warmed (37°C) LB plate. The plates were left standing at room temperature until the top agarose was solidified and then incubated at 37°C for 8 hours until the phage plaques were visible.

Detection of specific λ-phage plaques by southern blot

Detection and localisation of phage plaques containing a desired cDNA was performed by hybridisation of a specific radioactively labeled DNA probe to a nitrocellulose membrane containing a replica of the phage plaques on the growth plates. To transfer phages onto the nitrocellulose membrane, a membrane was placed on the surface of an infected plate so that the entire membrane would be in contact with the plate. The plate and membrane were marked for subsequent orientation. Transfer of the plaques was done for 5 minutes at room temperature. For isolation of viral DNA, the membranes were placed facing up in 0.5 N NaOH/1.5 M NaCl for 2 minutes at room temperature. After a neutralization step using 0.5 M Tris-HCl pH 8.0/1.5 M NaCl for 2 minutes, the membranes were air-dried for a few minutes. Phage DNA was immobilized by incubating the nitrocellulose membranes for 2 hours at 80°C. Detection and localization of specific phage plaques was performed using the Southern blot technique as described.

Picking λ-phage plaques

To isolate phage plaques, the tip of a Pasteur pipette was used to stab and separate an agarose piece containing the chosen plaque. The agarose piece was placed in an eppendorf tube containing 500 µl of suspension medium plus 10 µl chloroform. The tube was incubated O/N at 4°C to allow diffusion of the phage particles to the medium.

Extraction of λ-phage DNA

For preparation of DNA from individual clones of λ-phage, a suspension containing a phage clone was used to infect plating bacteria as described. To propagate a phage clone in soft agarose, the most appropriate dilution of a series of tenfold dilutions was chosen to give a confluent phage plaques plate. This dilution was used to generate four confluent plates. To harvest the phages, 5 ml of suspension medium were added to the plates and incubated O/N at 4°C with gentle shaking. All suspension medium containing a single phage clone was transferred into a polypropylene tube. DNA extraction from the suspension medium containing the propagated phage clone was performed using the Lambda mini kit (Qiagen) according to the manufacturer's instructions.

4.2.3 DNA - Genomic

Preparation of genomic DNA

For genomic DNA preparation from mouse tails, each tail was incubated O/N in 800 µl of tail buffer at 56°C. The following day, 300 µl of 6M NaCl was added, mixed by shaking and centrifuged for 10 minutes at 14000 rpm (Eppendorf) at RT to pellet the tail debris. 800 µl of the supernatant were transferred into a new reaction tube, mixed with 500 µl isopropanol and centrifuged at 14000 rpm for 5 minutes to pellet the genomic DNA. Supernatant was aspirated and the recovered DNA was washed in 70 % ethanol and dissolved in 100 µl TE.

For preparation of genomic DNA from ES-cells, a confluent well from a 24 well plate was washed twice in PBS, incubated O/N at 37°C with 600 µl ES-cell lysis buffer (10 mM Tris-HCl pH 8.0, 5 mM EDTA, 100 mM NaCl, 1 % SDS and 0.5 mg/ml Proteinase K). The next day DNA was precipitated in an eppendorf tube by addition of 500 µl isopropanol followed by mixing by shaking. The precipitated DNA was transferred to a new tube with a tip and

washed O/N with 70% ethanol. After spinning down the DNA was resuspended in 100 µl TE O/N at 37°C

Polymerase Chain Reaction (PCR)

For mouse genotyping, the standard genomic PCR reaction was performed with a hot start protocol that employs the HotStarTaq DNA polymerase. One reaction contained:

17 µl H2 O

2 µl 10xPCR buffer (QIAGEN)

0.5 µl dNTP solution (10 mM each dATP, dCTP, dGTP, dTTP)

0.2 µl each primer 50 mmol)

0.5-1U HotStarTaq DNA polymerase

5 ng DNA

The PCR reaction was initially denatured for 15 minutes at 94°C to activate the HotStarTaq DNA polymerase. PCR was typically performed with 36 cycles, each cycle consisting of 40 seconds denaturation at 95°C; 40 seconds annealing at the appropriate temperature for the oligonucleotides; 45 seconds of elongation at 72°C. The amplification products were assayed by gel electrophoresis.

For cloning purposes either the Pwo polymerase or the High Fidelity Expand was used, essentially as described above with the omission of the 15 minutes hot start.

Southern blot analysis

Detection and localisation of specific sequences within genomic or plasmid DNA was performed using the Southern blot technique. Typically the DNA (20mg of mouse genomic DNA or 1mg of plasmid DNA) was treated with one or more restriction enzymes. The resulting fragments were separated according to size by agarose gel electrophoresis (0.6 % gel cast in 0.5xTBE containing 0.5 µg/ml Ethidium Bromide was used for genomic DNA samples). After electrophoresis was completed, the gel was photographed with a fluorescent ruler for subsequent assessment of band sizes. The DNA was denatured by incubating the gel in 0.5 N NaOH, 1.5 M NaCl for 30 minutes with agitation. The gel was then briefly rinsed in deionized water before the DNA was transferred to a nylon membrane by capillarity under neutral conditions (20XSSC). The membrane was incubated for two hours at 80°C to immobilise the attached DNA, followed by a pre-hybridisation (2 hours minimum) in Church hybridisation solution at 65°C. The membrane was then probed O/N at 65°C with a radio-

labeled probe in 30 ml of Church buffer. After hybridisation, the membranes were washed in the following series of increasingly a stringent washing buffers: 2xSSC, 1 % SDS; 0.5xSSC, 1 %S DS; 0.1xSSC, 1 % SDS for 30 minutes each. Autoradiography was used to locate the positions of the bands complementary to the probe.

Radiolabelling of DNA probes for southern blot analysis

Labelling of DNA probes for southern blot analysis was performed PCR. Using a previously amplified sequence (in general with a size of 300 bp) as a template in the following reaction, radioactive dCTP-P^{32} was incorporated of into the probe:

8 µl H_2O

2 µl 10xPCR buffer

3 µl dNTP solution (0.5 mM each dATP, dGTP, dTTP)

5 µl P^{32}-dCTP (50 µCi)

0.5 µl each primer

2.5 U HotStarTaq DNA polymerase (QIAGEN)

5 ng Template DNA

The PCR reaction was initially denatured for 15 minutes at 94°C to activate the HotStarTaq DNA polymerase. PCR was usually performed with 30 cycles, each cycle consisting of 20 seconds denaturation at 95°C, 30 seconds annealing at 50°C, and 30 seconds of extension at 72°C. A final cycle of 5 minutes at 95°C was performed to denature the labelled probe. The probe was incubated on ice for 4-5 minutes and then added into the hybridisation solution.

4.2.4 RNA

Microarray analysis of pituitary gland expression pattern

13 week male mice were perfused with PBS, and the pituitary gland immediately removed. The pituitary glands were dissected with scissors in 600 µl RLT buffer (Qiagen), sheared with a p1000 pipette and with a Gauge21 syringe and snap frozen in liquid nitrogen. RNA was prepared using the Qiagen RNeasy kit in accordance with the protocol. The quantity of RNA was measured by spectrophotometry and the quality of the RNA was analysed by denaturing gel electophoresis (Gel: 1 % Agarose, 20 mM MOPS, 0.75 % formaldehyde, 0.5 µg/ml Ethidium Bromide. Running buffer: 20 mM MOPS.) on 2 µg of RNA. 1.8 µg of total RNA from each pituitary gland was labelled with biotin using the Codelink Expression Assay Reagent kit according to the protocol. The labelled mRNA was assayed by use of the Agilent

Bioanalyser and quantified by spectrophotometry. 10 μg of labelled mRNA were fragmented and loaded on the 20K mouse Bioarray as describe in the protocol and hybridised O/N at 37°C. The Bioarrays were then washed and bound biotin labelled probe detected with Cy5-streptavidin. The arrays were scanned in a GenePix Array scanner at 635 nm as described and analysed by Codelink Expression Analysis software. Microarray results were analysed using the software Genespring from Silicon Genetics.

4.2.5 DNA constructs

Construction of the *Men1* targeting vector

A 129 Mouse BAC library was screened with a probe corresponding to exon2 of mouse *Men1*. 4 positive BAC clones wereidentified: 7B24, 7D21, 7D23 and 7 F23 and the presence of *Men1* exon 2 was confirmed by PCR. Southern blot on BAC 7B24 and 7D21 revealed the presence of an approximately 8 kb EcoRV fragment that already published sequence (Guru *et al*., 1999) suggested would contain the entire *Men1* gene. The EcoRV fragment was cloned in the Bluescript vector. Unique HpaI and BstEII sites in intron 2 and 6 respectively (se Fig 2.1.1) was used to insert LoxP sites and a positive selection cassette in as described below.

A poly-linker was constructed from 4 oligos with the following sites:

SacI SgfI EcoRV LoxP HpaI LoxP AscI BstEII SpeI SgfI Asp718

First, a 3498 bp EcorV, HpaI 5´arm was inserted into the EcoRV site of the poly-linker. Next, a 1577 bp HpaI, BstEII Klenow blunted fragment was inserted into the HpaI site. Independently, a 2869 bp BstEII, EcoRV 3'arm fragment was fused to a PmeI, Spe1 fragment containing a negative selection Diphteria toxin A (DTA) cassette (Tajbakhsh, S.). This approximately 3900 bp fragment was inserted into the BstEII and SpeI sites of the construct. Finally the construct was partially digested with AscI (to avoid cutting an AscI site in the DTA cassette) and a 3500 bp FRT flanked positive selection neomycin resistance cassette was inserted as an AscI fragment.

Cloning of full length Gad67

A 1247 bp clone was isolated in a yeast two hybrid screening with Menin as a bait. Retransformation of the clone into AH109 showed that the clone supported growth in the presence of Menin-Gal4DNA binding domain but not in the presence of a vector encoding Gal4DNA binding domain alone.

The clone was used to screen a λ phage pituitary gland library as described. One clone containing a 3525 bp insert encoding the predicted 5' end of the gene was isolated. This

cloned overlapped the original yeast clone with only 92 bp. To clone the predicted 3' end of the gene, ESTs were studied and a PCR based approach based on a primer upstream of a SacI site in the 3' end of the yeast clone - Gad67SacI1, and a primer downstream of the predicted translation termination - Gad67PstI was chosen. A 924 bp fragment containing the predicted sequence was cloned.

To fuse the yeast clone with the λ phage fragment, a 591 bp BamHI, AseI fragment was cloned by PCR from the yeast two hybrid library using the primers Gad67BamHI and Gad67AseI. Finally, to clone the open reading frame, the 5' 108 bp of the open reading frame was cloned from the phage clone using the primers Gad67NotIXhoI and Gad67SacIDn. The cDNA was assembled from the 108 bp NotI, SacI fragment + 2921 SacI, BamHI fragment + 591 bp BamHI, AseI + 779 bp AseI, SacI fragment and 924 bp SacI, PstI fragment

Generation of *Pit-1-Cre* transgene

14.9 kb of *Pit-1* promoter containing sequences from –14.8 to +13 of the mouse Pit-1 promoter was cloned as a NotI, XhoI fragment (Rhodes *et al*., 1993) in front of an expression cassette consisiting of *Cre* recombinase flanked by a rabbit β-globin intron and polyadenylation signal in the BSSK$^-$ vector. This promoter fragment should be sufficient to ensure tissue specific expression of the transgene (Rhodes *et al*., 1993).

The plasmid was linealised with NotI and purified from the agarose gel using the BIOTRAP system. The DNA was dialysed against TE prepared from distilled tissue culture tested water (GibcoBRL) and diluted to 2 ng/μl in the same buffer.

DNA was injected into the pronuclei of fertilised Oocytes derived from BL-6, CD1 crosses by the EMBL transgenic facility. The injected Oocytes were implanted in pseudopregnant CD-1 foster-mothers.

DNA constructs for *in situ* probes

All probes were generated by cloning a DNA fragment containing either the complete cDNA or relevant parts of the cDNA of the gene to be probed into the BSSK vector. For all probe except cyclin B and the yeast two hybrid clones, the fragment were generated by PCR from a pituitary gland cDNA library. The probe for cyclin B was generated by PCR from chromosomal DNA and the probes from the yeast two hybrid clones were cloned from the yeast plasmids.

4.2.6 Cell culture methods

Culture conditions

Mouse embryonic stem (ES) cells were cultured in ES medium: glucose-rich (4500 mg/liter) DMEM medium supplemented with 15 % Fetal Calf Serum (FCS), 1 % MEM nonessential amino acids, 1 % Penicillin-Streptomycin, 1 % Glutamine, 1 % Sodium Pyruvat and Leukaemia Inhibitory Factor (LIF). The ES cells were grown on a layer of mouse embryo fibroblasts (MEFs) at 37°C with 5 % CO_2. Selection of ES cell clones that had integrated the replacement vectors was done by adding the antibiotic G418 (250 mg/ml) to the medium. Ongoing cultures of MEFs and ES cells were typically grown in 10-cm tissue culture dishes with 10 ml of medium. All ES-cell medium was changed daily.

Trypsinisation of cells

ES cells and fibroblasts at sub-confluent density were passed into new tissue culture dishes at lower density. The medium was aspirated and the cells were washed once with PBS. The cells were subsequently covered with 0.5 % (w/v) trypsin and incubated at room temperature until they were visibly detached from the dish. The trypsinisation reaction was stopped by addition of FCS containing medium. Cells were collected in a 50 ml tube, centrifuged (1500 rpm, 3 minutes) and the pellet was resuspended in new medium. The cells were counted using a Neubauer chamber and plated at appropriate numbers on new tissue culture dishes.

Mitomycin C treatment of Mouse Embryo Fibroblasts

To mitotically inactivate feeder cells, confluent layers of MEFs in tissue culture dishes were treated with medium containing 10 mg/ml of Mitomycin C for 3 hours at 37°C with 5 % CO_2. The dishes were washed three time with PBS and the cells collected by trypsinisation. After centrifugation, the cells were resuspended in feeder medium (glucose-rich (4500mg/liter) DMEM medium supplemented with 15 FCS, 1 % MEM nonessential amino acids, 1% penicillin-streptomycin, 1% glutamine), counted and the appropriate number was transferred to tissues culture dishes to ensure the production of a uniform confluent mono layer of cells.

Freezing and thawing cells

Cells were trypsinised, counted and centrifuged for 3 minutes at 1500 rpm. The supernatant was discarded and the pellet was resuspended in new medium at a density of $2.5x10^6$ cells/ml. Aliquots of $1x10^6$ cells were transferred into individual cryo vials and an equal volume of

medium containing 20% DMSO was added to each vial (10% DMSO final concentration). The cell suspension was frozen, by storing the vials at -80°C. For long-term storage, vials were transferred into liquid nitrogen. For thawing, cells the vials were rapidly warmed at 37°C and the cell suspension was transferred into a centrifuge tube containing medium. The cells were centrifuged at 1500 rpm for 3minutes, resuspended in new medium and transferred to tissue culture dishes. ES cells were transferred to tissue culture dishes containing a confluent layer of mitotically inactive MEFs.

Electroporation of ES cells

An exponentially growing culture of ES cells at passage #4 was prepared for electroporation by changing medium approximately 3 hours before harvesting the cells. The cells were trypsinised and medium added to stop the trypsinisation reaction. Cells were centrifuged for 4 minutes at 3000 rpm and RT, washed once and resuspended in PBS as a single cell suspension. The ES cell suspension was counted, and the cell suspension was centrifuged once more, washed and resuspended at a density of $1.5x10^7$ cells/ml in Ca^{2+} /Mg^{2+} free PBS. For each electroporation, 0.8 ml ($1.5x10^7$ cells) of cell suspension was placed in a sterile cuvette and 25 μg of linearised DNA were added and mixed well. This mixture was left at room temperature for 5 minutes and a single pulse of 240 V, 500 mF was applied to the cuvette. After electroporation, the cells were incubated on ice for 5 minutes and plated onto 10-cm tissue culture dishes of neo-resistant MEF feeder cells. Each 0.8 ml sample from the electroporation was divided and equally distributed on eight tissue culture dishes. The cells were allowed to recover for 48 hours in non-selective medium. The G418 selection of ES clones that had integrated the replacement vectors started 48 hours after electroporation.

Isolation of individual ES cell colonies

Selected individual ES cell colonies were isolated 9-10 days after electroporation. Sets of 96-well tissue culture dishes containing confluent mono-layers of MEFs in fresh medium were prepared in advance. Culture medium was replaced by PBS. The tip of a 10 μl micropippete was used to dissociate individual colonies to small aggregates of only a few cells. The dissociated colonies were transferred into the 96-well dishes and incubated at 37°C with 5 % CO_2. 48 hours after isolation, the individual clones were trypsinised and further cultured in the same well to give rise to an exponentially growing set of evenly distributed ES cell colonies. The growth of all ES cell clones was monitored daily and when considered appropriate (~50%

confluency for the highest number of clones) all clones in one dish were trypsinised and divided in the following way: Half of the ES cells of each clone were transferred to a new 96-well dish containing mitomycin C treated MEFs and these cells were subsequently frozen; the remaining cells from each clone were transferred to gelatin coated 24-well dishes for later preparation of genomic DNA. Homologous recombination was verified by southern blot.

ES cell injection into blastocysts and chimera production

Blastocyst injection was performed at the EMBL Transgenic Service. IB10 targeted ES cells with a 129/OLA genetic background were injected into E4.5 mouse blastocysts of the C57/Black6 strain produced by natural matings.

Establishment of MEFs

E11.5 embryos were isolated and the head removed for genotyping. The embryos were passed 5 times through an 18 gauge syringe and 5 times through a 21 gauge syringe. The resulting suspension was plated on in sterile tissue-culture dish (24 well) with medium (DMEM medium supplemented with 10 % FCS, 1% penicillin-streptomycin, 1% glutamine) and incubated O/N to allow cells to attach. The next day the medium was changed and cells allowed to grow to confluency. The cells were passaged with 1:3 to 1:10 splitting.

4.2.7 Tissue sectioning

Tissue preparation and fixation

Fixation of mouse tissues, organs and whole embryos was performed differently depending on whether the samples would be used for histology, Immunohistochemistry or *in situ* hybridisation.

For histological analysis of tissues using paraffin sections, pituitary glands were isolated from mice perfused in 4 % PFA and fixed 5 hours at 4°C in 4 % PFA. The pituitary glands were subsequently washed in PBS for 10 minutes at 4°C and stored indefinitely in 70% ethanol at 4°C.

For analysis of gene expression by *in situ* hybridisation, organs from mice perfused in 10 % formalin and embryos were properly dissected and stored indefinitely in 10% formalin.

Cryosectioning

After fixation, embryos and organs were incubated O/N at 4°C in RNAse-free 20 % Sucrose/PBS (w/v) solution O/N or until the tissue sank. OCT medium was placed in embedding molds and the tissue sample was introduced in the medium. The molds were placed in dry ice-cold ethanol to freeze the medium. Typically, 18 μm sections were cut on a Leica Cryotome with a chamber temperature of -20°C. Tissue sections were transferred onto glass slides and air dried for a minimum of 2 hours and stored at -20°C for later processing.

Paraffin embedding and mounting

Mouse organs preserved in 70% ethanol were dehydrated in a series of 85%, 96% and three times 100% ethanol at least for 1 hour for each step at room temperature. The samples were cleared in two changes of xylene for 30 minutes each and incubated O/N in xylene at room temperature. The organs were carried through a series of four changes in paraffin 1hour each at 60°C and embedded in the proper orientation in embedding molds. The molds were stored at 4°C until sectioning. The microtome was set to cut 7 μm sections.

Vibrotome sectioning

Pituitary glands from mice perfused in 4 % PFA were fixed in 4 % PFA for 4 hours at 4 °C, washed in PBS and embedded in 2 % Agarose in PBS. The agarose block was mounted on the vibrotome, and 50 μm section were cut. The agarose was removed when possible with a brush the tissue sections were stored in 0.5 % PFA in PBS at 4°C.

4.2.8 Histochemistry and Immunohistochemistry

Hematoxylene and Eosin staining

For hematoxylene and eosin staining of brain paraffin sections, slides were incubated twice for 10 minutes in xylene followed by rehydration in a series of 100%, 96% and 70% ethanol. After rinsing in distilled H_2O, sections were stained in hematoxylene solution (Sigma) for 10 minutes and washed in water for 10 minutes. Sections were subsequently stained in eosin solution (Sigma) for approximately 30 seconds, rinsed in distilled water, dehydrated in an ascending ethanol series, cleared in xylene and mounted.

Immunofluorescence

Imunofluorescence stainings were performed on 50 μm free floating vibrotomes sections prepared as described. Sections were rinsed for 10 minutes in PBS. For blocking, the tissue sections were incubated for 2 hours with 5 % (v/v) 2nd antibody species serum in TBS/0.4 % Triton X-100 at room temperature. sections were washed twice with TBS/0.4% triton X-100 and incubated with the primary antibody at the appropriate dilution in TBS/0.4% triton X-100 O/N at 4°C. The slides were rinsed twice with TBS/0.4% triton X-100 and incubated with fluorescent-labelled secondary antibody in TBS/0.4 % Triton X-100 for 1 hour at room temperature in the dark. The slides were washed twice in 1xTBS/0.4% triton X-100 and mounted with 60 μl of slow fade reagent (Prolong Antifade kit, Molecular Probes) according to the manufacturer's indications. Slides were stored at 4°C in the dark.

Immunohistochemistry

Immunohistochemical assays were performed on paraffin sections of embedded pituitary glands. The sections were initially deparaffinated by incubation in xylene for 3x5 minutes followed by rehydration in a series of 100%, 95% and 70% ethanol (3 minutes each). After washing in TBS for 5 minutes, antigen was unmasked and endogenous peroxidases were inactivated by one of two different methods.

1) Plain method. Sections were incubated for 10 minutes in 3 % H_2O_2/10 % MeOH in 1xTBS followed by 5 minutes washing in 1xTBS with agitation

2) Microwave method. Sections were heated in 250 ml unmasking solution (Vector) for 2x5 minutes at 540W in microwave oven. After cooling for 20 minutes, the sections were rinsed in water and then washed in 1xTBS for 5 minutes with agitation. The sections were then incubated for 10 minutes in 3 % H_2O_2/10 % MeOH in 1xTBS followed by 5 minutes washing in 1xTBS with agitation

The sections were incubated with blocking buffer (0.4 % Triton, 1 % Glycine, 3 % BSA, 10 % normal serum in 1xTBS) in a wet chamber for 2 hours at room temperature. After blocking, the sections were incubated with primary antibody in blocking buffer in a wet chamber ON at 4°C. The slides were washed for 3x20 minutes in wash buffer (0.4 % Triton, 1 % Glycine, 3 % BSA in 1xTBS) with agitation. The sections were incubated with biotinylated secondary antibody (vector) in was buffer in a wet chamber for 1 hour at room temperature and then washed as after primary antibody. The staining procedure using the ABC reagent and DAB substrate was performed according to the manufacturer's recommendations. The sections were

counterstained with methyl green stain (1:8 dilution from 2 % stock 10 minutes) dehydrated 2x10 minutes in 1-Butanol, cleared in xylene and mounted with 60 µl Eukitt.

4.2.9 *In situ* hybridisation

Generation of *in situ* probes by *in vitro* transcription

The radioactive labelling of RNA probes was performed using the Riboprobe® Combination System-SP6/T7. An *in vitro* transcription labelling reaction was set up and incubated for 1 hour at 37°C:

4 µl of 5xtranscription buffer

2 µl of 100 mM DTT

0.6 µl RNasin

4 µl of A/G/C mix (2.5mM each nucleotide)

1 µg of linearised template

Nuclease free H_2O to 14 µl

5 µl ^{35}S-UTP (100 µCi)

1 µl of RNA polymerase

The labelling reaction was followed by a treatment with DNaseI at 37°C for 15 minutes. This reaction was stopped by addition of 30 µl nuclease-free water and the labelled RNA was recovered using ProbeQuant™ G-50 Micro Columns according to the manufacturer's protocol. A probe concentration of $5x10^6$ cpm/ml was routinely used on the different tissue sections. The calculated amount of ^{35}S-labeled probe for 1 ml Hybridisation solution was initially mixed with 50 µl tRNA, 10 µl 1M DTT and nuclease-free H_2O to 200 µl. This mixture was incubated at 65°C for 5 minutes to denature annealed strands in the labelled probe and added to 800 µl Hybridisation solution (50 ml l Hybridisation solution: 25 ml formamide, 10 ml 50 % dextran sulphate, 3 ml 5 M NaCl, 1 ml 1xDenhardt's solution, 0.5 ml 1 M Tris-HCl pH 8.0, 0.1 ml 0.5 M EDTA pH 8.0, 0.4 ml nuclease free H_2O). The hybridisation mixture was stored at -20°C until the hybridisation step for a maximum of 1 week.

Hybridisation

18 µm frozen cryostat sections were used for *in situ* hybridisation. The tissue sections were initially treated with Proteinase K (10 mg/ml) in proteinase digestion buffer (0.1 M Tris-HCl pH 8.0, 50 mM EDTA pH 8.0) at 37°C for 30 minutes. Slides were rinsed briefly in dH_20 and

incubated in 0.1 M triethanolamine (TEA) pH 8.0 for 3 minutes at room temperature, and then acetylated in acetylation buffer (625 µl acetic anhydrid, 250 ml 0.1 M TEA) for 10 minutes at room temperature. Slides were then incubated in 2xSSC for 5 minutes and dehydrated through an ethanol series of 50%, 70%, 90% and 2 times 100% ethanol for 3 minutes each step. The slides were drained for 5 minutes and dried under vacuum in an exciccator for a minimum of 2 hours until hybridisation.

To hybridise the tissue sections with the a ^{35}S-labelled probe, an aliquot of the hybridisation mixture was placed at 65°C for 10 minutes and then centrifuged for 10 minutes at 3000 rpm to eliminate any dextran sulfate precipitates that may have formed. 65 µl of hybridisation mixture was applied to each slide (50x22 mm) and the tissue sections were then covered with a coverslip and sealed with the application of a bead of liquid DPX mounting medium. For hybridisation, the slides were incubated O/N on 60°C slide-warming tray. After hybridisation, the slides were cooled and incubated four times 15 minutes with 4xSSC. The slides were subsequently treated with RNaseA in RNase buffer (RNaseA 20 µg/ml, 25 ml 5 M NaCl, 2.5 ml 1 M Tris-HCl pH 8.0, 500 µl 0.5 M EDTA pH 8.0, dH_2O to 250 ml) for 37 minutes at 37°C. This was followed by a washing and gradual de-salting series of the following solutions: 2xSSC, 1 mM DTT for 5 minutes at RT; 1xSSC, 1 mM DTT for 5 minutes at RT; 0.5xSSC, 1mM DTT for 5 minutes at RT; 0.1xSSC, 1mM DTT for 37 minutes at 65°C; 0.1xSSC, 1mM DTT for 3 minutes at RT. Slides were then dehydrated through an ethanol series of 50 % ethanol (with 0.08xSSC, 1mM DTT), 70 % ethanol (with 0.08xSSC, 1mM DTT), 95 % ethanol and 100% ethanol each step for 3 min. The slides were finally drained for 5 minutes and dried under vacuum in an exciccator for a minimum of 2 hours.

4.2.10 Mouse methods

Mice were housed in a specific pathogen free environment and under controlled light, temperature (21°C) and humidity (50 % relative humidity) conditions. Water and food were provided as needed. Mice were routinely weaned from their parents at the age of 3 weeks with males and females being housed separately. Mice were tagged using six-digit number eartags and tail biopsies were taken for genotyping.

For experiments with embryos, breedings were set up with one male and one female. Vaginal plug-checks were performed daily, starting the morning following the set up of the breeding. The presence of a plug was considered day 0.5 of pregnancy. Embryos were taken from the mothers as previously described. For genotyping of embryos at day E12.5 or younger the yolk

sacs were separated from the placenta and used for DNA extraction. With embryos older than E12.5 tissue samples for genomic DNA were normally taken from the tail. The day of birth of the new litters was considered P0.

4.2.11 Proteins

Cell-extracts

All extracts from cell-culture and mouse tissues were done in RIPA buffer (50mM Tris-HCl pH 7.5, 150 mM NaCl, 1 % NP-40, 0.1 % SDS, 0.5 % Sodiumdeoxycholate, 0.05 % β-mercaptoethanol, protease and phosphatase inhibitors).

Mouse pituitary glands were removed after perfusion with PBS, snap frozen in liquid nitrogen and lysed in RIPA buffer in an eppendorf tube with a pestel. The extracts were sheared with a pipette tip and insoluble debris spun down at 14000 rpm.

Mouse Embryo Fibroblast cultures were lysed on ice in RIPA buffer with a cell scraper and the extracts treated as above.

Protein concentration meassurements

Protein concentrations were determined by Bio-Rad Bradford protein assay according to the manufactures protocol. In all assays, BSA was used as a standard.

SDS-PAGE

All SDS-PAGE gels were run on the Mini Protean 3 system and the gels wereprepared as follows:

Separation gel: 0.375 M Tris-HCl pH 8.8, 8-18 % acrylamide, 0.1 % SDS, 0.05 % APS and TEMED (3 µl in 5 ml)

Stacking gel: 0.125 M Tris-HCl pH 6.8, 3.9 % acrylamide, 0.1 % SDS, 0.05 % APS and TEMED (5 µl in 5 ml)

Extracts were heated to 90°C for 4 min. in Laemmli buffer (5xLeammli buffer: 0.15 M Tris-HCl pH 6.8, 5 % SDS, 25 % glycerol, and 0.050 % Bromidephenolblue) with 3 % β-mercapto-ethanol added freshly just before heating. The heated samples were spun at 14000 rpm for 2 minutes before loading on the gels. Gels were run at 100-200V in running buffer (25 mM Tris, 192 mM Glycine)

Western blotting

All blots weredone using the Mini Trans-Blot Cell. I all cases nitrocellulose membranes were used. The mini-gels were blotted in a buffer containing 20 % Methanol (analytic grade), 0.1 % SDS, 8.3 mM Tris, and 64 mM Glycine at 80 volts for 60-90 minutes at 4°C.

Probing

Membranes were blocked in PBS, 0.075% Tween20 + 5 % milk for an hour at room temperature or overnight at 4°C. All primary antibodies were used in 1:1000 times dilution in PBS, 0.075% + 1-5 % milk unless otherwise indicated in the figure legends. In all cases incubations were for 2 hours at RT or overnight at 4°C. All washes were done in PBS, 0.075% Tween20. All secondary antibodies were used in 1:5000 times dilution in PBS, 0.075% Tween20 (washing buffer) + 1-5 % milk for 1 hour at RT. Western blot were developed using ECL from Promega

Purification of GST-Menin

Bacteria transformed with pET-41a-Men1 were grown in 10 ml LB, 30 μg/ml Kanamycin O/N. The culture was diluted to 4000 ml in LB, 30 μg/ml Kanamycin and grown to an OD600 of 0.6. 1mM IPTG were added and the bacteria grown for four additional hours. The bacteria were spun down (4000 rpm, GSA) and resuspended in 50 ml PBS, 0,5 mM DTT + protease inhibitors. The bacteria were sonicated 8-10 times 30 seconds and Triton X-100 was added to 1% followed by mixing for 30 minutes at 4°C. The bacterial lysates were spun at 10000 rpm (SS34) for 10 minutes at 4°C to pellet insoluble aggregates. Glutathion-Sepharose was washed three times in cold PBS, added to the cleared bacterial lysate and incubated for 2 hours 4°C on a wheel. The beads werespun down at low speed (1000g) and washed 4 times with PBS- Triton X-100. GST-Menin was eluted in 2x1 ml of 20 mM reduced glutathione, 50 mM Tris-HCl, pH 8.0. Eluates were concentrated and the buffer changed to PBS using Centricon filter devises.

References

Abe H, Engler D, Molitch ME, Bollinger-Gruber J, Reichlin S. (1985) Vasoactive intestinal peptide is a physiological mediator of prolactin release in the rat. Endocrinology, 116, 1383-1390.

Agalioti T, Chen G, Thanos D. (2002) Deciphering the transcriptional histone acetylation code for a human gene. Cell, 111, 381-392.

Agarwal, SK, Guru, SC, Heppner, C, Erdos, MR, Collins, RM, Park, SY, Saggar, S, Chandrasekharappa, SC, Collins, FS, Spiegel, AM, Marx, SJ and Burns, AL. (1999) Menin interacts with the AP1 transcription factor JunD and represses JunD-activated transcription. Cell, 96, 143-152.

Agarwal SK, Novotny E, Crabtree JS, Weitzman JB, Yaniv M, Burns AL, Chandrasekharappa SC, Collins FS, Spiegel AM, Marx SJ. (2003) Transcription factor JunD, deprived of menin, switches from growth suppressor to growth promoter. Proc Natl Acad Sci, 100, 10770-10775.

Agulnick AD, Taira M, Breen JJ, Tanaka T, Dawid IB, Westphal H. (1996) Interactions of the LIM-domain-binding factor Ldb1 with LIM homeodomain proteins. Nature, 384, 270-272.

Ajiro K, Yoda K, Utsumi K, Nishikawa Y. (1996) Alteration of cell cycle-dependent histone phosphorylations by okadaic acid. Induction of mitosis-specific H3 phosphorylation and chromatin condensation in mammalian interphase cells. J Biol Chem, 271, 13197-13201.

Alexander, JM. (2001) Tumor suppressor loss in pituitary tumors. Brain Pathol, 11, 342-355.

Alleaume C, Eychene A, Caigneaux E, Muller JM, Philippe M. (2003) Vasoactive intestinal peptide stimulates proliferation in HT29 human colonic adenocarcinoma cells: concomitant activation of Ras/Rap1-B-Raf-ERK signalling pathway. Neuropeptides, 37, 98-104.

Angel P, Allegretto E, Okino ST, Hattori K, Boyle WJ, Hunter T, Karin M. (1988) Oncogene jun encodes a sequence-specific trans-activator similar to AP-1. Nature, 332, 166-171.

Angel P, Karin M. (1991) The role of Jun, Fos and the AP-1 complex in cell-proliferation and transformation. Biochim Biophys Acta, 1072, 129-157.

Asa SL, Kovacs K, Stefaneanu L, Horvath E, Billestrup N, Gonzalez-Manchon C, Vale W. (1992a) Pituitary adenomas in mice transgenic for growth hormone-releasing hormone. Endocrinology, 131, 2083-2089.

Asa SL, Kovacs K, Hammer GD, Liu B, Roos BA, Low MJ. (1992b) Pituitary corticotroph hyperplasia in rats implanted with a medullary thyroid carcinoma cell line transfected with a corticotropin-releasing hormone complementary deoxyribonucleic acid expression vector. Endocrinology, 131, 715-720.

Asa SL, Kelly M, Grandy DK, Low MJ. (1999) Pituitary lactotroph adenomas develop after prolonged lactotroph hyperplasia in dopamine D2 receptor-deficient mice. Endocrinology, 140, 5348-5355.

Ashcroft GS, Yang X, Glick AB, Weinstein M, Letterio JL, Mizel DE, Anzano M, Greenwell-Wild T, Wahl SM, Deng C, Roberts AB. (1999) Mice lacking Smad3 show accelerated wound healing and an impaired local inflammatory res. Nat Cell Biol, 1, 260-266.

Ayer DE, Lawrence Q, Eisenman RN. (1995) Mad-Max transcriptional repression is mediated by ternary complex formation with mammalian homologs of yeast repressor Sin3. Cell, 80, 767-776.

Balsa JA, Cacicedo L, Lara JI, Lorenzo MJ, Pazos F, Sanchez-Franco F (1996a). Autocrine and/or paracrine action of vasoactive intestinal peptide on thyrotropin-releasing hormone induced prolactin release. Endocrinology, 137, 144-150.

Balsa JA, Sanchez-Franco F, Lorenzo MJ, Pazos F, Lara JI, Cacicedo L. (1996b) Autoparacrine action of vasoactive intestinal peptide on dopaminergic control of prolactin secretion. Endocrinology, 137, 508-513.

Balsa JA, Sanchez-Franco F, Pazos F, Lara JI, Lorenzo MJ, Maldonado G, Cacicedo L.

(1998) Direct action of serotonin on prolactin, growth hormone, corticotropin and luteinizing hormone release in cocultures of anterior and posterior pituitary lobes: autocrine and/or paracrine action of vasoactive intestinal peptide. Neuroendocrinology, 68, 326-333.

Barradeau S, Imaizumi-Scherrer T, Weiss MC, Faust DM. (2000) Alternative 5'-exons of the mouse cAMP-dependent protein kinase subunit RIalpha gene are conserved and expressed in both a ubiquitous and tissue-restricted fashion. FEBS Lett, 476, 272-276.

Beg AA, Sha W, Bronson RT, Ghosh S, Baltimore D. (1995) Embryonic lethality and liver degeneration in mice lacking the RelA component of NF-kappa B. Nature, 376, 167-170.

Bertolino P, Radovanovic I, Casse H, Aguzzi A, Wang ZQ, Zhang CX. (2003a) Genetic ablation of the tumor suppressor menin causes lethality at mid-gestation with defects in multiple organs. Mech Dev, 120, 549-560.

Bertolino P, Tong W, Galendo D, Wang ZQ, Zhang CX. (2003b) Heterozygous Men1 mutant mice develop a range of endocrine tumors mimicking multiple endocrine neoplasia type 1. Mol Endocrinol, 17, 1880-1892.

Bertolino P, Tong W, Herrera PL, Casse H, Zhang CX, Wang ZQ. (2003c) Pancreatic beta-cell-specific ablation of the multiple endocrine neoplasia type 1 (MEN1) gene causes full penetrance of insulinoma development in mice. Cancer Res, 63, 4836-4841.

Biondi CA, Gartside M, Waring P, Loffler KA, Stark MS, Magnuson MA, Kay GF, Hayward NK. (2004) Conditional inactivation of the MEN1 gene leads to pancreatic and pituitary tumorigenesis but does not affect normal development of these tissues. Mol Cell Biol, 24, 3125-3131.

Blobe GC, SW, Lodish HF. (2000) Role of transforming growth factor beta in human disease. N Engl J Med, 342, 1350-1358.

Borrelli E, Schiemann P, Evans RM. (1992) Pituitary hyperplasia induced by ectopic expression of nerve growth factor. Proc Natl Acad Sci U S A, 89, 2764-2768.

Burrow GN, Wortzman G, Rewcastle NB, Holgate RC, Kovacs K. (1981) Microadenomas of the pituitary and abnormal sellar tomograms in an unselected autopsy series. N Engl J Med, 304, 156-158.

Carling, T. (2001) Molecular pathology of parathyroid tumors. Trends Endocrinol Metab, 12, 53-58.

Chandrasekharappa, SC, Guru, SC, Manickam, P, Olufemi, SE, Collins, FS, Emmert-Buck, MR, Debelenko, LV, Zhuang, Z, Lubensky, IA, Liotta, LA, Crabtree, JS, Wang, Y, Roe, BA, Weisemann, J, Boguski, MS, Agarwal, SK, Kester, MB, Kim, YS, Heppner, C, Dong, Q, Spiegel, AM, Burns, AL and Marx, SJ. (1997) Positional cloning of the gene for multiple endocrine neoplasia-type 1. Science, 276, 404-407.

Chang H, Huylebroeck D, Verschueren K, Guo Q, Matzuk MM, Zwijsen A. (1999) Smad5 knockout mice die at mid-gestation due to multiple embryonic and extraembryonic defects. Development, 126, 1631-1642.

Chang H, Zwijsen A, Vogel H, Huylebroeck D, Matzuk MM. (2000) Smad5 is essential for left-right asymmetry in mice. Dev Biol, 219, 71-78.

Chang KH, Chen Y, Chen TT, Chou WH, Chen PL, Ma YY, Yang-Feng TL, Leng X, Tsai MJ, O'Malley BW, Lee WH. (1997) A thyroid hormone receptor coactivator negatively regulated by the retinoblastoma protein. Proc Natl Acad Sci U S A, 94, 9040-9045.

Chanson P, Daujat F, Young J, Bellucci A, Kujas M, Doyon D, Schaison G. (2001) Normal pituitary hypertrophy as a frequent cause of pituitary incidentaloma: a follow-up study. J Clin Endocrinol Metab, 86, 3009-3015.

Chatzistamou I, Schally A, Varga JL, Groot K, Armatis P, Bajo AM. (2001) Inhibition of growth and reduction in tumorigenicity of UCI-107 ovarian cancer by antagonists of growth hormone-releasing hormone and vasoactive intestinal peptide. J Cancer Res Clin Oncol, 127, 645-652.

Chen Y, Chen P, Chen CF, Sharp ZD, Lee WH. (1999) Thyroid hormone, T3-dependent

phosphorylation and translocation of Trip230 from the Golgi complex to the nucleus. Proc Natl Acad Sci U S A, 96, 4443-4448.

Christofori G, Naik P, Hanahan D. (1994) A second signal supplied by insulin-like growth factor II in oncogene-induced tumorigenesis. Nature, 369, 414-418.

Coogan PF, Baron J, Lambe M. (1995) Parity and pituitary adenoma risk. J Natl Cancer Inst, 87, 1410-1.

Crabtree, JS, Scacheri, PC, Ward, JM, Garrett-Beal, L, Emmert-Buck, MR, Edgemon, KA, Lorang, D, Libutti, SK, Chandrasekharappa, SC, Marx, SJ, Spiegel, AM and Collins, FS. (2001) A mouse model of multiple endocrine neoplasia, type 1, develops multiple endocrine tumors. Proc Natl Acad Sci U S A, 98, 1118-1123.

Crabtree JS, Scacheri, PC, Ward JM, McNally SR, Swain GP, Montagna C, Hager JH, Hanahan D, Edlund H, Magnuson MA, Garrett-Beal L, Burns AL, Ried T, Chandrasekharappa SC, Marx SJ, Spiegel AM, Collins FS. (2003) Of mice and MEN1: Insulinomas in a conditional mouse knockout. Mol Cell Biol, 23, 6075-6085.

Duboule, D. (1995) Vertebrate Hox genes and proliferation: an alternative pathway to homeosis? Curr Opin Genet Dev, 5, 525-528.

Dasen JS, Rosenfeld MG. (1999) Signaling mechanisms in pituitary morphogenesis and cell fate determination. Curr Opin Cell Biol, 11, 669-677.

Datto MB, Li Y, Panus JF, Howe DJ, Xiong Y, Wang XF. (1995) Transforming growth factor beta induces the cyclin-dependent kinase inhibitor p21 through a p53-independent mechanism. Proc Natl Acad Sci U S A, 92, 5545-5549.

Davis, RJ. (2000) Signal transduction by the JNK group of MAP kinases. Cell, 103, 239-252.

Degerman A, Chun D, Nguyen TB, Bravo DT, Alanis J, Rokaeus A, Waschek JA. (2002) Local action of estrogen and thyroid hormone on vasoactive intestinal peptide (VIP) and galanin gene expression in the rat anterior pituitary. Neuropeptides, 36, 50-57.

del Peso L, Gonzalez-Garcia M, Page C, Herrera R, Nunez G. (1997) Interleukin-3-induced phosphorylation of BAD through the protein kinase Akt. Science, 278, 687-689.

Derynck R, Zhang Y. (2003) Smad-dependent and Smad-independent pathways in TGF-beta family signalling. Nature, 425, 577-584.

Dhalluin C, Carlson J, Zeng L, He C, Aggarwal AK, Zhou MM. (1999) Structure and ligand of a histone acetyltransferase bromodomain. Nature, 399, 491-496.

Dinc H, Esen F, Demirci A, Sari A, Resit Gumele H. (1998) Pituitary dimensions and volume measurements in pregnancy and post partum. MR assessment. Acta Radiol, 39, 64-69.

Djabali M, Selleri L, Parry P, Bower M, Young BD, Evans GA. (1992) A trithorax-like gene is interrupted by chromosome 11q23 translocations in acute leukaemias. Nat Genet, 2, 113-118.

Donis-Keller H, Dou S, Chi D, Carlson KM, Toshima K, Lairmore TC, Howe JR, Moley JF, Goodfellow P, Wells SA Jr. (1993) Mutations in the RET proto-oncogene are associated with MEN 2A and FMTC. Hum Mol Genet, 2, 851-856.

Doucas V, Spyrou G, Yaniv M. (1991) Unregulated expression of c-Jun or c-Fos proteins but not Jun D inhibits oestrogen receptor activity in human breast cancer derived cells. EMBO J, 10, 2237-2245.

Duyao MP, BA, Sonenshein GE. (1990) Interaction of an NF-kappa B-like factor with a site upstream of the c-myc promoter. Proc Natl Acad Sci U S A, 87, 4727-4731.

Ezzat S. (2001) The role of hormones, growth factors and their receptors in pituitary tumorigenesis. Brain Pathol, 11, 356-370.

Fagin JA, Fernandez-Mejia C, Melmed S. (1989) Pituitary insulin-like growth factor-I gene expression: regulation by triiodothyronine and growth hormone. Endocrinology, 125, 2385-2391.

Farrell WE, Simpson D, Bicknell J, Magnay JL, Kyrodimou E, Thakker RV, Clayton RN. (1999) Sequence analysis and transcript expression of the MEN1 gene in sporadic pituitary tumours. Br J Cancer, 80, 44-50.

Fernandez M, Sanchez-Franco F, Palacios N, Sanchez I, Villuendas G, Cacicedo L. (2003) Involvement of vasoactive intestinal peptide on insulin-like growth factor I-induced proliferation of rat pituitary lactotropes in primary culture: evidence for an autocrine and/or paracrine regulatory system. Neuroendocrinology, 77, 341-352.

Fernandez M, Sanchez-Franco F, Palacios N, Sanchez I, Villuendas G, Cacicedo L. (2003) Involvement of vasoactive intestinal peptide on insulin-like growth factor I-induced proliferation of rat pituitary lactotropes in primary culture: evidence for an autocrine and/or paracrine regulatory system. Neuroendocrinology, 77, 341-352.

FitzGerald KT, Diaz M. (1999) MLL2: A new mammalian member of the trx/MLL family of genes. Genomics, 59, 187-192.

Francis NJ, Kingston R. (2001) Mechanisms of transcriptional memory. Nat Rev Mol Cell Biol, 2, 409-421.

Franklin DS, Godfrey V, Lee H, Kovalev GI, Schoonhoven R, Chen-Kiang S, Su L, Xiong Y. (1998) CDK inhibitors p18(INK4c) and p27(Kip1) mediate two separate pathways to collaboratively suppress pituitary tumorigenesis. Genes Dev, 12.

Frederick JP, Liberati N, Waddell DS, Shi Y, Wang XF. (2004) Transforming growth factor beta-mediated transcriptional repression of c-myc is dependent on direct binding of Smad3 to a novel repressive Smad binding element. Mol Cell Biol, 24, 2546-2559.

Frost SJ, Simpson D, Farrell WE. (2001) Decreased proliferation and cell cycle arrest in neoplastic rat pituitary cells is associated with transforming growth factor-beta1-induced expression of p15/INK4B. Mol Cell Endocrinol, 176, 29-37.

Futreal PA, Coin L, Marshall M, Down T, Hubbard T, Wooster R, Rahman N, Stratton MR.

(2004) A census of human cancer genes. Nat Rev Cancer, 4, 177-183.

Gallo A, Cuozzo C, Esposito I, Maggiolini M, Bonofiglio D, Vivacqua A, Garramone M, Weiss C, Bohmann D, Musti AM. (2002) Menin uncouples Elk-1, JunD and c-Jun phosphorylation from MAP kinase activation. Oncogene, 21, 6434-6445.

Gerdes J, Lemke H, Baisch H, Wacker HH, Schwab U, Stein H. (1984) Cell cycle analysis of a cell proliferation-associated human nuclear antigen defined by the monoclonal antibody Ki-67. J Immunol, 133, 1710-1715.

Ghosh S, Karin M. (2002) Missing pieces in the NF-kappaB puzzle. Cell, 109, S81-96.

Gobl AE, BM, Lopez-Egido JR, Oberg K, Skogseid B, Westin G. (1999) Menin represses JunD-activated transcription by a histone deacetylase-dependent mechanism. Biochim Biophys Acta, 1447, 51-56.

Gomez O, Berg J. (2003) Autocrine/paracrine action of pituitary vasoactive intestinal peptide on lactotroph hyperplasia induced by estrogen. Endocrinology, 144, 4403-4409.

Gonsky R, Herman V, Melmed S, Fagin J. (1991) Transforming DNA sequences present in human prolactin-secreting pituitary tumors. Mol Endocrinol, 5, 1687-1695.

Gozes I, Fridkinb M, Hill JM, Brenneman DE. (1999) Pharmaceutical VIP: prospects and problems. Curr Med Chem, 11, 1019-1034.

Guru SC, Crabtree J, Brown KD, Dunn KJ, Manickam P, Prasad NB, Wangsa D, Burns AL, Spiegel AM, Marx SJ, Pavan WJ, Collins FS, Chandrasekharappa SC. (1999) Isolation, genomic organization, and expression analysis of Men1, the murine homolog of the MEN1 gene. Mamm Genome, 10, 592-596.

Guru SC, Goldsmith P, Burns AL, Marx SJ, Spiegel AM, Collins FS, Chandrasekharappa SC. (1998) Menin, the product of the MEN1 gene, is a nuclear protein. Proc Natl Acad Sci, 95, 1630-1634.

Guru SC, Prasad N, Shin EJ, Hemavathy K, Lu J, Ip YT, Agarwal SK, Marx SJ, Spiegel AM, Collins FS, Oliver B, Chandrasekharappa SC. (2001) Characterization of a MEN1 ortholog from Drosophila melanogaster. Gene, 263, 31-38.

Halleck MS, Pownall S, Harder KW, Duncan AM, Jirik FR, Schlegel RA. (1995) A widely distributed putative mammalian transcriptional regulator containing multiple paired amphipathic helices, with similarity to yeast SIN3. Genomics, 26, 403-406.

Hanahan D, Weinberg R. (2000) The hallmarks of cancer. cell, 100, 57-70.

Hannon GJ, Beach D. (1994) p15INK4B is a potential effector of TGF-beta-induced cell cycle arrest. Nature, 371, 257-261.

Hassig CA, Fleischer T, Billin AN, Schreiber SL, Ayer DE. (1997) Histone deacetylase activity is required for full transcriptional repression by mSin3A. Cell, 89, 341-347.

Heaney AP, Horwitz G, Wang Z, Singson R, Melmed S. (1999) Early involvement of estrogen-induced pituitary tumor transforming gene and fibroblast growth factor expression in prolactinoma pathogenesis. Nat Med, 5, 1317-1321.

Hentges S, Pastorcic M, De A, Boyadjieva N, Sarkar DK. (2000) Opposing actions of two transforming growth factor-beta isoforms on pituitary lactotropic cell proliferation. Endocrinology, 141, 1528-1535.

Heppner C, Bilimoria K, Agarwal SK, Kester M, Whitty LJ, Guru SC, Chandrasekharappa SC, Collins FS, Spiegel AM, Marx SJ, Burns AL. (2001) The tumor suppressor protein menin interacts with NF-kappaB proteins and inhibits NF-kappaB-mediated transactivation. Oncogene, 20, 4917-4925.

Heppner C, Kester M, Agarwal SK, Debelenko LV, Emmert-Buck MR, Guru SC, Manickam P, Olufemi SE, Skarulis MC, Doppman JL, Alexander RH, Kim YS, Saggar SK, Lubensky IA, Zhuang Z, Liotta LA, Chandrasekharappa SC, Collins FS, Spiegel AM, Burns AL, Marx SJ. (1997) Somatic mutation of the MEN1 gene in parathyroid tumours. Nat Genet, 16, 375-378.

Himes SR, Coles L, Katsikeros R, Lang RK, Shannon MF. (1993) HTLV-1 tax activation of the GM-CSF and G-CSF promoters requires the interaction of NF-kB with other transcription factor families. Oncogene, 8, 3189-3197.

Hinuma S, Habata Y, Fujii R, Kawamata Y, Hosoya M, Fukusumi S, Kitada C, Masuo Y, Asano T, Matsumoto H, Sekiguchi M, Kurokawa T, Nishimura O, Onda H, Fujino M. (1998) A prolactin-releasing peptide in the brain. Nature, 393, 272-276.

Hinz M, Krappmann D, Eichten A, Heder A, Scheidereit C, Strauss M. (1999) NF-kappaB function in growth control: regulation of cyclin D1 expression and G0/G1-to-S-phase transition. Mol Cell Biol, 19, 2690-2698.

Hoess RH, Ziese M, Sternberg N. (1982) P1 site-specific recombination: nucleotide sequence of the recombining sites. Proc Natl Acad Sci U S A, 79, 3398-3402.

Hoff, AO, Cote, GJ and Gagel, RF. (2000) Multiple endocrine neoplasias. Annu Rev Physiol, 62, 377-411.

Hofstra RM, Landsvater R, Ceccherini I, Stulp RP, Stelwagen T, Luo Y, Pasini B, Hoppener JW, van Amstel HK, Romeo G. (1994) A mutation in the RET proto-oncogene associated with multiple endocrine neoplasia type 2B and sporadic medullary thyroid carcinoma. Nature, 367, 375-376.

Hughes CM, Rozenblatt-Rosen O, Milne TA, Copeland TD, Levine SS, Lee JC, Hayes DN, Shanmugam KS, Bhattacharjee A, Biondi CA, Kay GF, Hayward NK, Hess JL, Meyerson M. (2004) Menin associates with a trithorax family histone methyltransferase complex and with the hoxc8 locus. Mol Cell, 13, 587-597.

Huntsman DG, Chin S, Muleris M, Batley SJ, Collins VP, Wiedemann LM, Aparicio S, Caldas C. (1999) MLL2, the second human homolog of the Drosophila trithorax gene, maps to 19q13.1 and is amplified in solid tumor cell lines. Oncogene, 18, 7975-7984.

Iavarone A, Massague J. (1997) Repression of the CDK activator Cdc25A and cell-cycle

arrest by cytokine TGF-beta in cells lacking the CDK inhibitor p15. Nature, 387, 417-422.

Infante C, Ramos-Morales F, Fedriani C, Bornens M, Rios RM. (1999) GMAP-210, A cis-Golgi network-associated protein, is a minus end microtubule-binding protein. J Cell Biol, 145, 83-98.

Itoh N, Obata K, Yanaihara N, Okamoto H. (1983) Human preprovasoactive intestinal polypeptide contains a novel PHI-27-like peptide, PHM-27. Nature, 304, 547-549.

Jacks T, Fazeli A, Schmitt EM, Bronson RT, Goodell MA, Weinberg RA. (1992) Effects of an Rb mutation in the mouse. Nature, 359, 295-300.

Jansen E, Steenberg P, LeRoith D, Roberts CT Jr, Sussenbach JS. (1991) Identification of multiple transcription start sites in the human insulin-like growth factor-I gene. Mol Cell Endocrinol, 78, 115-125.

Jeanmougin F, Wurtz J, Le Douarin B, Chambon P, Losson R. (1997) The bromodomain revisited. Trends Biochem Sci, 22, 151-153.

Jin S, Mao H, Schnepp RW, Sykes SM, Silva AC, D'Andrea AD, Hua X. (2003) Menin associates with FANCD2, a protein involved in repair of DNA damage. Cancer Res, 63, 4204-4210.

Joborn H, Larsson R, Rastad J, Nygren P, Akerstrom G, Ljunghall S. (1991) Vasoactive intestinal polypeptide stimulates parathyroid hormone release by interaction with cyclic adenosine monophosphate production of bovine parathyroid cells. Acta Endocrinol (Copenh), 124, 54-59.

Jurnak, F. (1985) Structure of the GDP domain of EF-Tu and location of the amino acids homologous to ras oncogene proteins. Science, 230, 32-36.

Kaji, H, Canaff, L, Lebrun JJ, Goltzman D and Hendy, GN. (2001) Inactivation of menin, a Smad3-interacting protein, blocks transforming growth factor type beta signaling. Proc Natl Acad Sci U S A, 98, 3837-3842.

Kaji H, Canaff L, Goltzman D, Hendy GN. (1999) Cell cycle regulation of menin expression. Cancer Res, 59, 5097-5101.

Karin M, Cao Y, Greten FR, Li ZW. (2002) NF-kappaB in cancer: from innocent bystander to major culprit. Nat Rev Cancer, 2, 301-310.

Kato I, Suzuki Y, Akabane A, Yonekura H, Tanaka O, Kondo H, Takasawa S, Yoshimoto T, Okamoto H. (1994) Transgenic mice overexpressing human vasoactive intestinal peptide (VIP) gene in pancreatic beta cells. Evidence for improved glucose tolerance and enhanced insulin secretion by VIP and PHM-27 in vivo. J Biol Chem, 269, 21223-21228.

Kerr LD, Miller D, Matrisian LM. (1990) TGF-beta 1 inhibition of transin/stromelysin gene expression is mediated through a Fos binding sequence. Cell, 61, 267-278.

Kim H, Lee J, Cho EJ, Liu JO, Youn HD. (2003) Menin, a tumor suppressor, represses JunD-mediated transcriptional activity by association with an mSin3A-histone deacetylase complex. Cancer Res, 63, 6135-6139.

Kineman RD, Teixeira L, Amargo GV, Coschigano KT, Kopchick JJ, Frohman LA. (2001) The effect of GHRH on somatotrope hyperplasia and tumor formation in the presence and absence of GH signaling. Endocrinology, 142, 3764-3773.

Kirschner LS, Carney J, Pack SD, Taymans SE, Giatzakis C, Cho YS, Cho-Chung YS, Stratakis CA. (2000) Mutations of the gene encoding the protein kinase A type I-alpha regulatory subunit in patients with the Carney complex. Nat Genet, 26, 89-92.

Kiyokawa H, Kineman R, Manova-Todorova KO, Soares VC, Hoffman ES, Ono M, Khanam D, Hayday AC, Frohman LA, Koff A. (1996) Enhanced growth of mice lacking the cyclin-dependent kinase inhibitor function of p27(Kip1). Cell, 85, 721-732.

Knudson, A. (1971) Mutation and cancer: statistical study of retinoblastoma. Proc Natl Acad Sci, 68, 820-823.

Kucharczak J, Simmons M, Fan Y, Gelinas C. (2003) To be, or not to be: NF-kappaB is the answer--role of Rel/NF-kappaB in the regulation of apoptosis. Oncogene, 22, 8961-8982.

Kurokawa M, Mitani K, Irie K, Matsuyama T, Takahashi T, Chiba S, Yazaki Y, Matsumoto K, Hirai H. (1998) The oncoprotein Evi-1 represses TGF-beta signalling by inhibiting Smad3. Nature, 394, 92-96.

Laburthe M, Couvineau A, Gaudin P, Maoret JJ, Rouyer-Fessard C, Nicole P. (1996) Receptors for VIP, PACAP, secretin, GRF, glucagon, GLP-1, and other members of their new family of G protein-linked receptors: structure-function relationship with special reference to the human VIP-1 receptor. Ann N Y Acad Sci, 805, 94-109.

Laherty CD, Yang W, Sun JM, Davie JR, Seto E, Eisenman RN. (1997) Histone deacetylases associated with the mSin3 corepressor mediate mad transcriptional repression. Cell, 89, 349-356.

Landis CA, Masters S, Spada A, Pace AM, Bourne HR, Vallar L. (1989) GTPase inhibiting mutations activate the alpha chain of Gs and stimulate adenylyl cyclase in human pituitary tumours. Nature, 340, 692-696.

Lania A, Mantovani G, Spada A. (2001) G protein mutations in endocrine diseases. Eur J Endocrinol, 145, 543-559.

Lara JI, Lorenzo M, Cacicedo L, Tolon RM, Balsa JA, Lopez-Fernandez J, Sanchez-Franco F. (1994) Induction of vasoactive intestinal peptide gene expression and prolactin secretion by insulin-like growth factor I in rat pituitary cells: evidence for an autoparacrine regulatory system. Endocrinology, 135, 2526-2532.

Laron, Z. (2001) Insulin-like growth factor 1 (IGF-1): a growth hormone. Mol Pathol, 54, 311-316.

Lawrence HJ, Helgason C, Sauvageau G, Fong S, Izon DJ, Humphries RK, Largman C. (1997) Mice bearing a targeted interruption of the homeobox gene HOXA9 have defects in myeloid, erythroid, and lymphoid hematopoiesis. Blood, 89, 1922-1930.

Lechleider RJ, Ryan J, Garrett L, Eng C, Deng C, Wynshaw-Boris A, Roberts AB. (2001) Targeted mutagenesis of Smad1 reveals an essential role in chorioallantoic fusion. Dev Biol., 240, 157-167.

Lee HH, Dadgostar H, Cheng Q, Shu J, Cheng G. (1999) NF-kappaB-mediated up-regulation of Bcl-x and Bfl-1/A1 is required for CD40 survival signaling in B lymphocytes. Proc Natl Acad Sci U S A, 96, 9136-9141.

Lee JW, Choi H, Gyuris J, Brent R, Moore DD. (1995) Two classes of proteins dependent on either the presence or absence of thyroid hormone for interaction with the thyroid hormone receptor. Mol Endocrinol, 9, 243-254.

Lemmens IH, Forsberg L, Pannett AA, Meyen E, Piehl F, Turner JJ, Van de Ven WJ, Thakker RV, Larsson C, Kas K. (2001) Menin interacts directly with the homeobox-containing protein Pem. Biochem Biophys Res Commun, 286, 426-431.

Li D, Roberts R. (2001) WD-repeat proteins: structure characteristics, biological function, and their involvement in human diseases. Cell Mol Life Sci, 58, 2085-2097.

Lidhar K, Korbonits M, Jordan S, Khalimova Z, Kaltsas G, Lu X, Clayton RN, Jenkins PJ, Monson JP, Besser GM, Lowe DG, Grossman AB. (1999) Low expression of the cell cycle inhibitor p27Kip1 in normal corticotroph cells, corticotroph tumors, and malignant pituitary tumors. J Clin Endocrinol Metab, 84, 3823-3830.

Lilling G, Wollman Y, Goldstein MN, Rubinraut S, Fridkin M, Brenneman DE, Gozes I. (1994-95) Inhibition of human neuroblastoma growth by a specific VIP antagonist. J Mol Neurosci, 5, 231-239.

Lin SC, Lin C, Gukovsky I, Lusis AJ, Sawchenko PE, Rosenfeld MG. (1993) Molecular basis of the little mouse phenotype and implications for cell type-specific growth. Nature, 364, 208-213.

Lin SY, Elledge S. (2003) Multiple tumor suppressor pathways negatively regulate

telomerase. Cell, 113, 881-889.

Liu JP, Baker J, Perkins AS, Robertson EJ, Efstratiadis A. (1993) Mice carrying null mutations of the genes encoding insulin-like growth factor I (Igf-1) and type 1 IGF receptor (Igf1r). Cell, 75, 59-72.

Lopez-Egido J, Cunningham J, Berg M, Oberg K, Bongcam-Rudloff E, Gobl A. (2002) Menin's interaction with glial fibrillary acidic protein and vimentin suggests a role for the intermediate filament network in regulating menin activity. Exp Cell Res, 278, 175-183.

Luo K, Stroschein S, Wang W, Chen D, Martens E, Zhou S, Zhou Q. (1999) The Ski oncoprotein interacts with the Smad proteins to repress TGFbeta signaling. Genes Dev, 13, 2196-2206.

Luo RX, Postigo A, Dean DC. (1998) Rb interacts with histone deacetylase to repress transcription. Cell, 92, 463-473.

Marks P, Rifkind R, Richon VM, Breslow R, Miller T, Kelly WK. (2001) Histone deacetylases and cancer: causes and therapies. Nat Rev Cancer, 1, 194-202.

Marmorstein R, Berger S. (2001) Structure and function of bromodomains in chromatin-regulating complexes. Gene, 272, 1-9.

Martin-Rivera L, Herrera E, Albar JP, Blasco MA. (1998) Expression of mouse telomerase catalytic subunit in embryos and adult tissues. Proc Natl Acad Sci U S A, 95, 10471-10476.

Maruno K, Absood A, Said SI. (1998) Vasoactive intestinal peptide inhibits human small-cell lung cancer proliferation in vitro and in vivo. Proc Natl Acad Sci U S A, 95, 14373-14378.

Mason AJ, Hayflick J, Zoeller RT, Young WS 3rd, Phillips HS, Nikolics K, Seeburg PH. (1986) A deletion truncating the gonadotropin-releasing hormone gene is responsible for hypogonadism in the hpg mouse. Science, 234, 1366-1371.

Massague J, Chen Y. (2000) Controlling TGF-beta signaling. Genes Dev, 14, 627-644.

Matthews JM, Visvader J. (2003) LIM-domain-binding protein 1: a multifunctional cofactor that interacts with diverse proteins. EMBO Rep, 4, 1132-1137.

Mayo KE. (1992) Molecular cloning and expression of a pituitary-specific receptor for growth hormone-releasing hormone. Mol Endocrinol, 6, 1734-1744.

Mayo KE, Hammer R, Swanson LW, Brinster RL, Rosenfeld MG, Evans RM. (1988a) Dramatic pituitary hyperplasia in transgenic mice expressing a human growth hormone-releasing factor gene. Mol Endocrinol, 2, 606-612.

McAndrew J, Paterson A, Asa SL, McCarthy KJ, Kudlow JE. (1995) Targeting of transforming growth factor-alpha expression to pituitary lactotrophs in transgenic mice results in selective lactotroph proliferation and adenomas. Endocrinology, 136, 4479-4488.

Melmed S. (2003) Mechanisms for pituitary tumorigenesis: the plastic pituitary. J Clin Invest, 112, 1603-1618.

Micheau O, Lens S, Gaide O, Alevizopoulos K, Tschopp J. (2001) NF-kappaB signals induce the expression of c-FLIP. Mol Cell Biol, 21, 5299-5305.

Moody TW, Leyton J, Chan D, Brenneman DC, Fridkin M, Gelber E, Levy A, Gozes I.(2001) VIP receptor antagonists and chemotherapeutic drugs inhibit the growth of breast cancer cells. Breast Cancer Res Treat, 68, 55-64.

Moody TW, Zia F, Draoui M, Brenneman DE, Fridkin M, Davidson A, Gozes I. (1993) A vasoactive intestinal peptide antagonist inhibits non-small cell lung cancer growth. Proc Natl Acad Sci U S A, 90, 4345-4349.

Muglia L, Jacobsen L, Dikkes P, Majzoub JA. (1995) Corticotropin-releasing hormone deficiency reveals major fetal but not adult glucocorticoid need. Nature, 373, 427-432.

Mukhopadhyay M, Teufel A, Yamashita T, Agulnick AD, Chen L, Downs KM, Schindler A, Grinberg A, Huang SP, Dorward D, Westphal H. (2003) Functional ablation of the mouse

Ldb1 gene results in severe patterning defects during gastrulation. Development, 130, 495-505.

Mulligan LM, Kwok J, Healey CS, Elsdon MJ, Eng C, Gardner E, Love DR, Mole SE, Moore JK, Papi L. (1993) Germ-line mutations of the RET proto-oncogene in multiple endocrine neoplasia type 2A. Nature, 363, 458-460.

Murphy M, Ahn J, Walker KK, Hoffman WH, Evans RM, Levine AJ, George DL. (1999) Transcriptional repression by wild-type p53 utilizes histone deacetylases, mediated by interaction with mSin3a. Genes Dev, 13, 2490-2501.

Nelson C, Albert V, Elsholtz HP, Lu LI, Rosenfeld MG. (1988) Activation of cell-specific expression of rat growth hormone and prolactin genes by a common transcription factor. Science, 239, 1400-1405.

Nicholson DW, Ali A, Thornberry NA, Vaillancourt JP, Ding CK, Gallant M, Gareau Y, Griffin PR, Labelle M, Lazebnik YA. (1995) Identification and inhibition of the ICE/CED-3 protease necessary for mammalian apoptosis. Nature, 376, 37-43.

Noma K, Allis C, Grewal SI. (2001) Transitions in distinct histone H3 methylation patterns at the heterochromatin domain boundaries. Science, 293, 1150-1155.

Novak A, Guo C, Yang W, Nagy A, Lobe CG. (2000) Z/EG, a double reporter mouse line that expresses enhanced green fluorescent protein upon Cre-mediated excision. Genesis, 28, 147-155.

Obungu VH, Lee Burns A, Agarwal SK, Chandrasekharapa SC, Adelstein RS, Marx SJ. (2003) Menin, a tumor suppressor, associates with nonmuscle myosin II-A heavy chain. Oncogene, 22, 6347-6358.

Ohkura N, Kishi M, Tsukada T, Yamaguchi K. (2001) Menin, a gene product responsible for multiple endocrine neoplasia type 1, interacts with the putative tumor metastasis suppressor nm23. Biochem Biophys Res Commun, 282, 1206-1210.

Oomizu S, Takeuchi S, Takahashi S. (1998) Stimulatory effect of insulin-like growth factor I on proliferation of mouse pituitary cells in serum-free culture. J Endocrinol, 157, 53-62.

Pachnis V, Mankoo B, Costantini F. (1993) Expression of the c-ret proto-oncogene during mouse embryogenesis. Development, 119, 4.

Pelengaris S, Khan M, Evan GI. (2002) Suppression of Myc-induced apoptosis in beta cells exposes multiple oncogenic properties of Myc and triggers carcinogenic progression. Cell, 109, 321-334.

Pernet-Gallay K, Antony C, Johannes L, Bornens M, Goud B, Rios RM. (2002) The overexpression of GMAP-210 blocks anterograde and retrograde transport between the ER and the Golgi apparatus. Traffic, 3, 822-832.

Pfarr CM, Mechta F, Spyrou G, Lallemand D, Carillo S, Yaniv M. (1994) Mouse JunD negatively regulates fibroblast growth and antagonizes transformation by ras. Cell, 76, 747-760.

Pickles LM, Roe S, Hemingway EJ, Stifani S, Pearl LH. (2002) Crystal structure of the C-terminal WD40 repeat domain of the human Groucho/TLE1 transcriptional corepressor. Structure (Camb), 10, 751-761.

Piroli GG, Pietranera L, Grillo CA, De Nicola AF. (2004) Gender differences in the expression of galanin and vasoactive intestinal peptide in oestrogen-induced prolactinomas of Fischer 344 rats. J Neuroendocrinol, 16, 64-71.

Pitts RL, Wang S, Jones EA, Symes AJ. (2001) Transforming growth factor-beta and ciliary neurotrophic factor synergistically induce vasoactive intestinal peptide gene expression through the cooperation of Smad, STAT, and AP-1 sites. J Biol Chem, 276, 19966-19973.

Plonowski A, Varga J, Schally AV, Krupa M, Groot K, Halmos G. (2002) Inhibition of PC-3 human prostate cancers by analogs of growth hormone-releasing hormone (GH-RH) endowed with vasoactive intestinal peptide (VIP) antagonistic activity. Int J Cancer, 98, 624-629.

Prezant TR, Levine J, Melmed S. (1998) Molecular characterization of the men1 tumor suppressor gene in sporadic pituitary tumors. J Clin Endocrinol Metab, 83, 1388-1391.

Prysor-Jones RA, Silverlight J, Kennedy SJ, Jenkins JS. (1988) Vasoactive intestinal peptide and the stimulation of lactotroph growth by oestradiol in rats. J Endocrinol, 116, 259-265.

Prysor-Jones RA, Silverlight J, Jenkins JS. (1989) Oestradiol, vasoactive intestinal peptide and fibroblast growth factor in the growth of human pituitary tumour cells in vitro. J Endocrinol, 120, 171-177.

Qian X, Jin L, Grande JP, Lloyd RV. (1996) Transforming growth factor-beta and p27 expression in pituitary cells. Endocrinology, 137, 3051-3060.

Ratineau C, Bernard C, Poncet G, Blanc M, Josso C, Fontaniere S, Calender A, Chayvialle JA, Zhang CX, Roche C. (2004) Reduction of menin expression enhances cell proliferation and is tumorigenic in intestinal epithelial cells. J Biol Chem, 279, 24477-84.

Reed JC, Bischoff JR. (2000) BIRinging chromosomes through cell division--and survivin' the experience. Cell, 102, 545-8.

Renehan AG, Zwahlen M, Minder C, O'Dwyer ST, Shalet SM, Egger M. (2004) Insulin-like growth factor (IGF)-I, IGF binding protein-3, and cancer risk: systematic review and meta-regression analysis. Lancet, 363, 1346-1353.

Renner U, Lohrer P, Schaaf L, Feirer M, Schmitt K, Onofri C, Arzt E, Stalla GK. (2002) Transforming growth factor-beta stimulates vascular endothelial growth factor production by folliculostellate pituitary cells. Endocrinology, 143, 3759-3765.

Rhodes SJ, Chen R, DiMattia GE, Scully KM, Kalla KA, Lin SC, Yu VC, Rosenfeld MG. (1993) A tissue-specific enhancer confers Pit-1-dependent morphogen inducibility and autoregulation on the pit-1 gene. Genes Dev, 7, 913-932.

Rich JN, Zhang M, Datto MB, Bigner DD, Wang XF. (1999) Transforming growth factor-beta-mediated p15(INK4B) induction and growth inhibition in astrocytes is SMAD3-

dependent and a pathway prominently altered in human glioma cell lines. J Biol Chem, 274, 35053-35058.

Rodriguez CI, Buchholz F, Galloway J, Sequerra R, Kasper J, Ayala R, Stewart AF, Dymecki SM. (2000) High-efficiency deleter mice show that FLPe is an alternative to Cre-loxP. Nat Genet, 25, 139-140.

Roguev A, Schaft D, Shevchenko A, Pijnappel WW, Wilm M, Aasland R, Stewart AF. (2001) The Saccharomyces cerevisiae Set1 complex includes an Ash2 homologue and methylates histone 3 lysine 4. EMBO J, 20, 7137-7148.

Romano D, Magalon K, Ciampini A, Talet C, Enjalbert A, Gerard C. (2003a) Differential involvement of the Ras and Rap1 small GTPases in vasoactive intestinal and pituitary adenylyl cyclase activating polypeptides control of the prolactin gene. J Biol Chem, 278, 51386-51394.

Sachdev D, Yee D. (2001) The IGF system and breast cancer. Endocr Relat Cancer, 8, 197-209.

Said SI, Mutt V. (1972) Isolation from porcine-intestinal wall of a vasoactive octacosapeptide related to secretin and to glucagon. Eur J Biochem, 28, 199-204.

Samson WK, Resch Z, Murphy TC, Chang JK. (1998) Gender-biased activity of the novel prolactin releasing peptides: comparison with thyrotropin releasing hormone reveals only pharmacologic effects. Endocrine, 9, 289-291.

Sarkar DK, Kim K, Minami S. (1992) Transforming growth factor-beta 1 messenger RNA and protein expression in the pituitary gland: its action on prolactin secretion and lactotropic growth. Mol Endocrinol, 6, 1825-1833.

Sauvageau G, Thorsteinsdottir U, Eaves CJ, Lawrence HJ, Largman C, Lansdorp PM, Humphries RK. (1995) Overexpression of HOXB4 in hematopoietic cells causes the selective expansion of more primitive populations in vitro and in vivo. Genes Dev, 9, 1753-1765.

Schreiber-Agus N, Chin L, Chen K, Torres R, Rao G, Guida P, Skoultchi AI, DePinho RA. (1995) An amino-terminal domain of Mxi1 mediates anti-Myc oncogenic activity and interacts with a homolog of the yeast transcriptional repressor SIN3. Cell, 80, 777-786.

Schule R, Rangarajan P, Kliewer S, Ransone LJ, Bolado J, Yang N, Verma IM, Evans RM. (1990a) Functional antagonism between oncoprotein c-Jun and the glucocorticoid receptor. Cell, 62, 1217-1226.

Schule R, Umesono K, Mangelsdorf DJ, Bolado J, Pike JW, Evans RM. (1990b) Jun-Fos and receptors for vitamins A and D recognize a common response element in the human osteocalcin gene. Cell, 61, 497-504.

Schussheim DH, Skarulis M, Agarwal SK, Simonds WF, Burns AL, Spiegel AM, Marx SJ. (2001) Multiple endocrine neoplasia type 1: new clinical and basic findings. Trends Endocrinol Metab. 12, 173-178.

Schwenk F, Baron U, Rajewsky K. (1995) A cre-transgenic mouse strain for the ubiquitous deletion of loxP-flanked gene segments including deletion in germ cells. Nucleic Acids Res, 23, 5080-5081.

Scully KM, Rosenfeld MG. (2002) Pituitary development: regulatory codes in mammalian organogenesis. Science, 295, 2231-5.

Seal LJ, Small C, Kim MS, Stanley SA, Taheri S, Ghatei MA, Bloom SR. (2000) Prolactin releasing peptide (PrRP) stimulates luteinizing hormone (LH) and follicle stimulating hormone (FSH) via a hypothalamic mechanism in male rats. Endocrinology, 141, 1909-1912.

Sornson MW, Wu W, Dasen JS, Flynn SE, Norman DJ, O'Connell SM, Gukovsky I, Carriere C, Ryan AK, Miller AP, Zuo L, Gleiberman AS, Andersen B, Beamer WG, Rosenfeld MG. (1996) Pituitary lineage determination by the Prophet of Pit-1 homeodomain factor defective in Ames dwarfism. Nature, 384, 327-333.

Sowa H, Kaji H, Canaff L, Hendy GN, Tsukamoto T, Yamaguchi T, Miyazono K, Sugimoto T, Chihara K. (2003) Inactivation of menin, the product of the multiple endocrine neoplasia

type 1 gene, inhibits the commitment of multipotential mesenchymal stem cells into the osteoblast lineage. J Biol Chem, 278, 21058-21069.

Sowa H, Kaji H, Kitazawa R, Kitazawa S, Tsukamoto T, Yano S, Tsukada T, Canaff L, Hendy GN, Sugimoto T, Chihara K. (2004) Menin inactivation leads to loss of transforming growth factor beta inhibition of parathyroid cell proliferation and parathyroid hormone secretion. Cancer Res, 64, 2222-2228.

Stewart C, Parente F, Piehl F, Farnebo F, Quincey D, Silins G, Bergman L, Carle GF, Lemmens I, Grimmond S, Xian CZ, Khodei S, Teh BT, Lagercrantz J, Siggers P, Calender A, Van de Vem V, Kas K, Weber G, Hayward N, Gaudray P, Larsson C. (1998) Characterization of the mouse Men1 gene and its expression during development. Oncogene, 17, 2485-2493.

Stork PJ, Schmitt J. (2002) Crosstalk between cAMP and MAP kinase signaling in the regulation of cell proliferation. Trends Cell Biol, 12, 258-266.

Stratakis C. (2001) Clinical genetics of multiple endocrine neoplasias, Carney complex and related syndromes. J Endocrinol Invest, 24, 370-383.

Stroschein SL, Wang W, Zhou S, Zhou Q, Luo K. (1999) Negative feedback regulation of TGF-beta signaling by the SnoN oncoprotein. Science, 286, 771-4.

Struthers RS, Vale W, Arias C, Sawchenko PE, Montminy MR. (1991) Somatotroph hypoplasia and dwarfism in transgenic mice expressing a non-phosphorylatable CREB mutant. Nature, 350, 622-624.

Sukhodolets KE, Hickman A, Agarwal SK, Sukhodolets MV, Obungu VH, Novotny EA, Crabtree JS, Chandrasekharappa SC, Collins FS, Spiegel AM, Burns AL, Marx SJ. (2003) The 32-kilodalton subunit of replication protein A interacts with menin, the product of the MEN1 tumor suppressor gene. Mol Cell Biol, 23, 493-509.

Suphapeetiporn K, Greally J, Walpita D, Ashley T, Bale AE. (2002) MEN1 tumor-suppressor protein localizes to telomeres during meiosis. Genes Chromosomes Cancer, 35, 81-85.

Surmacz E. (2003) Growth factor receptors as therapeutic targets: strategies to inhibit the insulin-like growth factor I receptor. Oncogene, 22, 6589-6597.

Suzuki S, Yamamot I, Arita J. (1999) Mitogen-activated protein kinase-dependent stimulation of proliferation of rat lactotrophs in culture by 3',5'-cyclic adenosine monophosphate. Endocrinology, 140, 2850-2858.

Symes AJ, Pitts R, Conover J, Kos K, Coulombe J. (2000) Synergy of activin and ciliary neurotrophic factor signaling pathways in the induction of vasoactive intestinal peptide gene expression. Mol Endocrinol, 14, 429-439.

Takizawa CG, MD. (2000) Control of mitosis by changes in the subcellular location of cyclin-B1-Cdk1 and Cdc25C. Curr Opin Cell Biol, 12, 658-665.

Tamkun JW, Deuring R, Scott MP, Kissinger M, Pattatucci AM, Kaufman TC, Kennison JA. (1992) brahma: a regulator of Drosophila homeotic genes structurally related to the yeast transcriptional activator SNF2/SWI2. Cell, 68, 561-572.

Tanaka R, Tsushima T, Murakami H, Shizume K, Obara T. (1994) Insulin-like growth factor I receptors and insulin-like growth factor-binding proteins in human parathyroid tumors. World J Surg, 18, 635-641.

Tang Y, Katuri V, Iqbal S, Narayan T, Wang Z, Lu RS, Mishra L, Mishra B. (2002) ELF a beta-spectrin is a neuronal precursor cell marker in developing mammalian brain; structure and organization of the elf/beta-G spectrin gene. Oncogene, 21, 5255-5267.

Tang Y, Katuri V, Dillner A, Mishra B, Deng CX, Mishra L. (2003) Disruption of transforming growth factor-beta signaling in ELF beta-spectrin-deficient mice. Science, 299, 574-577.

Treier M, Gleiberman A, O'Connell SM, Szeto DP, McMahon JA, McMahon AP, Rosenfeld MG. (1998) Multistep signaling requirements for pituitary organogenesis in vivo. Genes Dev, 12, 1691-1704.

Treier M, Rosenfeld M. (1996) The hypothalamic-pituitary axis: co-development of two organs. Curr Opin Cell Biol, 8, 833-843.

Tremblay KD, Dunn N, Robertson EJ. (2001) Mouse embryos lacking Smad1 signals display defects in extra-embryonic tissues and germ cell formation. Development, 128, 3609-3621.

Umayahara Y, Kawamori R, Watada H, Imano E, Iwama N, Morishima T, Yamasaki Y, Kajimoto Y, Kamada T. (1994) Estrogen regulation of the insulin-like growth factor I gene transcription involves an AP-1 enhancer. J Biol Chem, 269, 16433-16442.

Vallar L, Spada A, Giannattasio G. (1987) Altered Gs and adenylate cyclase activity in human GH-secreting pituitary adenomas. Nature, 330, 566-568.

Verges B, Boureille F, Goudet P, Murat A, Beckers A, Sassolas G, Cougard P, Chambe B, Montvernay C, Calender A. (2002) Pituitary disease in MEN type 1 (MEN1): data from the France-Belgium MEN1 multicenter study. J Clin Endocrinol Metab, 87, 457-465.

Verweij CL, Geerts M, Aarden LA. (1991) Activation of interleukin-2 gene transcription via the T-cell surface molecule CD28 is mediated through an NF-kB-like response element. J Biol Chem, 266, 14179-14182.

Wall MA, Coleman D, Lee E, Iniguez-Lluhi JA, Posner BA, Gilman AG, Sprang SR. (1995) The structure of the G protein heterotrimer Gi alpha 1 beta 1 gamma 2. Cell, 83, 1047-1058.

Wang L, Wang X, Adamo ML. (2000) Two putative GATA motifs in the proximal exon 1 promoter of the rat insulin-like growth factor I gene regulate basal promoter activity. Endocrinology, 141, 1118-1126.

Wang Q, Wang X, Evers BM. (2003) Induction of cIAP-2 in human colon cancer cells through PKC delta/NF-kappa B. J Biol Chem, 278, 51091-51099.

Wanke IE, Rorstad O. (1990) Receptors for vasoactive intestinal peptide in rat anterior pituitary glands: localization of binding to lactotropes. Endocrinology, 126, 1981-1988.

Woloschak M, Yu A, Xiao J, Post KD. (1996) Frequent loss of the P16INK4a gene product in human pituitary tumors. Cancer Res, 56, 2493-2496.

Woloschak M, Yu A, Post KD. (1997) Frequent inactivation of the p16 gene in human pituitary tumors by gene methylation. Mol Carcinog, 19, 221-224.

Wong C, Rougier-Chapman E, Frederick JP, Datto MB, Liberati NT, Li JM, Wang XF. (1999) Smad3-Smad4 and AP-1 complexes synergize in transcriptional activation of the c-Jun promoter by transforming growth factor beta. Mol Cell Biol, 19, 1821-1830.

Xu L, Lavinsky R, Dasen JS, Flynn SE, McInerney EM, Mullen TM, Heinzel T, Szeto D, Korzus E, Kurokawa R, Aggarwal AK, Rose DW, Glass CK, Rosenfeld MG. (1998) Signal-specific co-activator domain requirements for Pit-1 activation. Nature, 395, 301-306.

Yaguchi H, Ohkura N, Tsukada T, Yamaguchi K. (2002) Menin, the multiple endocrine neoplasia type 1 gene product, exhibits GTP-hydrolyzing activity in the presence of the tumor metastasis suppressor nm23. J Biol Chem, 277, 38197-38204.

Yamada M, Saga Y, Shibusawa N, Hirato J, Murakami M, Iwasaki T, Hashimoto K, Satoh T, Wakabayashi K, Taketo MM, Mori M. (1997) Tertiary hypothyroidism and hyperglycemia in mice with targeted disruption of the thyrotropin-releasing hormone gene. Proc Natl Acad Sci U S A, 94, 10862-10867.

Yang X, Castilla L, Xu X, Li C, Gotay J, Weinstein M, Liu PP, Deng CX. (1999) Angiogenesis defects and mesenchymal apoptosis in mice lacking SMAD5. Development, 126, 1571-1580.

Yokoyama A, Wang Z, Wysocka J, Sanyal M, Aufiero DJ, Kitabayashi I, Herr W, Cleary ML. (2004) Leukemia proto-oncoprotein MLL forms a SET1-like histone methyltransferase complex with menin to regulate Hox gene expression. Mol Cell Biol, 24, 5639-5649.

Yu BD, Hess J, Horning SE, Brown GA, Korsmeyer SJ. (1995) Altered Hox expression and segmental identity in Mll-mutant mice. Nature, 378, 505-508.

Yumita W, IY, Yamauchi K, Sakurai A, Hashizume K. (2003) Suppression of insulin-induced

AP-1 transactivation by menin accompanies inhibition of c-Fos induction. Int J Cancer, 103, 738-744.

Zeisig BB, Milne T, Garcia-Cuellar MP, Schreiner S, Martin ME, Fuchs U, Borkhardt A, Chanda SK, Walker J, Soden R, Hess JL, Slany R. (2004) Hoxa9 and Meis1 are key targets for MLL-ENL-mediated cellular immortalization. Mol Cell Biol, 24, 617-628.

Zhu JL, Kaytor E, Pao CI, Meng XP, Phillips LS. (2000) Involvement of Sp1 in the transcriptional regulation of the rat insulin-like growth factor-1 gene. Mol Cell Endocrinol, 164, 205-218.

Zhu, Y, Richardson, JA, Parada, LF and Graff, JM. (1998) Smad3 mutant mice develop metastatic colorectal cancer. Cell, 94, 703-714.

Zhuang Z, Vortmeyer A, Pack S, Huang S, Pham TA, Wang C, Park WS, Agarwal SK, Debelenko LV, Kester M, Guru SC, Manickam P, Olufemi SE, Yu F, Heppner C, Crabtree JS, Skarulis MC, Venzon DJ, Emmert-Buck MR, Spiegel AM, Chandrasekharappa SC, Collins FS, Burns AL, Marx SJ, Lubensky. (1997) Somatic mutations of the MEN1 tumor suppressor gene in sporadic gastrinomas and insulinomas. Cancer Res, 57, 4682-4686.